

# Techno-economic analysis of integration possibilities for fluctuating renewable energy sources in the Power and Biomass to Liquid process

A thesis accepted by the Faculty of Energy-, Process- and Bio-Engineering of  
the University of Stuttgart to fulfill the requirements for the degree of Doctor  
of Engineering Sciences (Dr.-Ing.)

by **Felix Habermeyer**

born in Munich

First assessor: Prof. Dr. André D. Thess

Second assessor: Prof. Dr. Magne Hillestad

Date of oral exam: April 9, 2024

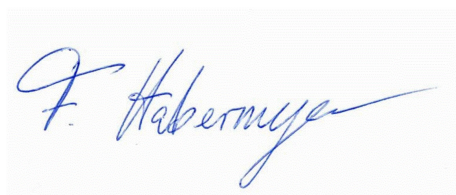
Institute for Building Energetics, Thermotechnology and Energy Storage  
at the University of Stuttgart

2024

# Eigenständigkeitserklärung

Ich erkläre, dass ich abgesehen von den ausdrücklich bezeichneten Hilfsmitteln diese Dissertation selbstständig verfasst habe.

Signature:

A handwritten signature in blue ink, appearing to read 'F. Habermeyer', written on a light-colored background.

Date:

November 16, 2023

# Acknowledgements

This dissertation would not have been possible without the invaluable support of numerous individuals. I would like to express my heartfelt gratitude to those who played particularly significant roles in guiding me on this academic journey.

First and foremost, I am thankful to Esa and Minna Kurkela for providing me with the opportunity to participate in the FLEXCHX project, which was a great learning experience. My heartfelt appreciation goes to Esa for engaging in countless discussions on gasification and fuel processes, which eventually led to our joint publications.

I am also grateful for the smooth and pleasant collaboration with Veatriki Papantoni. The insightful feedback from both Veatriki and Urte Brandt was extremely helpful in reaching our common goal.

I am looking back at some great years spend with my DLR colleagues Julia Weyand, Sandra Adelung, Simon Maier and Moritz Raab. Your critical feedback helped me to improve my work but has also changed me as a person. I'd like to especially acknowledge Simon Maier for his efforts in extending and maintaining TEPET.

I would like to express my appreciation to Marc Linder for his support during challenging times. Your courage and kindness will always be remembered.

My heartfelt thanks to Uwe Dietrich and Prof. André Thess for providing me with the opportunity to prepare this dissertation under their supervision. I am grateful for the fruitful discussions and their guidance, which steered this work in the right direction.

Lastly, I extend my gratitude to my family for their unwavering support. Mama, Papa, Fanny, Sophie, Peter, and Valerie, thank you for always having my back, offering advice, and for your love even during the toughest times.

# Abstract

Sustainable aviation fuels provide the opportunity to reduce the aviation industry's climate impact while avoiding a complete replacement of the current aircraft fleet. The European Union directs its member states to a gradual uptake of sustainable aviation fuel from 2 %<sub>vol.</sub> in 2025 to 63 %<sub>vol.</sub> by 2050 with the ReFuelEU directive. Yet, biomass-based fuel production in Europe is limited by the availability of sustainable biomass. This limitation can be mitigated by the Power Biomass to Liquid process, which attains near full biogenic carbon conversion to fuel by the addition of electrolytic hydrogen.

This work evaluates the economic feasibility and global warming impact of sustainable aviation fuel production via the Power Biomass to Liquid process. Different options to enhance process performance and reduce its footprint are analyzed. This includes a discussion of process configurations and integration options for fluctuating energy sources. Based on flowsheet simulations in Aspen Plus, production costs, emissions and fuel production volume are estimated under different economic and regional boundary conditions.

The production cost for the Power Biomass to Liquid process is highly sensitive to the electricity price. In fact, the electricity cost is the largest cost contributor followed by the cost for the biomass and the electrolyzer investment. The electricity's carbon footprint is also shown to be the determining factor for the fuel's global warming potential. Therefore, regions with inexpensive and green electricity, either from their national grid mix or their renewable energy potential, are the ideal sites for the Power Biomass to Liquid process. In a region-specific analysis, Norway and Sweden present good production sites due to their suitable grid conditions. Ireland is a promising production site based on its onshore wind potential.

High electricity prices and emissions can also be avoided by operating the Power Biomass to Liquid process dynamically. Yet, dynamically operated electrolysis units add substantial cost when over-dimensioned. Therefore, an optimum between reduced electricity costs and increased

capital expenses has to be found.

A cost reduction can also be achieved by identifying process configurations suited for the region-specific boundary conditions. A higher CO<sub>2</sub> recycle ratio, for example, leads to an enhanced product yield at the cost of a larger hydrogen demand. Due to the increased electricity demand for hydrogen production, this is only cost-effective at low electricity prices.

When considering forest residues with an availability of 33 % as the feedstock for the Power Biomass to Liquid process, around 25 Mt/a sustainable aviation fuel can be produced within Europe. This output could be even higher when agricultural residues can also be utilized. Yet, this production volume of sustainable aviation fuel depends upon low-carbon electricity. When considering grid connected operation in Europe today, only around 5 Mt/a can be produced when adhering to the European sustainable aviation fuel definition of 70 % emission reduction compared to fossil fuel.

# Kurzzusammenfassung

Nachhaltige Flugkraftstoffe bieten die Möglichkeit die Klimawirkung der Luftfahrt zu verringern und gleichzeitig einen vollständigen Austausch der derzeitigen Flotte zu vermeiden. Die Europäische Union verpflichtet ihre Mitgliedstaaten mit der ReFuelEU-Richtlinie zu einer schrittweisen Erhöhung der Beimischquote nachhaltiger Flugkraftstoffe von 2 %<sub>vol.</sub> im Jahr 2025 auf 63 %<sub>vol.</sub> bis 2050. Die Produktion von Treibstoff auf Biomassebasis ist in Europa jedoch durch die Verfügbarkeit von nachhaltiger Biomasse begrenzt. Diese Limitierung kann durch das Power Biomass to Liquid Verfahren verringert werden, bei dem durch die Zugabe von elektrolytischem Wasserstoff eine nahezu vollständige Umwandlung von biogenem Kohlenstoff zu Fischer-Tropsch-Kraftstoff erreicht wird.

In dieser Arbeit werden die wirtschaftliche Machbarkeit und die Umweltauswirkungen einer nachhaltigen Flugkraftstoffproduktion mit dem Power Biomass to Liquid-Verfahren untersucht. Es werden verschiedene Optionen zur Steigerung der Prozessleistung und zur Verringerung des ökologischen Fußabdrucks analysiert. Dies beinhaltet eine Diskussion von unterschiedlichen Prozesskonfigurationen und Integrationsoptionen für fluktuierende Energiequellen. Auf der Grundlage von Fließbildsimulationen in Aspen Plus werden Produktionskosten, Emissionen und Kraftstoffproduktionsmengen unter verschiedenen wirtschaftlichen und regionalen Randbedingungen ermittelt.

Die Produktionskosten für das Power Biomass to Liquid Verfahren hängen stark vom Strompreis ab. Die Stromkosten sind der größte Kostenfaktor, gefolgt von den Biomassekosten und der Investition in den Elektrolyseur. Der Kohlenstoff-Fußabdruck des Stroms ist zudem auch der entscheidende Faktor für das Treibhauspotenzial des Kraftstoffs. Daher sind Regionen mit preiswertem und grünem Strom, entweder aus dem nationalen Stromnetz oder aus lokal verfügbarer erneuerbarer Energie, die idealen Standorte für den Power Biomass to Liquid Prozess. Eine regionsspezifische Analyse zeigt, dass Norwegen und Schweden aufgrund des

hohen Anteils an erneuerbarer Energie im Stromnetz gute Produktionsstandorte für diesen Prozess darstellen. Irland wäre aufgrund seines Onshore-Windpotenzials ein vielversprechender Produktionsstandort.

Hohe Strompreise und Emissionen können auch durch den dynamischen Betrieb des Power Biomass to Liquid Verfahrens vermieden werden. Allerdings verursachen dynamisch betriebene Elektrolyseeinheiten bei Überdimensionierung erhebliche Mehrkosten. Daher muss ein Optimum zwischen reduzierten Stromkosten und erhöhten Kapitalkosten gefunden werden.

Eine Kostensenkung kann auch durch die Identifizierung von Prozesskonfigurationen erreicht werden, die für die regionsspezifischen Randbedingungen geeignet sind. Eine höhere CO<sub>2</sub>-Recyclierungsrate führt zum Beispiel zu einer höheren Produktausbeute auf Kosten eines höheren Wasserstoffbedarfs. Aufgrund des dadurch erhöhten Strombedarfs ist dies nur bei niedrigen Strompreisen wirtschaftlich.

Nimmt man forstwirtschaftliche Reststoffe mit einer Verfügbarkeit von 33 % als Ausgangsmaterial für den Power Biomass to Liquid Prozess an, können in Europa rund 25 Mt/a nachhaltiger Flugkraftstoff hergestellt werden. Die Produktmenge könnte sogar noch höher sein, wenn auch landwirtschaftliche Reststoffe als Ausgangsstoffe verwendet werden können. Diese Produktionsmenge ist jedoch nur mit emissionsarmer Elektrizität möglich. Betrachtet man den netzgebundenen Betrieb in Europa, können heute nur etwa 5 Mt/a produziert werden, wenn man die europäische Definition für nachhaltigen Flugkraftstoff von 70 % Emissionsreduzierung im Vergleich zu fossilem Kraftstoff einhält.

# Contents

<b>1</b>	<b>Introduction</b>	<b>2</b>
1.1	Motivation . . . . .	2
1.2	SAF production . . . . .	3
1.3	SAF production via the PBtL process . . . . .	4
1.4	Published literature and contributions of this work . . . . .	6
1.4.1	Techno-economic analysis . . . . .	6
1.4.2	Discussion of plant configuration . . . . .	8
1.4.3	Life cycle analysis and SAF quantity . . . . .	9
1.4.4	Integration options for fluctuating energy sources . . . . .	10
<b>2</b>	<b>Methodology</b>	<b>12</b>
2.1	Aspen Plus process simulation . . . . .	13
2.2	Fortan Fischer-Tropsch reaction kinetic . . . . .	14
2.3	Techno-economic analysis with TEPET . . . . .	14
<b>3</b>	<b>Publications</b>	<b>17</b>
<b>4</b>	<b>Results and Discussion</b>	<b>74</b>
4.1	Techno-economic results . . . . .	74
4.2	Process configuration . . . . .	76
4.3	Integration of fluctuating energy sources . . . . .	78
4.4	GHG abatement cost . . . . .	79
4.5	Production potential . . . . .	79
<b>5</b>	<b>Conclusion</b>	<b>81</b>
5.1	Outlook . . . . .	83



# List of Figures

- 1.1 Schematic flowsheet for the Power Biomass to Liquid process (PBtL) [13]. . . . . 5
- 1.2 Schematic flowsheet for the Biomass to Liquid process (BtL) [13]. . . . . 6
  
- 2.1 Methodology overview. . . . . 12

# List of Tables

1.1	ASTM certified drop-in fuel production routes and main production characteristics [4]. . . . .	3
1.2	Comprehensive literature overview on the PBtL process . . . . .	7
2.1	Summary of main characteristics of the three published PBtL process models. . .	13
4.1	PBtL process performance for all published simulations compared to results from literature. All shown results represent the base case in each publication along with the key assumptions. . . . .	75

# Nomenclature

ASU Air separation unit

AtJ Alcohol to jet

BtL Biomass to liquid

CAPEX Capital expenditure

CFB Circulating fluidized bed

CH Catalytic hydrothermolysis

FCI Fixed capital investment

GHG Greenhouse gas

GWP Global warming potential

HEFA Hydrotreated ester and fatty acid

LCA Life cycle analysis

LCOE Levelized cost of electricity

LCOH Levelized cost of hydrogen

NPC Net production cost

PBtL Power Biomass to Liquid

PEMEL Proton exchange membrane electrolysis

PV Photovoltaics

RED II Second renewable energy directive

RWGS Reverse water gas shift

SAF Sustainable aviation fuel

SBCR Slurry bubble column reactor

SiP Synthesized iso-paraffine

SNG Synthetic natural gas

SOEC Solid oxide electrolysis cell

SPK Synthesized paraffinic kerosene

SXB Staged fixed bed

TEA Techno-economic analysis

TEPET Techno economic process evaluation tool

WGS Water gas shift

# Chapter 1

## Introduction

### 1.1 Motivation

Limiting climate change well below 2 degrees above pre-industrial levels is the central goal of the Paris Agreement. This agreement was adopted by 196 nations [1]. To limit the temperature rise, greenhouse gas emissions have to be cut. This poses the challenge for governments to find an economically optimal and socially acceptable way to transform today's industrial and societal practices towards lower greenhouse gas (GHG) emissions.

The European Union has set itself the goal of reducing GHG emissions by at least 55 % compared to 1990 until 2030 and reaching net-zero by 2050 [2]. The way to decarbonize many sectors has been politically defined. For the aviation industry, blending rates for sustainable aviation fuel (SAF) have been defined in the ReFuelEU package. These will be gradually increased from 2 %<sub>vol.</sub> in 2025 to 63 %<sub>vol.</sub> by 2050 [3]. Yet, the optimal fuel production route still has to be identified. Here, many factors including social acceptance and greenhouse gas abatement cost, which all may vary based on time or location, have to be considered in finding the optimal energy provision for aviation.

This work aims to enhance the understanding of one particular production route for sustainable aviation fuel, the Power Biomass to Liquid (PBtL) process. The PBtL process converts biomass and electrolytic hydrogen via the Fischer-Tropsch route to hydrocarbons. After some refining steps, the produced fuel can be blended into conventional fossil jet fuel. To assess the process in comparison with other SAF production routes, this work answers the following questions:

- What are the production cost and GHG emissions for the PBtL process? How can these

values be minimized via the selection of the process configuration?

- How to incorporate electricity supply fluctuations into the process for minimal production cost and GHG emissions?
- How much sustainable aviation fuel can be produced within Europe given the limited availability of biomass and renewable power?

## 1.2 SAF production

Several SAF production routes have achieved certification as drop-in fuels. Table 1.1 offers an overview of these routes, including their maximum blending rates, estimated production costs, and associated greenhouse gas (GHG) emissions. The latter two characteristics should be viewed as rough indications as they are derived from a review study on today’s state-of-the-art knowledge on these processes [4].

The FT route (FT-SPK and FT-SPK/A) is certified for a 50 % blending rate similar to the alcohol to jet (AtJ), catalytic hydrothermolysis (CH) and hydrotreated ester and fatty acid (HEFA) route. The high blending rate sets these routes apart from the synthesized iso-paraffine (SiP) and the HEFA route that includes algae-derived hydrocarbons as feedstock (HC-HEFA), which is restricted to 10 %. While all other routes have to be refined in a separate facility, up to 5 % of FT product can be added to conventional oil refining processes.

**Table 1.1.** ASTM certified drop-in fuel production routes and main production characteristics [4].

Route	Certified Blending [%vol.]	Feedstock	Production Cost (> 0.18 Mt/a)	GHG Emissions
AtJ	50	Lignocellulosic biomass, sugar-based feedstock	High	Intermediate
SiP	10	Lignocellulosic biomass, sugar-based feedstock	High	Intermediate
HEFA	50	Oil-based feedstock	Low	High
HC-HEFA	10	Algae-derived hydrocarbons + fatty acid and esters		
FT-SPK	50	Carbon-based biomass	Intermediate	Low
FT-SPK/A	50	Co-processing of a benzene-rich stream from coal gasification		
FT Co-processing	5	Carbon-based biomass	Intermediate	Low
CH	50	Algae, waste oil, oil plant		

The FT route was found to have lower production cost than the AtJ and SiP route [4]. However, it's important to note that the AtJ process demonstrates cost advantages at smaller plant sizes due to its lower capital intensity in comparison to the FT route. While the HEFA route appears to be the most cost-effective production route, it is associated with a significant GHG footprint and limited feedstock availability [4]. The FT route, on the other hand, is connected to low emissions and has a relatively large feedstock base. In addition, the FT route is a mature process technology with many commercially operated coal- and natural gas-based plants and a number of biomass-based projects [5].

Although, FT appears to be a promising production route for SAF, there are certain caveats to consider. Some novel routes are in the certification process as SAF with a blending rate of 50 %. Routes such as methanol to SAF could be a better alternative to FT. In fact, studies have found the methanol to SAF route to have a higher process efficiency and lower production cost [6, 7].

The FT process under investigation in this work relies on biomass as feedstock. Many studies consider CO<sub>2</sub> from direct air capture or industrial flue gas removal as an alternative renewable carbon source for the FT process [8–10]. The advantage of using biomass over CO<sub>2</sub> is that less energy is needed for the conversion of the feedstock. Biomass, with a typical composition of CH<sub>1.4</sub>O<sub>0.61</sub> [11], would need to be fully oxidized to have the same hydrogen demand as CO<sub>2</sub>, i.e. 3 mol<sub>H<sub>2</sub></sub>/mol<sub>feedstock</sub>. Gasification and reformation retain a certain amount of CO and H<sub>2</sub>. Therefore, these steps are considered not full but partial oxidation steps. Consequently, less hydrogen (< 3 mol<sub>H<sub>2</sub></sub>/mol<sub>feedstock</sub>) is needed for the conversion of biomass to hydrocarbons than CO<sub>2</sub>. However, the availability issues and discussions about feedstock sustainability can be avoided by using renewable CO<sub>2</sub> from direct air capture as feedstock [12].

### 1.3 SAF production via the PBtL process

The PBtL conversion route from biomass and electricity to FT syncrude is shown in Figure 1.1. Throughout this work, the process proposed in the FLEXCHX project has been used as the base case design [14]. Dried biomass is converted to syngas by the addition of steam, oxygen and recycled CO<sub>2</sub>. The syngas consists mainly of components that find their chemical equilibrium according to the water gas shift (WGS) equilibrium ( $CO + H_2O \rightleftharpoons CO_2 + H_2$ ). These components, together with some inert gas components such as nitrogen or methane,

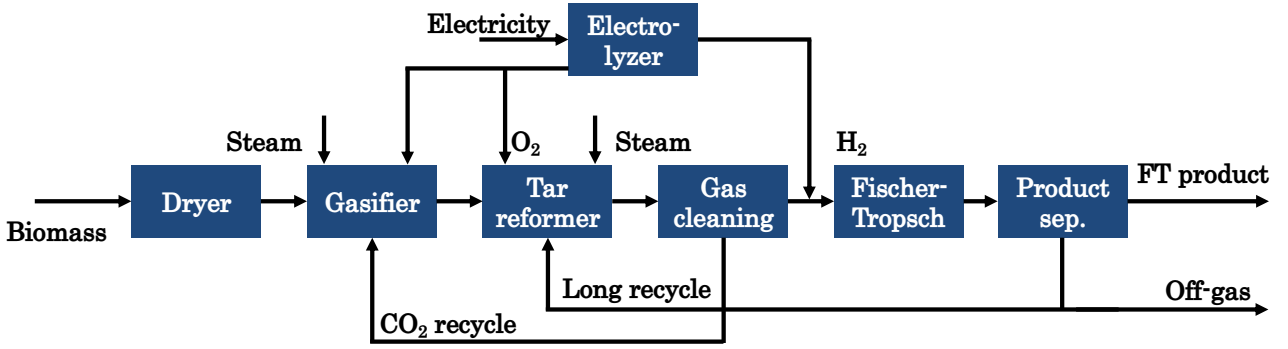
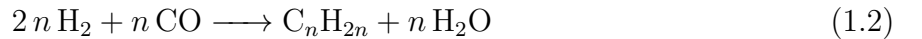
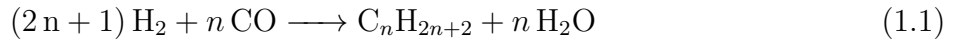


**Figure 1.1.** Schematic flowsheet for the Power Biomass to Liquid process (PBtL) [13].

have to be separated from components that act as catalyst poison such as tars or hydrogen sulfide. To do so, the gas mixture is introduced into the tar reformer. Here, a catalytic tar cracking reaction occurs over a nickel catalyst under the addition of oxygen [14]. Further, in the tar reformer recycled short chained hydrocarbons  $C_{1-4}$ , by-products of the FT reaction, can be partly reformed to syngas components. After the removal of the remaining catalyst poisons and the addition of hydrogen from the electrolyzer unit, the gas mixture is fed to the FT reactor. Here,  $H_2$  and CO react according to Equation 1.1 and Equation 1.2 over a Cobalt catalyst to paraffines and olefins of various chain lengths. The fraction with a carbon chain length higher than five ( $C_{5+}$ ) is separated from the generated  $H_2O$ , unconverted syngas and the shorter fraction  $C_{1-4}$ . The  $C_{5+}$  fraction can be converted to SAF in subsequent refining steps, which are not within the scope of this work.



Contrary to PBtL, no hydrogen is added to the BtL process. Consequently, no electrolysis unit is needed. The oxygen for gasifier and reformer is produced in an air separation unit (ASU), as depicted in Figure 1.2. Additionally, no  $CO_2$  recycle is employed in the BtL process. The FT reactant should be fed to the reactor in a ratio of  $H_2/CO = 2.1$  [15]. In the PBtL process, the recycling of  $CO_2$  leads to a shift towards CO and  $H_2O$  in the WGS equilibrium, resulting in significantly lower  $H_2/CO$  ratios. The adjustment of this ratio in the PBtL process can only be achieved by adding hydrogen from the electrolyzer. In contrast, the BtL process allows for



the ratio to be adjusted by introducing steam at the equilibrium stages. As a consequence, a larger part of the biogenic carbon leaves the BtL process in the form of  $\text{CO}_2$ , which ultimately results in a lower product yield for the BtL compared to the PBtL process. The BtL process, on the other hand, can be operated without the additional investment and operation costs for the electrolyzer. Furthermore, the far lower electrical power requirement means that the BtL process is less dependent upon its electricity's carbon footprint to reach a low process GWP.

A number of BtL processes are in operation today. Thyssen is operating a biomass gasification plant in combination with a Fischer-Tropsch synthesis in Dunkirk [16]. Moreover, the Fulcrum project relies on a municipal solid waste gasification and a Fischer-Tropsch synthesis [17]. Yet, other BtL projects had to be shut down such as the CHOREN project [18].

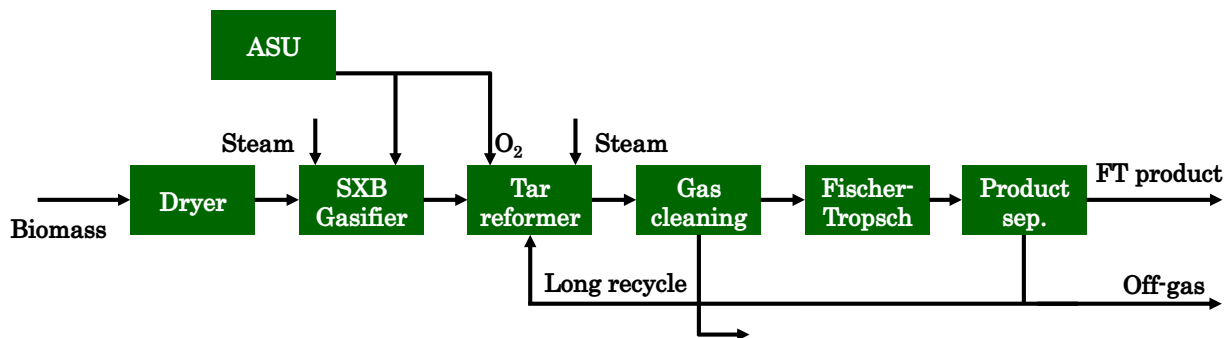


**Figure 1.2.** Schematic flowsheet for the Biomass to Liquid process (BtL) [13]

## 1.4 Published literature and contributions of this work

The following section gives an overview of all studies on the PBtL process and highlights the areas in which the present work has added new aspects to the scientific discussion. Table 1.2 lists publications on the PBtL process with their methodologies and main results. This table solely focuses on the FT route excluding studies that apply the principle of adding electrolytic hydrogen to increase carbon conversion to other biomass conversion routes such as methanol [19], [20] or SNG [21].

### 1.4.1 Techno-economic analysis

A number of techno-economic analyses (TEA) have been conducted for the PBtL process. Three studies focus on a specific production site for the estimation of production costs. Hillestad

**Table 1.2.** Comprehensive literature overview on the PBtL process

Study	Study type	Main finding	Reference year	Geographical scope	Key assumptions	Plant size (biomass input)	Variation of plant configuration	Integration options for RES
Hillestad et al. [22]	TEA	NPC 1.7 \$/l	2014	Norway	50 \$/MWh <sub>grid</sub>	435 MW <sub>th</sub>	H <sub>2</sub> distribution to RWGS and FT reactor	
Albrecht et al. [9]	TEA	NPC 2.06 €/l	2014	Germany	105 €/MWh <sub>grid</sub>	100 MW <sub>th</sub>		
Isaacs et al. [23]	TEA, GWP focused LCA	Grid: NPC 2016 1.84 \$/l, GWP 2016 187 gCO <sub>2,eq</sub> /MJ <sub>fuel</sub>	2016, 2030 and 2050	USA	67.3 \$/MWh <sub>grid</sub>	1000 t <sub>dry</sub> /d (200 MW <sub>th, dry</sub> )		Off-grid PV and wind or a combination of both
Bernical et al. [24]	TEA, GWP focused LCA	NPC 1.5 €/l, GWP 41 gCO <sub>2,eq</sub> /kWh <sub>fuel</sub>	2011	France	70 €/MWh <sub>grid</sub> 55 gCO <sub>2,eq</sub> /kWh	500 MW <sub>th</sub>		
Dossow et al. [25]	Technical analysis	Carbon efficiency 67 – 97 % depending on the hydrogen feed rate	2021				Comparison of SOEC and PEMEL; water gas shift options	
Putta et al. [26]	TEA	Optimal energy distribution identified; AEL most economic electrolyzer technology	2022	Norway	50 \$/MWh	130 MW <sub>th</sub>	Energy distribution gasifier/electrolyzer; electrolyzer technology	
Müller et al. [27]	Experimental	Dynamic H <sub>2</sub> addition to the FT reactor feed is technically feasible	2018					Experimental validation
Ostadi et al. [28]	Technical analysis	Higher H <sub>2</sub> /CO ratio leads to higher hydrogen demand and higher product output	2019		Three-stage FT reactor		H <sub>2</sub> /CO ratio in the FT input	
Ostadi et al. [29]	Exergy analysis	Gasifier followed by FT and SOEC have the largest exergy destruction	2019					
Weyand et al. [30]	LCA	Electricity and biomass transport radius identified as the largest GWP contributors	2023	Finland		200 MW <sub>th</sub>	H <sub>2</sub> /CO ratio in the FT input	FLEXCHX alternating concept
Peduzzi et al. [11]	Optimization study	NPC and GWP values for all analyzed process configurations in a PBtL process exceed those of the BtL process	2018		100.5 €/MWh 320 gCO <sub>2,eq</sub> /kWh	200 MW <sub>th</sub>	Different technology options and technical parameters)	

et al. find production costs of 1.7  $\$/_{2014}$ /l at an electricity price of 50  $\$/\text{MWh}$  in Norway, while Albrecht et al. [9] estimate production costs of 2.06  $\$/_{2014}$ /l at an electricity price of 105  $\$/\text{MWh}$  in Germany. Bernical et al. [24] present production cost estimates of 1.5  $\text{€}_{2011}$ /l for an electricity price of 70  $\text{€}/\text{MWh}$  in France.

Isaacs et al. [23], on the other hand, perform a region-specific production cost analysis for the Eastern USA. They find production costs of 1.84  $\$/_{2016}$ /l when assuming a grid electricity price of 67.3  $\$/\text{MWh}$ . When local biomass costs and hydrogen production under local PV and wind conditions are considered on a US county level, the cheapest production quartile has production costs of 3.24 and 2.64  $\$/\text{l}$  for PV and wind, respectively.

Techno-economic studies are predominantly based on technical models taken from literature. The publications encompassed in this work are based, in part, on new models and cost functions developed within the EU project FLEXCHX. For example, the novel SXB gasification technology was modelled based on experimental data and insights provided by the technology developers [13]. Similarly, the cost function for the SXB technology was established based on input from the technology developers. A similar approach was taken for the sorbent-based gas cleaning section, which was also developed in the course of the FLEXCHX project. With that, this work broadens the techno-economic discussion by adding novel technology options.

TEA studies typically focus on specific production sites, which suffice for a fundamental understanding of the technology while assuming a single set of biomass, electricity price, and availability conditions. However, for an actual roll-out analysis in a specific region multiple production sites entailing a variety of production conditions have to be considered. Such a study is presented for the USA by Isaacs et al. [23]. However, no study for the European scope was available before the publication by Habermeyer et al. [31].

### 1.4.2 Discussion of plant configuration

While some studies only analyze one plant configuration, others compare different flowsheet or operation points to find optimization potential in terms of technical efficiency or process economics. Some studies only focus on the technical analysis of the PBtL process. Dossow et al. [25] compare different options for the hydrogen addition in the water gas shift equilibrium reaction. They find that the more hydrogen is added to the process, as defined by the configuration, the more product is generated. Moreover, using an SOEC instead of a PEMEL system increases the process efficiency. Similarly, Ostadi et al. [28] show that an increased

H<sub>2</sub>/CO ratio in the FT feed leads to an increased product output while requiring more hydrogen from the electrolyzer. The same author employs an exergy analysis to identify the gasifier as the primary source of exergy destruction, followed by the FT reactor and electrolyzer.

Studies investigating different plant configurations are also integrated into techno-economic analyses. Hillestad et al. [22] demonstrate that hydrogen addition to the reverse water gas shift stage instead of the FT reactor feed increases the product output. Similar to the findings of Dossow et al. [25], the additional product output comes at the cost of a higher hydrogen demand. However, the economic implications of this parameter variation are not discussed. Putta et al. [26] demonstrate the existence of an optimum point concerning efficiency and production costs for a specific ratio of thermal energy supplied to the gasifier in relation to electrical energy provided to the electrolyzer. Nonetheless, the economic results are also not directly stated but given as a dimensionless index.

Peduzzi et al. [11] combine the discussion of fuel GWP and production costs in an optimization study. Their optimization framework includes different technological routes for the conversion of biomass to FT fuel, encompassing BtL and PBtL process concepts with different gasification and gas cleaning technologies. The optimization algorithm minimizes performance indicators, e.g., the production cost or the GWP of routes by manipulating defined process variables such as the FT temperature. Yet, in this study boundary conditions, such as electricity price or GWP, are not varied. For the relatively high electricity price (100.5 €/MWh) and footprint (320 g<sub>CO<sub>2,eq</sub></sub>/kWh), the results show the BtL process as superior compared to the PBtL process in terms of production costs and process GWP for all analyzed technology routes.

The present work addresses this gap by jointly discussing technical and economic implications of process configuration variations. These include process design variations such as the selection of electrolysis technology or reformation options for FT off-gas [13]. But also parameter variations such as the CO<sub>2</sub> recycle ratio, the FT operation temperature and conversion, the FT off-gas recycle ratio [13], the H<sub>2</sub>/CO in the FT inlet [32] as well as the electrolyzer efficiency [13] are addressed by this work. These results show under which economic boundary condition, e.g., electricity price, a specific process configuration is advantageous.

### 1.4.3 Life cycle analysis and SAF quantity

A life cycle analysis typically describes the environmental impact of a process in many categories. As seen in Weyand et al. [30], this includes impact categories such as global warming potential

(GWP) or land and water use. In Tab. 2 the term LCA is also used for studies [23, 24] that only focus on the GWP.

Across all studies on the GWP of the Power Biomass to Liquid (PBtL) process, a consistent consensus prevails: the electricity demand emerges as the most influential factor affecting the total GWP of fuel production [23, 24, 30]. This convergence of findings is mirrored in a study on a methanol production route using biomass and electrolytic hydrogen as feedstock [33].

The novelty of the approach presented in this work lies in the combination of GWP with economic findings to determine the sustainable fuel potential within the EU. The calculation of GHG abatement costs [13, 32] contributes a measure for the cost of defossilization, which makes PBtL SAF comparable to other GHG abatement measures. This measure is especially important in a climate policy context. Moreover, the combination of GHG emissions with the fuel potential analysis allows for the appraisal of fuel quantity that fulfils certain sustainability criteria. In the context of EU legislation, it has been shown how much SAF can be produced within the EU in accordance with the RED II directive within the third publication featured in this work [31]. A similar fuel production quantity analysis on the PBtL process has not been published before. However, these results are highly important for the comparison of PBtL to other conversion pathways. The increased fuel output is the key advantage of the PBtL process over routes such as the BtL process.

#### **1.4.4 Integration options for fluctuating energy sources**

Some studies on the PBtL process deviate from steady-state operation. Renewable energy sources can offer inexpensive and low-GHG electricity, but integration strategies for the fluctuating energy have to be found. Müller et al. [27] show that a dynamic hydrogen addition to the FT reactor is technically feasible. Weyand et al. conduct an LCA for an alternating production system switching from PBtL to BtL operation depending on the availability of renewable energy in the grid [30]. This operation strategy is taken from the EU project FLEXCHX [34]. Moreover, Isaacs et al. [23] calculate LCOH for an off-grid system including battery and hydrogen storage with the algorithm described in [35]. This algorithm minimizes the LCOH for PV and wind profiles for every region within the Eastern USA under the constraint of constant hydrogen output.

The first paper within this work [32] provides the techno-economic basis for the analysis of Weyand et al. [30] with the first analysis of the FLEXCHX operation concept. In addition,

process configurations to improve the techno-economic performance of such an alternating process are proposed with the variation of the  $H_2/CO$  ratio. Consequently, this work adds not only a techno-economic appraisal of this novel operation strategy to the literature on this topic but also suggests improved process configurations.

Moreover, with the third publication [31], this work contributes to the discussion of integration of fluctuating energy sources within the EU. Similar to Isaacs et al. [23], a constant hydrogen output from an off-grid hydrogen plant is analyzed. For around 300 NUTS regions the production costs of hydrogen are estimated based on local PV and wind capacity factors. These results uncover promising production sites for an off-grid PBtL process.

# Chapter 2

## Methodology

This section highlights the methodical advances that were necessary to answer the research questions at hand. Figure 2.1 provides a summary of the methodology, outlining the key developments made in this work along with the main results. In accordance with Figure 2.1, the methodological advances can be allocated to the three programs Aspen Plus, Fortran and TEPET. For each publication an Aspen Plus flowsheet, as summarized in Table 2.1, has been implemented in connection with a FT Fortran kinetic. Moreover, specific techno-ecologic-economic analysis methods were developed in TEPET to generate the respective results.

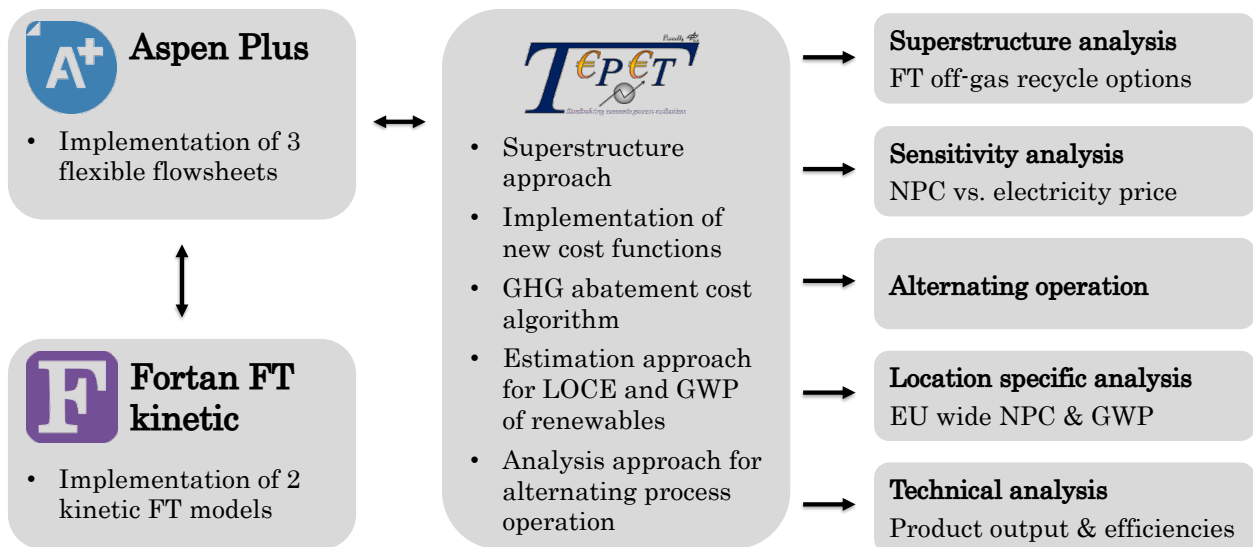


Figure 2.1. Methodology overview.

## 2.1 Aspen Plus process simulation

The basis for every techno-economic evaluation is a unique Aspen Plus flowsheet. Table 2.1 gives an overview over the key process design and modeling decisions. Some of these technologies were modeled based on novel developments from the EU project FLEXCHX. The staged fixed bed gasifier (SXB), for example, is modeled based on the experimental results from the FLEXCHX project [36]. The SXB gasifier was newly developed and tested within the course of this project. Hence, the model and the derived results can be considered as new findings on this field. Moreover, the SXB gasifier was developed for small-scale applications. Therefore, publication II features a much smaller plant ( $50 \text{ MW}_{th}$ ) compared to the other studies on CFB gasifiers.

**Table 2.1.** Summary of main characteristics of the three published PBtL process models.

<b>Publication</b>	<b>I</b>	<b>II</b>	<b>III</b>
Plant size [ $\text{MW}_{th}$ ]	200	50	400
Electrolyzer capacity [ $\text{MW}_{el}$ ]	188	42	890
Product output [ $\text{Mt/a}$ ]	0.13	0.032	0.4
Gasifier technology	CFB	SXB	CFB
FT model	Todic 2013 [37]	Todic 2017 [38]	Todic 2013 [37]
$\text{CO}_2$ recycling rate [%]	33	44	100

In addition, some of the flowsheets contain process superstructures. This means that several process configurations are implemented in one flowsheet. This was done to easily and time-effectively simulate a number of process configurations using TEPET’s simulation control function. Within this function an array of process configurations can be defined, e.g., a PBtL and BtL process with a high and low FT temperature. TEPET then automatically adjusts the simulation parameters and runs the corresponding simulation. Each of the four simulation results is then used to automatically calculate the techno-economic process results for every specified configuration.

A similar approach was pursued for the cost estimation for the alternating process operation in paper I. Here, both operation modes were simulated within one Aspen Plus flowsheet. For alternating processes, the operation mode with the larger unit size defines the required capital investment. For each case in this study, the operation mode with the largest unit size was manually selected. This was done for all units in order to calculate the complete investment



sum for the alternating process.

## 2.2 Fortran Fischer-Tropsch reaction kinetic

Various upstream process parameters have an effect on the FT reaction. Parameters like the  $H_2/CO$  ratio, studied in paper I, have a direct effect on the reactor's product selectivity and the amount of catalyst needed to attain a defined conversion. To accurately simulate the FT reaction, two kinetic reaction models were implemented [37, 38] in a Fortran kinetic which is linked to Aspen Plus as shown in Table 2.1. The link between Fortran and Aspen Plus enables a rapid solution of the model's system of equations. The algorithm's fast convergence time is necessary for any process simulation that includes a recycle. Due to the complexity of the kinetic reaction model no solution was viable within Aspen Plus itself. Therefore, implementing a Fortran user subroutine was a necessary step.

The FT model introduced by Todic et al. in 2013 [37] offers a comprehensive description of paraffin and olefin product distributions. This model accounts for the influence of reactor temperature, pressure, catalyst loading, feed throughput, and composition within a slurry bubble column reactor. This model finds application in both paper I and III.

The same research group has published an updated model with a closer fit to the experimental data in 2017 [38]. The closer fit has been achieved by including a secondary methane formation rate and a secondary 1-olefin hydrogenation reaction mechanism. The later mechanism accounts for the re-adsorption of olefins to the catalyst and is therefore especially worth considering when olefins are recycled to the FT reactor. The model by Todic et al. 2017 is used in paper II. The respective Fortran codes can be found in the supplementary information of each paper.

## 2.3 Techno-economic analysis with TEPET

The production cost estimation method by Peters et al. [39] is implemented in DLR's software tool TEPET. TEPET is equipped with an extensive database encompassing investment and operational cost functions, sourced from various references. This database was extended by the functions needed for the evaluation of the PBtL process. Notably, a investment cost function for the novel SXB gasification technology was derived from project internal cost estimations and added to TEPET [13].

Indirect investment costs, such as the cost of installation or piping, are estimated by multiplying

Lang factors with the base investment cost [39]. For some units in the PBtL flowsheet standard Lang factors could not be applied. For electrolyzers, for instance, lower Lang factors than the standard chemical equipment should be used as the integration effort for electro-chemical equipment is typically lower. Here, electrolyzer specific Lang factors were established in an expert interview and accordingly implemented in TEPET [32].

In instances where project-specific data on investment costs is unavailable, literature-derived functions were used. In the case of the FT slurry bubble column reactor (SBCR), the investment cost function has to be dependent upon the amount of catalyst in the reactor. This is of importance when different reactor conversion rates are techno-economically compared, as a higher catalyst loading leads to higher reaction rates at a constant syngas input [40]. Since no such function has been available in literature, a novel investment cost function for the FT SBCR has been developed. Here, the costs for catalyst and the vessel are estimated separately. A detailed description of the cost function can be found in paper I [41].

Two different methodologies for the estimation of the process' GWP have been established in collaboration with the respective co-authors. In the second publication, a simplified approach considering only biomass harvesting, transport and electricity production for the GWP calculation is pursued [13]. For the assessment of European production conditions, only the electricity GWP is varied for each country while biomass related emissions are assumed as constant. For the approach applied in paper III [31], electricity GWP and biomass transport are calculated based on local conditions within Europe. The biomass density in a specific region determines the transportation distance to the PBtL plant.

The GHG abatement cost calculation combines economic and ecologic analysis. The value gives an indication of additional cost incurred for the GHG emission savings of synthetic fuels in comparison to crude oil. It is established as the difference of PBtL net production cost  $NPC_{PBtL}$  and crude oil price  $Price_{Crude\ oil}$  divided by the GHG emission  $m_{CO_2,eq}$  reduction as seen in Equation 3. The according calculation algorithm has been implemented in TEPET as part of paper II and III [13, 31].

$$GHG\ abatement\ cost = \frac{NPC_{PBtL} - Price_{crudeoil}}{m_{CO_2,eq,crudeoil} - m_{CO_2,eq,PBtL}} \quad (2.1)$$

Based on the previously described calculation algorithms for NPC, GWP and abatement costs, a region-specific analysis for Europe has been conducted. The challenge has been to account for the different boundary conditions across approximately 300 NUTS regions. Local parameters affecting the production cost including biomass, labor and electricity prices have been collected

in a database. The same has been done for the local parameters influencing production emissions, such as the biomass transport radius and the carbon intensity of the used electricity. A special estimation algorithm has been pursued for electricity price and carbon intensity. While the price and carbon intensity values for grid electricity could be directly taken from datasets, they had to be estimated for the renewable energy sources wind and PV. Both values were estimated based on the local capacity factors. The higher the local capacity factor, i.e. the share of full load hours per year, the lower the levelized cost of electricity LCOE and carbon intensity could be found.

# Chapter 3

## Publications

The following publications have been published in peer reviewed journal. Statements about the author's contributions can be found before each publication:

**Publication I: Techno-Economic Analysis of a Flexible Process Concept for the Production of Transport Fuels and Heat from Biomass and Renewable Electricity**

F. Habermeyer, E. Kurkela, S. Maier, R.-U. Dietrich

Frontiers in Energy Research 2021 Vol. 9 Pages 684

DOI: <https://doi.org/10.3389/fenrg.2021.723774>

**Publication II: Power Biomass to Liquid – an option for Europe's sustainable and independent aviation fuel production**

F. Habermeyer, J. Weyand, S. Maier, E. Kurkela and R.-U. Dietrich

Biomass Conversion and Biorefinery 2023

DOI: [10.1007/s13399-022-03671-y](https://doi.org/10.1007/s13399-022-03671-y)

**Publication III: Sustainable aviation fuel from forestry residue and hydrogen – a techno-economic and environmental analysis for an immediate deployment of the PBtL process in Europe**

F. Habermeyer, V. Papantoni, U. Brand-Daniels and R.-U. Dietrich

Sustainable Energy & Fuels

Additionally, the scientific work has been presented at the following national and international conferences:

- Felix Habermeyer and Ralph-Uwe Dietrich (2018) FLEXCHX Project: Flexible combined production of power, heat and transport fuels from renewable energy sources.  
4. Wissenschaftliches SCI-Treffen „Sektorkopplung“, 20.-21. Sep. 2018, Stuttgart, Germany.
- Felix Habermeyer and Ralph-Uwe Dietrich (2019) Flexibility in renewable fuel production from biomass – the role of electrolysis boosted Fischer-Tropsch synthesis. Jahrestreffen der ProcessNet-Fachgruppe Energieverfahrenstechnik und des Arbeitsausschusses Thermische Energiespeicherung, 6.-7. March 2019, Frankfurt am Main, Germany.
- Felix Habermeyer (2019) Flexibility in renewable fuel production from biomass – the role of electrolysis boosted Fischer-Tropsch synthesis. 27th European Biomass Conference & Exhibition, 27.-30. May 2019, Lisbon, Portugal.
- Felix Habermeyer, Julia Weyand, Simon Maier and Ralph-Uwe Dietrich (2022) Power and Biomass to Liquid - An economic and sustainable process for the production of aviation fuel. ProcessNet EVT, 30. March - 1. April 2022, Bamberg, Germany.
- Felix Habermeyer, Julia Weyand, Simon Maier and Ralph-Uwe Dietrich (2022) Power and Biomass to Liquid - Unlocking the full potential of biomass for sustainable aviation fuel production. 30th European Biomass Conference & Exhibition, 9.-12. May 2022, Online.
- Felix Habermeyer, Veatriki Papantoni, Simon Maier and Ralph-Uwe Dietrich (2022) Power and Biomass to Liquid - An option for Europe’s sustainable and independent aviation fuel production. ProcessNet (Bio)Process Engineering, 12.-15. Sept. 2022, Aachen, Germany.
- Felix Habermeyer, Julia Weyand, Simon Maier and Ralph-Uwe Dietrich (2023) Sustainable aviation fuel from renewable hydrogen and biomass – a techno-economic analysis for Europe. 11th FSC International Conference, 23. - 25. May 2023, Aachen, Germany.
- Habermeyer, Felix Veatriki Papantoni, Julia Weyand, Simon Maier and Ralph-Uwe Dietrich (2023) Power and Biomass to Liquid – lifting the biomass limitation for Europe’s sustainable and independent aviation fuel production. 31th European Biomass Conference & Exhibition, 5.-8. June 2023, Bologna, Italy.

## Publication I

### **Techno-Economic Analysis of a Flexible Process Concept for the Production of Transport Fuels and Heat from Biomass and Renewable Electricity**

F. Habermeyer, E. Kurkela, S. Maier, R.-U. Dietrich

Frontiers in Energy Research 2021 Vol. 9 Pages 684

DOI: <https://doi.org/10.3389/fenrg.2021.723774>

#### **Author Contributions:**

The study is based on Esa Kurkela's process design as studied in the EU project FLEXCHX. Modeling, simulation and analysis was done by Felix Habermeyer under the guidance of Ralph-Uwe Dietrich and Esa Kurkela. The software tool TEPET was provided by Simon Maier. The authors Felix Habermeyer and Simon Maier prepared the manuscript. Ralph-Uwe Dietrich, Esa Kurkela and Simon Maier discussed and commented the manuscript.



# Techno-Economic Analysis of a Flexible Process Concept for the Production of Transport Fuels and Heat from Biomass and Renewable Electricity

Felix Habermeyer<sup>1\*</sup>, Esa Kurkela<sup>2</sup>, Simon Maier<sup>1</sup> and Ralph-Uwe Dietrich<sup>1</sup>

<sup>1</sup>DLR e.V., Institute of Engineering Thermodynamics, Stuttgart, Germany, <sup>2</sup>VTT Technical Research Centre of Finland Ltd., Teknologian Tutkimuskeskus VTT Oy, Espoo, Finland

## OPEN ACCESS

### Edited by:

Erik Furusjö,  
Research Institutes of Sweden (RISE),  
Sweden

### Reviewed by:

Ganapati D. Yadav,  
Institute of Chemical Technology, India  
Abu Yousuf,  
Shahjalal University of Science and  
Technology, Bangladesh

### \*Correspondence:

Felix Habermeyer  
felix.habermeyer@dlr.de

### Specialty section:

This article was submitted to  
Bioenergy and Biofuels,  
a section of the journal  
Frontiers in Energy Research

**Received:** 11 June 2021

**Accepted:** 07 October 2021

**Published:** 23 November 2021

### Citation:

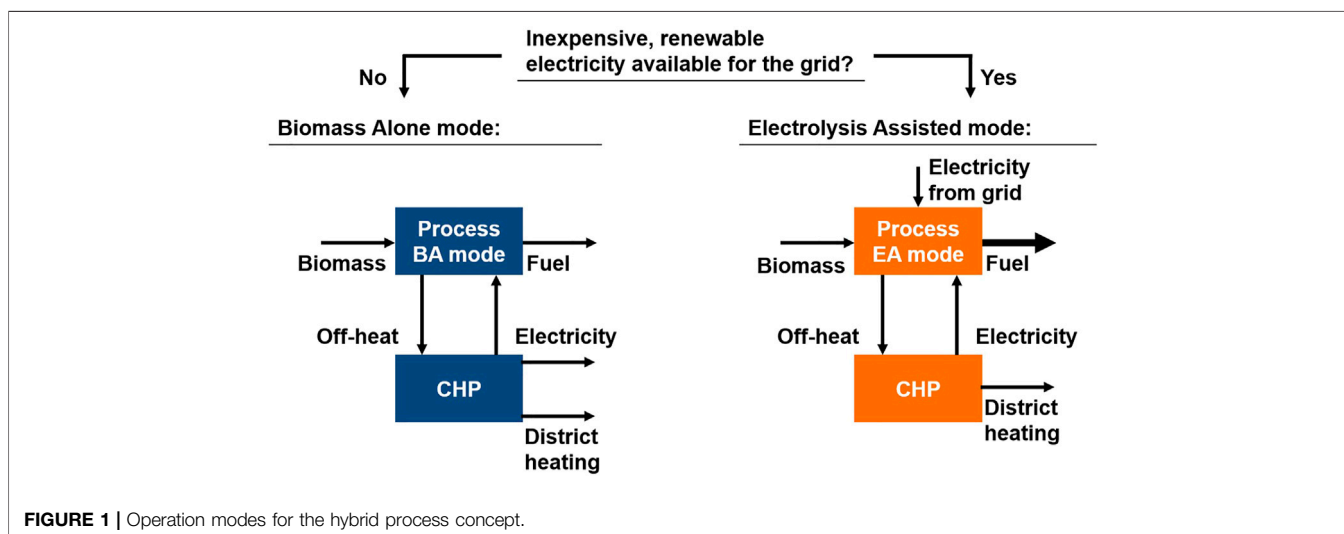
Habermeyer F, Kurkela E, Maier S and  
Dietrich R-U (2021) Techno-Economic  
Analysis of a Flexible Process Concept  
for the Production of Transport Fuels  
and Heat from Biomass and  
Renewable Electricity.  
Front. Energy Res. 9:723774.  
doi: 10.3389/fenrg.2021.723774

Different processes have been proposed to meet the global need for renewable fuel. The Biomass to Liquid process (BtL) converts biomass via the Fischer-Tropsch route to hydrocarbon chains that can be refined to transport fuel. With the addition of electrolytic hydrogen to the Power and Biomass to Liquid process (PBtL), the carbon efficiency can be increased relative to the BtL process. It was shown in previous studies that the PBtL concept has an economic edge over BtL when cheap electricity is available to maximize the fuel yield. In this study, a techno-economic analysis is conducted for a hybrid process concept which can switch operation modes from electrolysis enhanced to only biomass conversion. In case studies the effect of the Fischer-Tropsch conversion, H<sub>2</sub>/CO ratio of the Fischer-Tropsch feed and the biomass feed rate in the electrolysis enhanced mode are analyzed. Every process configuration is modeled based on experimentally validated unit models from literature in the commercial software Aspen Plus and analyzed using DLR's software tool TEPET. For a 200 MW<sub>th</sub> biomass input plant, production costs of 1.08 €<sub>2019</sub>/L for the hybrid concept with a carbon efficiency of 53.3% compared to 0.66 €<sub>2019</sub>/L for BtL with 35.4% and 1 €<sub>2019</sub>/L for PBtL with 61.1% were found based on the Finnish day-ahead market for the base case. The net production cost for the hybrid concept can be decreased by 0.07 €<sub>2019</sub>/L when a Fischer-Tropsch H<sub>2</sub>/CO ratio of 1.6 instead of 2.05 is used.

**Keywords:** power and biomass to liquid, biomass to liquid, fischer-tropsch, techno-economic analysis, alternative fuel process, dynamic process operation

## INTRODUCTION

With the European Green Deal, the European Union (EU) aspires to become carbon neutral by 2050. To that end, the share of renewable fluctuating electricity production is aimed to be ramped up from 32% today to 65% by 2030 (European Commission, 2020). This poses a challenge to the existing energy system, as short-term and seasonal mismatches of energy supply and demand have to be addressed. Various energy scenarios show that only a combination of measures, involving energy storage and flexible demand, enable an efficient energy transition (Mathiesen et al., 2015; Papaefthymiou and Dragoon, 2016; Blanco and Faaij, 2018; Kotzur et al., 2018).



The increasing share of renewables on the energy market has displaced already installed infrastructure. Especially, in Northern Europe the combined heat and power (CHP) plant infrastructure is under financial pressure competing on the power market (Helin et al., 2018). As a result, district heating is prioritized over the combined heat and electricity production. Thus, a solution for the continued operation of biomass fired CHP plants is needed to avoid idling existing infrastructure.

At the same time, the EU aims to reduce the carbon emissions from the transport sector. Here, the electrification of light-duty vehicles is only one step. Heavy-duty transportation, especially aviation and shipping, will continue to rely on liquid fuels for their higher energy density. Therefore, the European commission states that the technology development and deployment for renewable, low-carbon fuels has to be achieved by 2030 (European Commission, 2020).

The process concept proposed in the EU-project FLEXCHX offers a solution for the three fields of the energy transition: The fuel process converts biomass to liquid hydrocarbons via the Fischer-Tropsch (FT) route. Whenever cheap renewable electricity is available from the grid, an electrolysis unit is operated to enhance the fuel yield. In an adjacent CHP plant the process off-heat is used to generate district heating and electrical power (Kurkela et al., 2020). The two operation modes are shown in **Figure 1**.

The conversion of biomass to liquid fuels has been widely discussed in literature under the acronym BtL. The term includes all conversion routes, i.e. methanol, ethanol or DME (Olofsson et al., 2005). Yet, here it is only used to refer to the FT route. In a review of 15 different techno-economic BtL studies, Haarlemmer et al. found the realistic production cost range to be 1–4 €<sub>2011</sub>/L for a 400 MW<sub>th</sub> biomass input plant (Haarlemmer et al., 2012). The BtL process is continuously approaching a higher technological maturity. Successful demo plants (Ail and Dasappa, 2016) are waiting for market entry, until sustainable fuels get promoted for commercial implementation.

Processes with the addition of electrolytic hydrogen to a BtL plant are referred to as power biomass to liquid (PBtL) (Albrecht

et al., 2017). Hillestad et al. show that production costs for a PBtL process can be lower compared to a BtL plant of the same biomass input of 435 MW<sub>th</sub>, if electricity is available for less than 100 \$<sub>2018</sub>/MWh (Hillestad et al., 2018). A similar result was found by Albrecht et al. (Albrecht et al., 2017). Here, the PBtL concept has lower production costs at electricity prices below 70 €<sub>2018</sub>/MWh when comparing two plants with the product capacity of 240 kt/year. Further, both studies point out that the carbon efficiency for the PBtL is significantly higher than for BtL. Therefore, a smaller amount of the finite biomass feedstock has to be consumed per amount of fuel. Hannula and Reiner argue that not only biomass supply will be a limiting factor but also the availability of renewable power (Hannula and Reiner, 2019). Thus, PBtL might offer a middle way between feeding only biomass with BtL or relying solely on electrical energy with process concepts such as carbon capture and utilization (CCU).

Process concepts with flexible electricity sourcing have also gained attention in literature. Müller et al. show that it is experimentally possible to integrate H<sub>2</sub> from a wind park profile into an FT-BtL process (Müller et al., 2018). To attain a constant H<sub>2</sub>/CO ratio at the FT input, the gasification train is continuously controlled responding to the electrolyzer H<sub>2</sub> profile. Sigurjonsson and Clausen analyze a system that switches operation modes. Here, a system composed of a gasifier, an SOEC/SOFC unit and a methane reactor is simulated (Sigurjonsson and Clausen, 2018). Depending on the electricity price, the process is either used to produce synthetic natural gas (SNG) or electricity and heat. A techno-economic analysis shows that the hybrid system can be operated more economically than a stand-alone SNG plant, especially if electricity prices are highly volatile. For the same system Butera et al. show an energy efficiency of 70.5% in the SNG mode and 37.5% in the electricity mode (Butera et al., 2020).

Hybrid processes have higher investment costs than steady-state processes because part of the equipment is inactive or only used in part-load. The advantage of a hybrid system lies in the lower operation costs. The PBtL concept can produce fuel at



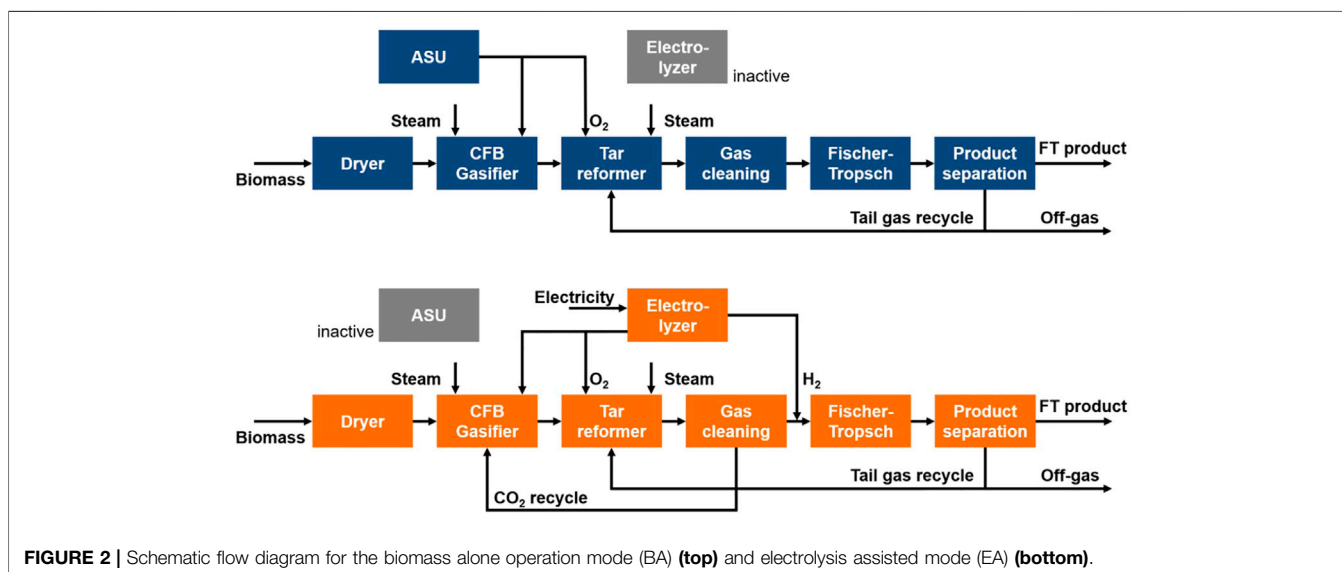


**FIGURE 2 |** Schematic flow diagram for the biomass alone operation mode (BA) (top) and electrolysis assisted mode (EA) (bottom).

lower cost and with lower biomass consumption compared to BtL, if inexpensive electricity is available (Albrecht et al., 2017; Hillestad et al., 2018). In a market with fluctuating energy prices, a cost advantage for the hybrid system can be gained by avoiding high electricity prices with the temporary shut-down of the electrolyzer. To understand the trade-off between higher investment and lower operation costs, this study estimates the conversion efficiency and production cost for the presented hybrid process concept in comparison to the BtL and the PBtL concept. The evaluation is based on the electricity price profile on the Finnish day-ahead market for the reference year 2019. Further, the techno-economic impact of key process parameters, H<sub>2</sub>/CO ratio at the FT inlet, FT reactant conversion and biomass feed rate in the electrolysis assisted mode, are studied. To evaluate a broader set of energy market conditions, a sensitivity analysis over the electricity price and the share of operation hours in each mode is conducted.

## PROCESS CONCEPT

The concept studied here describes a process operated in two modes: In the biomass alone mode (BA), biomass is converted to fuel via the FT synthesis. In the electrolysis assisted mode (EA), hydrogen is produced by a grid-connected electrolyzer, which is used to enhance the fuel output of the process. For both modes, off-heat is converted to electricity and district heating in a CHP plant. A schematic flow diagram of the two operation modes is depicted in **Figure 2**. The operation concept is based on the EU project FLEXCHX (Kurkela et al., 2020).

### Biomass Alone Operation Mode

The biomass alone mode is depicted in a schematic flow diagram in **Figure 2**. In a first step, the biomass moisture content is reduced in the dryer. With the addition of oxygen and steam, the dry biomass is then converted to raw syngas in a circulating

fluidized bed (CFB) gasifier. Besides hydrogen and carbon monoxide the syngas also contains carbon dioxide, steam, tars, ash and other trace components like ammonia or hydrogen sulfide. Components poisoning the FT catalyst have to be removed. The auto-thermal tar reformer reduces the tar content while simultaneously increasing the H<sub>2</sub>/CO ratio of the syngas. Oxygen for gasifier and reformer is produced in a cryogenic air separation unit (ASU).

In the gas cleaning section water, CO<sub>2</sub> and trace components are removed from the syngas. The clean syngas then reacts over the FT catalyst to hydrocarbon chains. Here, hydrocarbon chains with a chain length higher than five are considered product and are separated from the shorter hydrocarbons. Further upgrading steps such as cracking of longer chains is not considered in this study. The separated tail gas consisting of short hydrocarbons and unconverted syngas is partly recycled to the reformer. The remaining tail gas leaves the process and is burned. The energy content of the off-gas is used in the CHP.

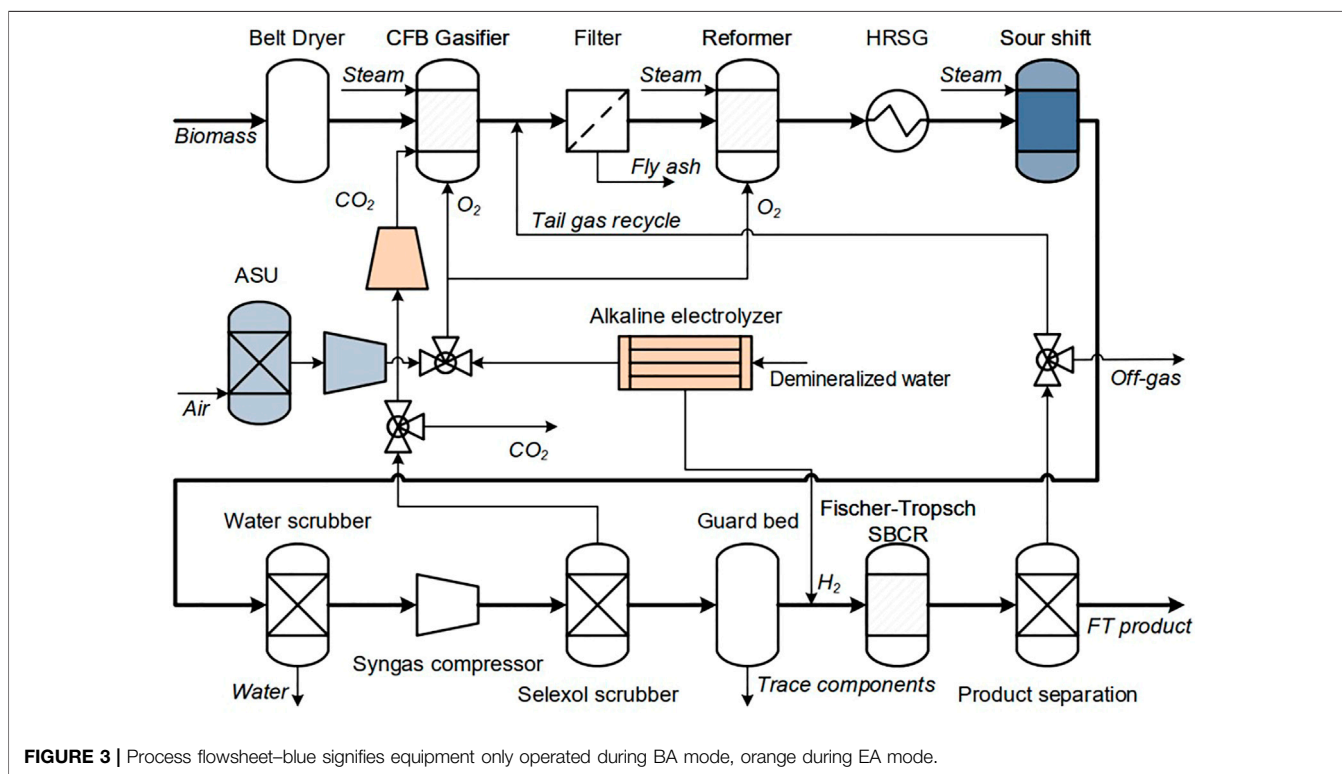
### Electrolysis Assisted Operation Mode

In contrast to the BA mode, the electrolysis assisted mode features a CO<sub>2</sub> recycle. As can be seen in **Figure 2**, CO<sub>2</sub> from the gas cleaning section is reintroduced into the gasifier. This leads to a higher carbon efficiency. However, it also lowers the H<sub>2</sub>/CO ratio in the FT feed. To reach the stoichiometric H<sub>2</sub>/CO ratio of ~2, hydrogen from an electrolyzer is added. In addition, the oxygen produced in the electrolyzer can be used in gasifier and reformer.

Overall, the EA mode requires less biomass feedstock to produce an equal amount of FT product compared to the BA mode. Yet, the higher biomass conversion has to be weighed against the additional cost for the electrolysis power demand.

### Process Flowsheet

The flowsheet for the FLEXCHX process concept is depicted in **Figure 3**. It contains the equipment for BA and EA mode. In addition, equipment types selected for this study are highlighted.



A CFB gasifier is used to convert the dried biomass into syngas. This gasifier type is suitable for the FLEXHCX operation strategy because of its high load flexibility. Warnecke reports an operation range of 50%–120% relative to standard load for a CFB gasifier (Warnecke, 2000). Moreover, CFB gasifiers feature a high carbon efficiency (Warnecke, 2000; Molino et al., 2016). The steam/oxygen gasification is selected here for its higher carbon efficiency compared to steam gasification (Hannula, 2016). Fly ash produced in the gasifier is removed from the syngas in a hot gas filtration unit. The gasification pressure of 4 bar and temperature of 900°C are selected based on experimental results (Kurkela et al., 2014), which show that under these conditions high carbon efficiency is achieved and the calcium-based bed material catalyzes initial tar decomposition and helps to avoid filter blinding by soot and heavy tars.

The catalytic tar reformer not only lowers the tar content but also the hydrocarbon gas content produced in gasifier and FT reactor. With the addition of oxygen, both component types undergo an autothermal reformation reaction (Shen and Yoshikawa, 2013). An alternative technology to tar reforming is organic solvent scrubbing. With it, only tar components are removed from the syngas. It can therefore be argued that for fuel processes the catalytic tar reformation is a more suitable technology due to the significantly higher yields of CO and H<sub>2</sub> attained by the hydrocarbon gas reformation (Hannula, 2016; Kurkela et al., 2020).

A cryogenic ASU is used for the oxygen production for gasifier and reformer. This production method is reported to be the most economical option for large scale oxygen production (Smith and Klosek, 2001; Hillestad et al., 2018). In the EA mode the oxygen is mainly produced in the electrolyzer. Only in cases where the

electrolytic oxygen does not suffice, the remaining oxygen is produced in the ASU. The pure oxygen feeding instead of air is chosen in this study because it allows for higher syngas recycle ratios. This leads to a higher product output and lower production costs as shown for a BtL process in (Ostadi and Hillestad, 2017).

To adjust the syngas H<sub>2</sub>/CO up to a stoichiometric ratio of ~2 (Hillestad et al., 2018), a sour shift reactor is used. For that the gas is firstly cooled in the heat recovery steam generation system (HRSG). Then, the syngas reacts in the sour shift reactor according to the water gas shift equilibrium (Unde, 2012):



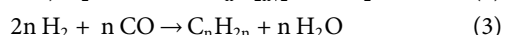
The addition of steam in the shift reactor entails the reaction of CO to CO<sub>2</sub>, which decreases the overall carbon efficiency of the process. To avoid the additional formation of CO<sub>2</sub> in the EA mode the sour shift reactor can be bypassed. In this mode the H<sub>2</sub>/CO is adjusted by adding hydrogen from the electrolyzer.

The gas cleaning train consists of a water scrubber, syngas compression, Selexol scrubber and a guard bed (Hannula, 2016). As the FT pressure level typically is higher than the gasification pressure, a compressor is required for the process. A higher FT pressure level is associated with higher catalyst productivity (Van Der Laan and Beenackers, 1999). Further, a Selexol scrubber is chosen for its economic and energy efficiency advantages compared to other physical absorption methods (Padurean et al., 2012). As the FT catalyst is sensitive to impurities, a guard bed is required to lower their concentration in the syngas feed (Kurkela et al., 2020).

**TABLE 1** | Properties of biomass feedstock (Hannula, 2016).

Proximate analysis, wt% dry basis	
Fixed carbon	25.3
Volatile matter	70.8
Ash	3.9
Ultimate analysis, wt% dry basis	
Ash	3.9
C	53.2
H	5.5
N	0.3
Cl	0
S	0.04
O (difference)	37.06
Other properties	
HHV, MJ/kg	20.67
Initial moisture content, wt%	50

The FT reaction can be characterized as a polymerization reaction. The reactants  $H_2$  and  $CO$  form hydrocarbon molecules of different chain lengths. The production of paraffines and olefins can be described with the chemical reactions in Eqs 2, 3 (Van Der Laan and Beenackers, 1999).



Although a multitude of reactor types have been presented in the past, the most notable designs are the slurry bubble column reactor and the fixed bed reactor (Ail and Dasappa, 2016). Both reactor types are of high technical maturity as they are utilized in large scale Gas-to-Liquid plants (Hillestad et al., 2018). Recently, the FT microchannel reactor design has gained some attention (LeViness et al., 2014; Piermartini et al., 2017). Although arguments can be made for all of the aforementioned reactor designs, in this study a slurry bubble column is modeled. The advantages of this reactor type are low capital cost for large plant sizes and a high thermal stability (LeViness, 2013).

At the outlet hydrocarbon products  $C_{5+}$  are separated from water and tail gas. Tail gas, consisting of short chained hydrocarbon gases  $C_{1-4}$  as well as unconverted syngas, is partly recycled to the filter unit.

In this study the alkaline electrolysis AEL technology is chosen for the production of hydrogen and oxygen in the EA mode. Compared to other technologies, specifically proton exchange membrane electrolysis (PEMEL) and solid oxide electrolysis (SOEL), AEL is the most mature technology with the lowest investment costs (Schmidt et al., 2017). The SOEL technology features the highest system efficiency, up to 81%<sub>LHV</sub> compared to 60%<sub>LHV</sub> for AEL and 60%<sub>LHV</sub> PEM (Buttler and Spliethoff, 2018). However, an SOEL is not suitable for intermittent operation. Thermal stress during start-up and shut-down are detrimental to stack lifetime (Buttler and Spliethoff, 2018). The PEMEL might become a more suitable technology for the proposed process in the future as investment costs are predicted to decrease and system efficiency to increase (Schmidt et al., 2017).

**TABLE 2** | Gasifier yield model (Kurkela et al., 2014).

Biomass	Conversion [%]	Selectivity [%]	Product
Nitrogen	98	12.8	$N_2$
		86.7	$NH_3$
		0.5	HCN
Sulfur	100	98	$H_2S$
		2	COS
Carbon	2	100	Fly ash
		0	Bottom ash
Ash	100	1	Fly ash
		99	Bottom ash

## Comparison Cases BtL and PBtL

To give reference points, a BtL and PBtL process are simulated and techno-economically evaluated. Both processes rely on the same equipment and flowsheet layout as the hybrid concept. The hybrid plant requires additional investment costs compared to BtL and PBtL. This is due to units that are only active in one mode and over-dimensioned units.

The BtL plant is comprised of all units operated in the BA mode, i.e. no electrolyzer and  $CO_2$  compressor are needed for this process. For the PBtL, on the other hand, only equipment types that are used in the EA mode are required. Therefore, ASU and sour shift reactor are excluded.

One hybrid operation mode defines the equipment size. If e.g. the syngas stream in the EA mode is larger than in the BA mode, a larger water scrubber is needed for the EA mode. Therefore, the water scrubber is over-dimensioned for the BA mode. For the comparison cases, BtL and PBtL, no equipment has to be over-dimensioned.

## PROCESS MODELING AND SIMULATION

The process was simulated using the commercial software Aspen Plus (V10). The Soave-Redlich-Kwong equation of state is chosen (Hannula, 2016). This method is recommended for hydrocarbon processes (Aspen Technology Inc., 2013). All unit operation models are based on experimentally validated literature models.

### Biomass and Dryer

The biomass properties are taken from Hannula et al. (Hannula, 2016) and displayed in Table 1. Here, forest residue chips are considered as feedstock. Forest residue is composed of bark, needles and stem wood from harvesting and industrial wood residues (Hannula, 2016). Annually 40 Mt forest residue are estimated to be available in the EU (Searle and Malins, 2013). In Aspen Plus biomass is defined as a non-conventional component with a higher heating value (HHV) of 20.67 MJ/kg based on dry matter.

The initial moisture content of 50 wt% is reduced in a belt dryer to 12 wt%. For the dryer an electrical power consumption of 32 kWh/t based on dry feedstock mass and a heat demand of 1,300 kWh/t based on the evaporated water mass is assumed (Hannula, 2016).

## Gasification and Air Separation Unit

The CFB gasifier is modeled as a combination of an RYield reactor and an RGibbs reactor (Hannula and Kurkela, 2010). The yield for the first reactor at an operation point of 4 bar and 900°C is displayed in **Table 2**. Conversion and selectivity values for the biomass components are taken from the experimental results published in (Kurkela et al., 2014). Here, unconverted biomass nitrogen is passed to fly ash.

The yield for the carbon species formed during gasification can be taken from the **Supplementary Material**. Here, benzene and naphthalene are modeled for the larger variety of tar species. The modeled tar yield amounts to a molar concentration of 0.3% in the gasifier output. The remaining carbon, hydrogen and oxygen atoms react according to the water gas shift equilibrium in the RGibbs reactor.

The gasifier is assumed to have a heat loss of 1% of the dry biomass input LHV (Hannula, 2016). To fulfill this constraint, the oxygen feed rate is iterated. Further, the steam to oxygen feed mass ratio, or the steam to oxygen and CO<sub>2</sub> ratio in the EA mode, is fixed to 1.3. CO<sub>2</sub> is recycled to the gasifier in such a way that the mass ratio of CO<sub>2</sub> to steam and CO<sub>2</sub> is equal to 65%<sub>wt.</sub>

Gasification ash is completely removed from the syngas. Bottom ash can be removed from the gasifier directly. For fly ash the filter unit is required. At a high syngas temperature filter blinding may occur due to the soot formation tendency of the tar components (Hannula, 2016). To avoid this, the raw gas temperature is lowered to 600°C before filtration (Kurkela et al., 1993). This is partly accomplished by adding the cooler tail gas recycle stream.

The ASU is assumed to have an energy demand of 1 MW<sub>e</sub>/(kg/s) with an output pressure of 1 bar (Clausen et al., 2010). The oxygen purity is assumed to be 100% for the simulation. This is a reasonable assumption given the reported oxygen purity of >99 mol% (Smith and Klosek, 2001; Clausen et al., 2010). Subsequently, ASU oxygen is compressed to the gasification pressure of 4 bar by an 80% isentropic efficiency one-stage compressor.

## Tar Reforming and Sour Shift

The tar reformer is modeled as an adiabatic RGibbs reactor with an operation temperature of 900°C. In the autothermal reformer oxygen is added to attain this temperature level. The steam to oxygen feed mass ratio is set to 1 (Hannula, 2016). All input components C<sub>2+</sub> and tars are simulated to reach chemical equilibrium (Hannula, 2016). Only for the components CH<sub>4</sub>, NH<sub>3</sub> and HCN a conversion limit of 80% is assumed.

In the subsequent sour-shift reactor steam at 4 bar is added to attain a defined H<sub>2</sub>/CO ratio in the syngas. It is modeled as an REquil reactor in which only the water gas shift reaction is taking place (cf. Eq. 1). To avoid catalyst deactivation steam is added to reach a molar steam/CO input ratio of 1.8. The output temperature for the adiabatic reactor is also limited by the catalyst to 404°C (Hannula, 2016). To meet this constraint the outlet temperature in the HRSG is iterated. Further, the sour shift reactor has a by-pass stream. The amount of bypassed syngas is iterated to attain the defined H<sub>2</sub>/CO ratio (Hannula, 2016). In the EA mode the sour shift reactor is bypassed entirely.

## Gas Cleaning

The water scrubber is modeled as two flash units with an outlet temperature of 60°C for the first and 30°C for the second stage. The syngas is cooled to 200°C at the scrubber inlet by the HRSG system in both modes (Hannula, 2016).

The subsequent syngas compression is modeled as a five-stage compressor with equal pressure ratio and intercooling to 80°C (Hannula, 2016). The outlet pressure is 25 bar as defined by the upper limit of the used FT model. The isentropic efficiency is assumed as 80% for every stage.

For a 90% CO<sub>2</sub> removal rate the energy consumption for the Selexol process is assumed to be 74 kJ/kg<sub>CO<sub>2</sub>,removed</sub> (Hamelinck and Faaij, 2006; Albrecht and Dietrich, 2018). The pressure in the desorption column is set to 1 bar. Therefore, a re-compression of CO<sub>2</sub> to the gasification level of 4 bar is modeled with a one-stage compression with an isentropic efficiency of 80%.

As the reduction of H<sub>2</sub>S to an acceptable level for the FT reactor, below 10 ppb (Hillestad et al., 2018), cannot be accomplished with the Selexol scrubber alone, a ZnO adsorption bed is needed at the end of the gas cleaning train. For that a separator block removing all trace components is simulated.

## Electrolyzer

The AEL unit is modeled as a splitter with a system energy demand of five kWh/Nm<sup>3</sup>, which amounts to a system efficiency of 70.8%<sub>HHV</sub> (Buttler and Spliethoff, 2018). The demineralized water input is assumed to be split into pure oxygen and hydrogen streams at 25 bar and 60°C. The hydrogen is introduced into the syngas stream prior to the FT reactor where the gas mixture is heated to reaction temperature of 230°C. The oxygen stream is used in gasifier and reformer. The power input is calculated such that a defined H<sub>2</sub>/CO is reached in the FT feed.

## Fischer-Tropsch

In this study, the kinetic reaction model proposed in Todic et al. (Todic et al., 2013) is used to describe the FT reaction in a slurry bubble column reactor over a Co.-Re/Al<sub>2</sub>O<sub>3</sub> catalyst. The model is based on the carbide mechanism and fitted to experimental data for a temperature range of 478–503 K, a pressure range of 15–25 bar, an H<sub>2</sub>/CO ratio in the range of 1.4–2.1 and a weight hourly space velocity (WHSV) in the range of 1–22.5 NI/(g<sub>cat</sub> h).

The model describes the production rate of n-paraffins and 1-olefins up to a carbon length of 30 as a differential-algebraic system of equations. The system has six input variables reactor temperature, pressure and total molar feed rate as well as the partial pressure of H<sub>2</sub>, CO and H<sub>2</sub>O at the reactor output and one design parameter, catalyst loading. Further, the kinetic reaction model assumes that the slurry bubble column reactor can be idealized as a continuously stirred tank reactor (CSTR) (Todic et al., 2013). In Aspen Plus the FT reactor is represented by an RCSTR block. The reaction rate functions are listed in Eqs 4–7. For each product molecule a reaction rate is determined based on its respective growth probability  $\alpha$  and the fraction of vacant catalyst sites [S], which in turn is a function of all growth probabilities  $\alpha$  in the model. Due to its complexity the reaction model is implemented in a FORTRAN user kinetic

subroutine. The code can be found in the **Supplementary Material**.

$$R_{CH_4} = k_{5M} K_7^{0.5} p_{H_2}^{1.5} \alpha_1 [S] \quad (4)$$

$$R_{C_2H_4} = k_{6E,0} e^{2c} \sqrt{K_7 p_{H_2}} \alpha_1 \alpha_2 [S] \quad (5)$$

$$R_{C_nH_{2n+2}} = k_5 K_7^{0.5} p_{H_2}^{1.5} \alpha_1 \alpha_2 \prod_{i=3}^n \alpha_i [S] \quad n \geq 2 \quad (6)$$

$$R_{C_nH_{2n}} = k_{6,0} e^{cn} \sqrt{K_7 p_{H_2}} \alpha_1 \alpha_2 \prod_{i=3}^n \alpha_i [S] \quad n \geq 2 \quad (7)$$

In this study, the operation conditions for the FT reactor are set to 230°C and 25 bar. Higher pressure level has been shown to increase the selectivity and reaction rate for the FT Co. catalyst (Van Der Laan and Beenackers, 1999; Todic et al., 2014). The upper temperature limit was selected as the operation point because the catalyst activity increases with temperature (Todic et al., 2014).

To avoid a large recycle stream the FT reactor should be designed to maximize the CO conversion and the product selectivity  $C_{5+}$  i.e. the selectivity for hydrocarbons with a chain length higher than 4. Given the reactor's operation conditions, the gas hourly space velocity (GHSV) can be adjusted to maximize product output. Lowering the GHSV leads to an increased CO conversion and product selectivity (Schanke et al., 2001). However, the product selectivity drops sharply when surpassing a certain threshold. Commonly, this limit can be found at 75%–80% CO conversion for an SBCR (Rytter and Holmen, 2015). In this conversion range, the increased water-gas-shift activity leads to catalyst oxidation and consequently to its deactivation (Rytter and Holmen, 2015).

For the reactor simulation the  $H_2$  conversion is set to a value as defined in the case studies cf. *Process Analysis*. This is achieved by iterating the catalyst mass in the reactor and thereby the GHSV.

Since the FT reactor is operated in two modes, BA and EA, one requires a lower catalyst mass. It is therefore assumed that the reactor consists of two modules, of which one can be by-passed. For the cost analysis the larger catalyst mass is considered.

## Product Separation and Syngas Recycle

An idealized complete separation is assumed for the reaction water, tail gas and product  $C_{5+}$ . Part of the longer hydrocarbon products accumulate in the FT slurry and have to be removed by a filter unit (Schweitzer and Vigié, 2009). However, this filtration process is not included in the simulation. For the economic analysis an auxiliary flash unit is simulated at 5°C to gauge the necessary flash volume. The  $C_{5+}$  fraction is viewed as the main product of the process. Any additional processing steps are assumed to be carried out in a central processing facility.

To increase the process carbon efficiency, tail gas containing hydrocarbon gases  $C_{1-4}$  and the unconverted syngas is recycled to the reformer. A recycle rate of 95% of the total tail gas is modeled here. Various studies point out that to avoid the accumulation of inert gas content the recycle ratio has to be below 100% (Albrecht et al., 2017; Hillestad et al., 2018). As a reference, the recycle ratio is set to 93% for the BtL process in the study by Hillestad et al. For PBtL the recycle ratio is kept in a range of 98.5%–91.8%

depending on the process design (Hillestad et al., 2018). Since only small amounts of nitrogen are produced in the gasifier and the 90%  $CO_2$  removal is sufficient to avoid  $CO_2$  accumulation, the 95% recycle assumption can be justified here.

## Combined Heat and Power Plant

The CHP plant is modeled as a steam cycle fed by the process off-heat. In addition, the heat from burning FT off-gas, which is not recycled, is counted as a source for the CHP plant. It is assumed that 90% of the off-gas's LHV can be recovered. The electrical efficiency for the CHP system is set to 40% relative to its heat input (Wang et al., 2019). The remaining energy is converted to district heating. Surplus electrical power is fed to the grid.

## PROCESS ANALYSIS

### Definition Of Case Studies

**Table 3** shows the parameters varied for every simulation case. In this study the effect of  $H_2$  conversion in the FT reactor,  $H_2/CO$  ratio in the FT feed and the biomass feed rate for EA mode on the process performance and economics is gauged. In the base case (1.1) the FT reactor is modeled with a conservative  $H_2$  conversion of 70% at the stoichiometric  $H_2/CO$  ratio of 2.05 (Hillestad et al., 2018). BA and EA have an equal biomass feed of 200  $MW_{th}$ .

Lowering the  $H_2/CO$  ratio to 1.6 has several positive effects on the process. Firstly, a lower  $H_2/CO$  is associated with a higher product selectivity (Van Der Laan and Beenackers, 1999; Todic et al., 2014). Secondly, in the EA mode less hydrogen is needed to reach the  $H_2/CO$  ratio. Thereby, lower costs for electricity and the electrolyzer can be expected. Thirdly, in the BA mode less CO has to be converted to  $CO_2$  in the water gas shift reactor to reach the higher  $H_2/CO$  ratio. Consequently, the process will have a higher carbon efficiency.

The conversion limit for the FT reactor is lower for operation points with an under-stoichiometric  $H_2/CO$  ratio (Lillebø et al., 2017). Yet, to the author's knowledge no study quantifies the impact of  $H_2/CO$  ratio on the conversion limit. To account for this, the  $H_2$  conversion is simulated at 55% and 70% for both  $H_2/CO$  ratios. Here, the  $H_2$  conversion is used instead of the commonly used CO conversion to make cases with different  $H_2/CO$  ratios more comparable. In **Table 3** all odd cases have a conversion of 70%.

Feeding 100 MW instead of 200 MW biomass in the EA mode is advantageous in two aspects: For the smaller syngas stream less hydrogen is needed to attain the defined  $H_2/CO$  ratio. Therefore, the electrolyzer, which is not operated for a part of the year, can be designed with a lower capacity. On the other hand, the plant is over dimensioned for the EA mode. All cases with 100  $MW_{th}$  biomass input are listed under case 2.1–2.4 in **Table 3**.

### Definition Of Efficiencies

Three performance indicators are used to evaluate the simulated process performance: carbon efficiency  $\eta_C$ , fuel efficiency and process efficiency (Albrecht et al., 2017).

Carbon efficiency  $\eta_C$ , as defined in **Eq. 8**, can be interpreted as the fraction of carbon molecules in the biomass that is converted to FT product.

$$\eta_C = \frac{\dot{n}_{C,Prod.}}{\dot{n}_{C,Biom.}} \tag{8}$$

The energetic fuel efficiency is stated in Eq. 9. It describes the ratio of chemical energy in the product based on its lower heating value (LHV) to the input energy streams. Here, the input is regarded as the energy content of the biomass feed and the electrolysis power input  $P_{AEL}$ .

$$\eta_{Fuel} = \frac{\dot{m}_{Prod.} LHV_{Prod.}}{\dot{m}_{Biom.} LHV_{Biom.} + P_{AEL}} \tag{9}$$

The energetic plant efficiency (Eq. 10) also takes the by-products heat and electricity into account.

$$\eta_{process} = \frac{\dot{m}_{Prod.} LHV_{Prod.} + P_{Elec.out} + \dot{Q}_{distr.}}{\dot{m}_{Biom.} LHV_{Biom.} + P_{AEL}} \tag{10}$$

### Economic Analysis

The economic analysis is conducted with the DLR software tool TEPET. The tool retrieves stream and unit dimension data from Aspen Plus. By linking the modelled units with according cost data within the TEPET database, a transparent cost estimation can be obtained. The calculation method is described in depth by Albrecht et al. (Albrecht et al., 2017) and has been extended to allow the estimation of a flexible process operation. All applied estimation parameters are detailed in the **Supplementary Material**.

In this study investment costs are updated using the Chemical Engineering Place Cost Index (CEPCI) for the year 2019 taken from (Jenkins, 2020). The plant lifetime is assumed to be 20 years with 8,100 full load hours to be divided between the two modes. For the timespan the interest rate is fixed to 7% (Albrecht et al., 2017). The number of total employee hours is estimated according to the heuristic outlined in (Peters et al., 1968) as 39,200 h/a with labor costs of 43.83 €/h (Krebs, 2015).

The investment cost  $E$  for the process equipment is estimated according to Eq. 11. Here, the equipment size  $S$  is set into relation with a reference unit of size  $S_{ref}$  and equipment cost  $E_{ref}$ . To account for the economy-of-scale effect, a cost degression exponent  $k$  is considered (Albrecht et al., 2017). All investment cost assumptions can be found in the **Supplementary Material**.

$$E = E_{ref} \left( \frac{S}{S_{ref}} \right)^k \tag{11}$$

The net production costs (NPC) are calculated according to Eq. 12 from the capital expense CAPEX and the operational expense OPEX. The NPC are stated as €/l. To that end, the costs have to be divided by the production rate and the product density  $\rho_{Prod}$ , which is assumed to be 0.729 kg/L for FT product (Albrecht et al., 2017). The CAPEX for the process is found by adding cost factors to the equipment costs obtained from Eq. 11 yielding the fixed capital investment costs FCI. That way, indirect capital expenses such as the installation cost for the units is included. Besides the utility and labor costs, the OPEX also entail indirect operational expenses. Cost items, such as administrative cost, are considered in this category. The corresponding estimation method for indirect operation and capital expenses can be found in the **Supplementary Material**.

**TABLE 3 |** Case definition for the simulation.

Case	1.1 (base)	1.2	1.3	1.4	2.1	2.2	2.3	2.4
H <sub>2</sub> conversion [%]	70	55	70	55	70	55	70	55
H <sub>2</sub> /CO [-]	2.05	2.05	1.6	1.6	2.05	2.05	1.6	1.6
Biomass feed rate	200	200	200	200	200	200	200	200
BA [MW <sub>th</sub> ]								
Biomass feed rate	200	200	200	200	100	100	100	100
EA [MW <sub>th</sub> ]								

$$NPC \left[ \frac{\text{€}}{\text{l}} \right] = \frac{CAPEX + OPEX}{\dot{m}_{Prod} \rho_{Prod}^{-1}} \tag{12}$$

All utility prices are listed in Table 4. Further, the electricity prices for the year 2019 are taken from the day-ahead market provided by Nord Pool AS (Nord Pool AS, 2021). The Finnish electricity tax of 0.5 €/MWh (class II) and the electricity price of 8.84 €/MWh in winter months (Dec.–Feb.) and 12.3 €/MWh for the rest of the year are added to the electricity price ((HSV, 2021; Verohallinto, 2021) as cited in (Helen, 2021)). The resulting price profile can be found in the **Supplementary Material**. The yearly average price amounts to 55.49 €/MWh.

### Economic Analysis of the Hybrid Process

For the hybrid capital expense estimation, the characteristic size  $S$  (cf. Eq. 11) is defined by the mode with the larger equipment. For the mode with the smaller characteristic size, part load operation is assumed. For example, the gasifier in case 2.1 has twice the capacity in BA compared to EA mode. The gasifier investment costs for both modes are defined by the BA mode. In the EA mode the gasifier is operated on part load as an over-dimensioned unit.

The operation costs are defined by each mode independently. Therefore, net production costs (NPC) can be calculated assuming that one mode is active for all 8,100 h. This is subsequently denoted as  $NPC_{BA/EA}$ . The  $NPC_{hy}$  for the hybrid operation of both modes follows from Eq. 13. Here,  $cf_{BA}$  and  $cf_{EA}$  stand for the capacity factors in BA and EA mode, i.e. the share of all 8,100 h spent in each mode.

$$NPC_{hy} = cf_{BA} NPC_{BA} + cf_{EA} NPC_{EA} \tag{13}$$

To calculate the hours spent in BA and EA mode according to the electricity price profile on the Finnish day-ahead market, the electricity price for which BA and EA mode have the same NPC has to be found. Days with electricity prices below this threshold are operated in EA, above in BA mode. For further calculations, the average electricity price in BA and EA mode operation have to be determined. It is assumed that the hours the plant is not operated do not affect these average electricity costs.

### Economic Analysis of the Reference Processes

The cases defined in Table 3 are also applicable to the BtL and the PBtL concept. To keep the cases comparable, all cases are analyzed with a biomass input of 200 MW<sub>th</sub>. For the

**TABLE 4** | Utility prices.

Utility	Prices	Source
Wet biomass	42.232 €/t	Hannula, (2016)
Electricity selling price	50.4 €/MWh	Hannula, (2016)
Demineralized water for electrolysis	2 €/m <sup>3</sup>	Albrecht and Dietrich, (2018)
Fresh water	0.434 €/m <sup>3</sup>	Kempegowda et al. (2015)
District heating	40 €/MWh	Hannula, (2016)
FT catalyst <sup>a</sup>	33 €/kg	Swanson et al. (2010)
Selexol <sup>b</sup>	4.346 €/kg	Albrecht et al. (2017)
Waste water	0.907 €/m <sup>3</sup>	Peters et al. (1968)

<sup>a</sup>Catalyst replacement rate 0.5%/day (Bechtel, 1998).

<sup>b</sup>Selexol makeup 0.00018 kg<sub>makeup</sub>/kmol<sub>syngas</sub> (Albrecht et al., 2017).

analysis the same flowsheets are used. Therefore, no difference in terms of carbon, fuel or process efficiency can be found and thus also in direct operation costs. Only the investment costs will differ for BtL and the BA mode for the same case, because the BtL process does not require an electrolyzer and a CO<sub>2</sub> compressor. Also, certain equipment types are over-dimensioned for the BA mode since the EA mode requires the larger equipment size. Here, the BtL process also has lower investment costs.

Correspondingly, the PBtL will require lower investment costs compared to the EA mode. Sour shift reactor and ASU are not included. This extends to cases where the oxygen from the electrolyzer not sufficient. For the small oxygen stream only the energy demand for its production is included in the calculation.

### Sensitivity Analysis

The aim of this study is to analyze a hybrid process over a broad range of operation conditions. To that end, a sensitivity study over the electricity price and the capacity factor of each mode is conducted. Here, only the electricity price for the energy input is varied. Further, to provide a reference point to BtL, the electricity price for which the hybrid concept and the BtL process have equal NPC is calculated.

The production costs are estimated for a specific set of economic parameters which may change in the future. To account for this possible change, a sensitivity analysis is conducted for the largest cost contributors biomass price, electrolyzer investment cost and investment costs for the BtL plant.

The investment costs for the BtL plant entail all equipment except the electrolyzer and CO<sub>2</sub> recycle. Haarlemmer et al. find investment costs in the range of 300–1200 M€<sub>2011</sub> for 400 MW BtL plants (Haarlemmer et al., 2012). To assess what BtL plant investment costs mean for the hybrid process NPC, they are increased by + 100%.

The biomass cost contributes substantially to the overall NPC in the BtL and PBtL concept (Hillestad et al., 2018). Haarlemmer et al. report biomass prices in the range of 7.2–37.08 €<sub>2011</sub>/MWh (Haarlemmer et al., 2012). In this study a biomass price of 18 €<sub>2019</sub>/MWh is used. To gauge the effect of a higher biomass price, it is increased by 100%.

Lastly, the electrolyzer investment costs are predicted to fall in the coming years (Schmidt et al., 2017). The technology could reach investment cost levels below 0.6 M€/MW (Schmidt et al., 2017). To account for this the AEL investment costs are reduced by—50% to around 0.6 €/MW.

## RESULTS AND DISCUSSION

This section presents carbon and energy efficiency alongside the production costs for all simulation cases, as shown in **Table 3**. The reference processes BtL and PBtL are also analyzed. It should be noted that in terms of carbon and energy efficiency the results for BtL are equivalent to BA cases. The same applies for PBtL and EA cases. Only the economic results differ for the hybrid process and the reference processes.

### Carbon Efficiency

In the base case a carbon efficiency of 35.4% was found for the BA mode. As depicted in the Sankey diagram in **Figure 4**, the remaining carbon is converted to CO<sub>2</sub> (60.3%), off-gas (1.9%) and ash (2.4%).

An advantage of the EA mode over the BA mode is the higher carbon efficiency. In the base case, 61.1% of the biomass carbon instead of 35.4% is converted into FT product. The higher carbon efficiency is mainly due to the amount of carbon converted to CO<sub>2</sub>—a similar share of carbon leaves the process in the form of ash and FT off-gas in both modes. For the BA mode almost twice the amount of CO<sub>2</sub> is produced in the WGS reaction (cf. **Table 5**). This is caused by the steam addition needed to reach the defined H<sub>2</sub>/CO ratio in the sour shift reactor. In the EA mode no additional steam is introduced. Instead the H<sub>2</sub>/CO ratio is adjusted with electrolytic H<sub>2</sub>.

As highlighted in **Table 5**, the highest carbon efficiency for the BA mode can be found for case 1.3 or 2.3 at 35.6%. This can be attributed to the lower amount of CO<sub>2</sub> produced to reach an H<sub>2</sub>/CO ratio of 1.6. Further, a higher FT yield, CO conversion multiplied with C<sub>5+</sub> selectivity, affects the carbon efficiency positively, because the amount of FT-off gas is reduced.

In the EA mode the highest carbon efficiency is found for case 1.1. at 61.1%. The combination of high FT yield and low CO<sub>2</sub> production lead to the highest carbon efficiency. In both modes, the EA biomass feed amount has no influence on the carbon efficiency.

### Fuel and Process Efficiency

For all analyzed cases fuel and process efficiency is found to be higher in the BA mode compared to the EA mode cf. **Table 5**. This is mainly due to the additional energy loss in the electrolyzer. The energy streams for case 1.1 BA and EA mode are depicted in **Figure 5**. Here, it can be seen that of the 200 MW<sub>LHV</sub> biomass input in BA mode 57.6% is converted to fuel, 18.8% to district heating and

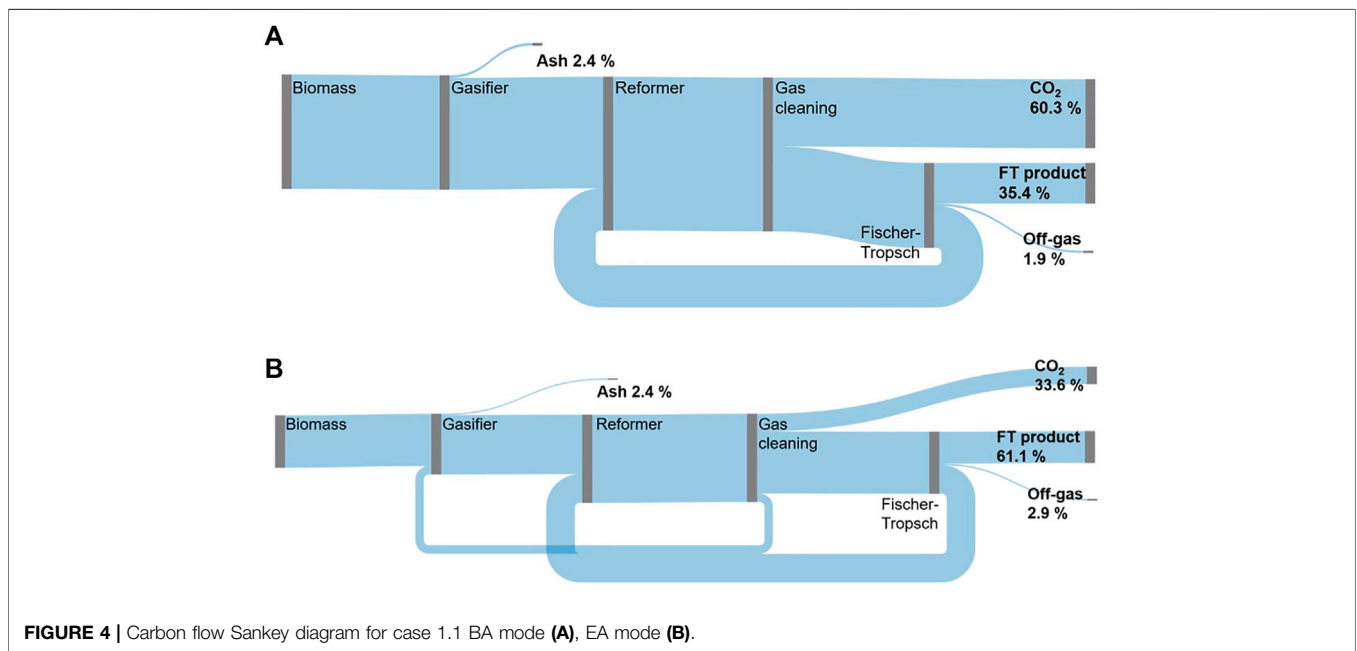


**FIGURE 4 |** Carbon flow Sankey diagram for case 1.1 BA mode (A), EA mode (B).

**TABLE 5 |** Efficiency values and key process results for all simulated cases.

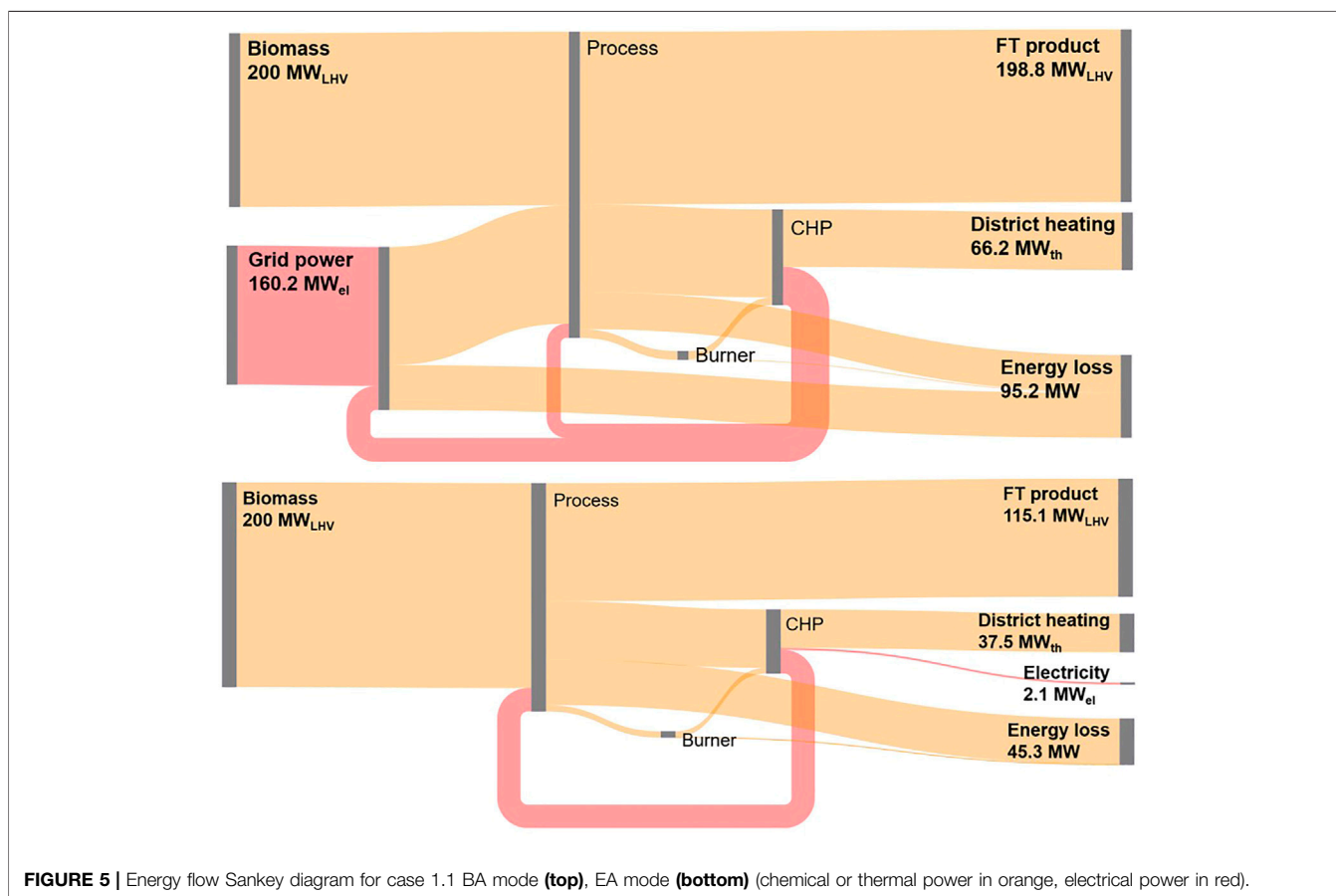
Case number	1.1	1.2	1.3	1.4	2.1	2.2	2.3	2.4
H <sub>2</sub> conversion [%]	70	55	70	55	70	55	70	55
H <sub>2</sub> /CO [-]	2.05	2.05	1.6	1.6	2.05	2.05	1.6	1.6
Biomass feed rate BA [MW <sub>th</sub> ]	200	200	200	200	200	200	200	200
Biomass feed rate EA [MW <sub>th</sub> ]	200	200	200	200	100	100	100	100
<b>BA/BtL</b>								
Fuel Efficiency [%]	57.6	55.6	<b>58.4</b>	56.0	57.6	55.6	58.4	56.0
Process Efficiency [%]	77.4	78.5	77.8	<b>79.0</b>	77.4	78.5	77.8	79.0
Carbon Efficiency [%]	35.4	34.2	<b>35.9</b>	34.5	35.4	34.2	35.9	34.5
CO <sub>2</sub> produced [kg/s]	14.00	14.11	13.72	13.84	14.00	14.11	13.72	13.84
FT C <sub>5+</sub> Selectivity [%]	83.2	84.4	87.3	87.5	83.2	84.4	87.3	87.5
Per-pass FT CO Conversion	67.2	52.7	53.1	41.6	67.2	52.7	53.1	41.6
FT product output [kg/s]	2.62	2.53	2.66	2.56	2.62	2.53	2.66	2.56
Electricity output [MW]	2.1	3.4	1.8	3.3	2.1	3.4	1.8	3.3
District heating output [MW]	37.5	42.3	37.1	42.6	37.5	42.3	37.1	42.6
<b>EA/PBtL</b>								
Fuel Efficiency [%]	55.2	53.6	<b>56.1</b>	54.2	55.2	53.6	56.1	54.2
Process Efficiency [%]	73.6	74.3	74.4	<b>75.3</b>	73.6	74.3	74.4	75.3
Carbon Efficiency [%]	<b>61.1</b>	60.4	56.0	54.5	61.1	60.4	56.0	54.5
CO <sub>2</sub> produced [kg/s]	7.83	7.67	8.83	8.80	3.91	3.84	4.41	4.40
FT C <sub>5+</sub> Selectivity [%]	83.5	84.6	87.5	87.7	83.5	84.6	87.5	87.7
Per-pass FT CO Conversion	67.2	52.7	53.1	41.6	67.2	52.7	53.1	41.6
Power input AEL [MW]	187.9	198.7	145.2	151.8	93.9	99.4	72.6	75.9
FT product output [kg/s]	<b>4.53</b>	4.48	4.15	4.04	2.26	2.24	2.07	2.02
District heating output [MW]	66.2	76.3	59.3	69.0	33.1	38.2	29.6	34.5

*Bold values signify best process performance within case 1.*

1.1% to electricity. The bulk of the generated electricity is used for the auxiliary process power requirement. In the EA mode the remaining electricity is fed to the AEL. Thereby, the electricity demand from the grid can be reduced from 187.9 to 160.2 MW<sub>el</sub>. With that 55.2% of process power input can be converted to FT fuel, while 18.4% are converted to district heating.

The highest fuel efficiency is found for cases with high H<sub>2</sub> conversion and a low H<sub>2</sub>/CO ratio i.e. case 1.3 and 2.3. In the BA mode a fuel efficiency of 58.4% and 56.1% in the EA mode is reached as shown in **Table 5**. Like for the carbon efficiency, the biomass feed rate in the EA mode has no influence on the fuel or process efficiency. High FT conversion and low H<sub>2</sub>/CO ratio lead





to the highest fuel efficiency in the BA mode, because these conditions have the highest FT product output. For the EA mode, on the other hand, case 1.3 does not feature the highest product output. However, the lower feed rate of hydrogen, needed for the H<sub>2</sub>/CO ratio of 1.6, results in the highest fuel efficiency.

When including the by-products district heating and electricity for the process efficiency, the highest process efficiency values can be found for case 1.4 and 2.4. With the lower H<sub>2</sub> conversion of 55% and an H<sub>2</sub>/CO ratio of 1.6 a process efficiency of 79% BA and 75.3% EA can be attained (cf. Table 5). As less reactant can be converted to FT product, the process output is shifted towards heat and electricity production. This affects the process efficiency positively.

## Economic Results

For the base case NPC of 1.08 and 1.04 €<sub>2019</sub>/L for continuous operation in BA and EA mode are found. The average electricity price of 55.49 €/MWh is used to determine the continuously operated EA NPC. BtL and PBtL, in contrast, have NPC of 0.66 and 1 €<sub>2019</sub>/L (cf. Table 6). The difference in NPC for BA and BtL or EA and PBtL is due to the lower investment cost. As the electrolysis unit and CO<sub>2</sub> recycle are not needed for a BtL plant, only 50.9% of the FCI has to be considered relative to the hybrid plant. Similarly, PBtL has 92.2% of the FCI for the hybrid plant.

When applying the Finnish day-ahead price profile, the NPC for the hybrid process in the base configuration is found to be

1.02 €<sub>2019</sub>/L. If the electricity price is lower than 61 €/MWh, the hybrid process is operated in EA mode. The remaining 30% of the year the process is operated in BA mode. The resulting electricity price for all hours operated in EA mode amounts to 50.65 €/MWh. Under this operation regime the hybrid process has a carbon efficiency of 53.5%.

The lowest production costs are found for case 1.3. Figure 6 juxtaposes the net production costs for the EA and BA mode for case 1.1 and case 1.3. In the BA mode case 1.3 has production costs of 0.98 €<sub>2019</sub>/L. This is 0.10 €/l lower than for case 1.1. For the EA mode, this difference is only 0.06 €/l. The lower production costs are due to the lower H<sub>2</sub>/CO ratio leading to reduced investment costs for the electrolyzer. Compared to the base case the electrolyzer investment costs are 21% lower for case 1.3. At the same time, the fuel efficiency is increased by around 1% in both modes. However, the lower H<sub>2</sub>/CO ratio comes at the cost of a reduced carbon efficiency.

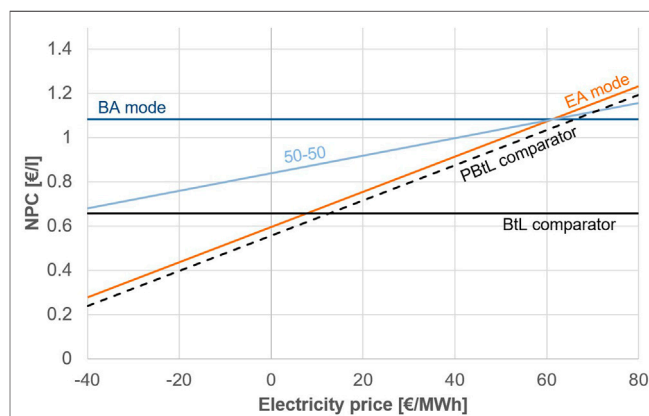
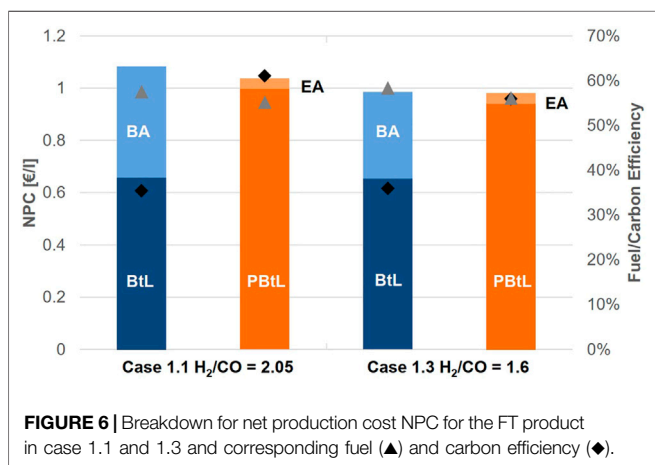
The hybrid process in case 1.3 operated under the conditions of the Finnish day-ahead market has the lowest NPC of 0.95 €<sub>2019</sub>/L—0.07 €<sub>2019</sub>/L less than in case 1.1. With 50% operation in EA mode, the average price for electricity is 47.51 €/MWh. The overall carbon efficiency amounts to 46%.

The reduced EA biomass feed rate in cases 2 leads to a decrease in the BA NPC at the expense of the EA NPC. The cost reduction for the BA mode can be attributed predominantly to the lower capital investment for the electrolyzer, as less hydrogen is needed for 100 MW biomass input. On the other hand, the higher NPC in

**TABLE 6 |** Net production cost NPC and fixed capital investment FCI for all studied cases.

Case number	1.1	1.2	1.3	1.4	2.1	2.2	2.3	2.4
H <sub>2</sub> conversion [%]	70	55	70	55	70	55	70	55
H <sub>2</sub> /CO [-]	2.05	2.05	1.6	1.6	2.05	2.05	1.6	1.6
Biomass feed rate BA [MW <sub>th</sub> ]	200	200	200	200	200	200	200	200
Biomass feed rate EA [MW <sub>th</sub> ]	200	200	200	200	100	100	100	100
NPC <sub>BA</sub> [€ <sub>2019</sub> /L]	1.08	1.13	<b>0.98</b>	1.03	0.85	0.87	0.80	0.82
NPC <sub>EA</sub> [€ <sub>2019</sub> /L]	1.04	1.07	<b>0.98</b>	1.01	1.29	1.33	1.26	1.30
FCI hybrid plant [M€ <sub>2019</sub> ]	535	554	482	500	390	401	367	376
FCI AEL [M€ <sub>2019</sub> ]	224	236	176	184	118	124	93	97
NPC BtL [€ <sub>2019</sub> /L]	0.66	0.66	0.65	0.66	0.66	0.66	0.65	0.66
FCI BtL relative to hybrid plant [%]	50.9	49.8	56.8	55.7	50.9	49.8	56.8	55.7
NPC PBtL [€ <sub>2019</sub> /L]	1.00	0.99	0.94	0.97	1.00	0.99	0.94	0.97
FCI PBtL relative to hybrid plant [%]	92.2	92.8	91.8	92.0	50.9	49.8	56.8	55.7
Electricity price for equal NPC BA-EA [€ <sub>2019</sub> /MWh]	61.0	62.9	56.1	57.5	-0.13	1.63	-13.1	-12.3
c <sub>fBA</sub> [%]	30	24	50	42	100	100	100	100
Average electricity price during EA operation [€/MWh]	50.65	51.43	47.51	48.69	—	—	—	—
NPC <sub>hy</sub> [€ <sub>2019</sub> /L]	1.02	1.06	0.95	0.99	—	—	—	—
Carbon efficiency hybrid concept [%]	53.5	54.0	46.0	46.0	—	—	—	—

Bold values signify lowest production costs for case 1.



the EA mode is due to the lower product output for all cases with 100 MW input.

On the Finnish day-ahead market cases 2 could not be sensibly applied. The NPC of the EA mode are only lower than BA NPC, when electricity is available at negative prices. Since this is not the case for 2019, the process would only be operated in the BA mode. Consequently, on the present energy markets of Finland, the electrolyzer would have to be inactive for the entire year.

### Sensitivity Analysis

To assess under what conditions on the energy market the hybrid operation principle is economical, a sensitivity analysis is conducted for the electricity price. **Figure 7** displays the production costs for case 1.1 in EA and BA mode for an electrical price range from -40 to 80 €/MWh. The resulting production costs of the plant operated half a year in BA and half a year EA mode is denoted as 50-50. Further, the production costs for a BtL and a PBtL plant of the same size are shown.

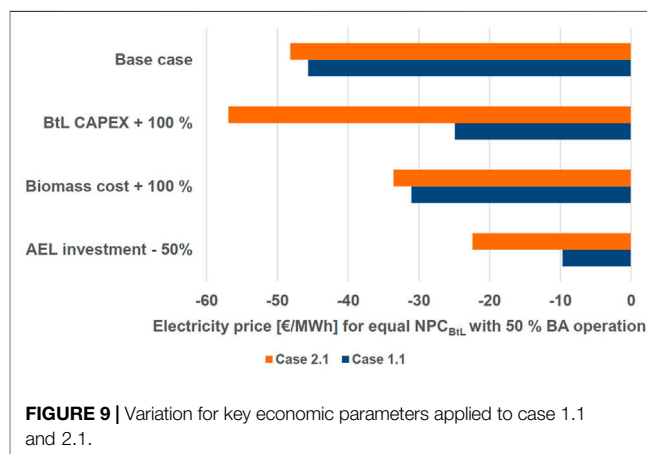
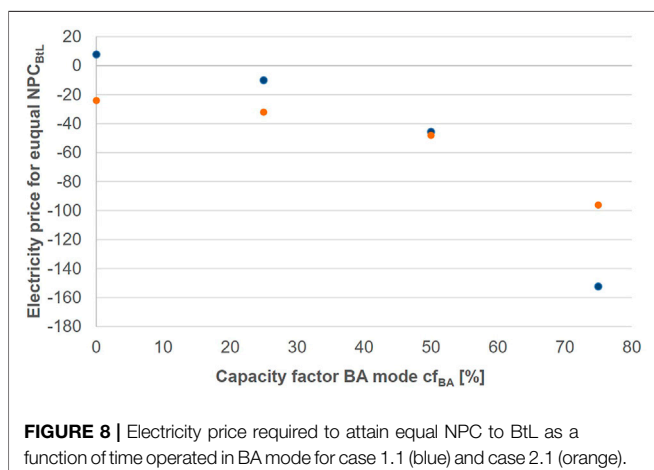
The PBtL and BtL comparator production costs stay below those of EA and BA mode respectively. This is due to investment

costs of inactive equipment. The inactive electrolyzer accounts for most of the price spread between BA mode and BtL comparator.

The EA mode would have to be operated for the entire year at a price of 8 €/MWh to reach the same production costs of a BtL plant. If the EA mode is only operated for half a year electricity prices of below -40 €/MWh would have to be available for the same time period to reach the BtL price level.

In **Figure 8** the share of operation hours in the BA mode are varied for cases 1.1 and 2.1. Based on this, the diagram shows the electricity price for the EA operation hours such that the hybrid process concept reaches equal NPC as the corresponding BtL plant.

It can be seen that none of the cases reaches an equal electricity price above -40 €/MWh at 50-50 operation. For a lower EA operation share the required electricity prices asymptotically approach negative infinity. Further, it can be taken from **Figure 8** that the cost advantage for cases 1 over 2 can only be found, if BA operation shares stay below 50%. When the



process is predominantly operated in BA mode, designing the process with a lower EA biomass input is advantageous.

In **Figure 9** three economic parameters are varied and compared to the cases 1.1 and 2.1. For all parameter changes the electricity price is calculated with which the hybrid process concept, operated in 50% EA and 50% BA mode, reaches an equal NPC with the corresponding BtL plant. As seen in **Figure 7**, equal production costs to BtL are reached at an electricity price below—40 €/MWh for half a year.

The investment costs for the BtL plant, which entail all equipment except the electrolyzer and CO<sub>2</sub> recycle, are estimated as 272 M€<sub>2019</sub> for case 1.1 at 200 MW biomass input. Therefore, the BtL investment costs increased by +100% would be 544 M€ at 200 MW biomass input. This estimate is in line with the upper range of the cost estimates of 1200 M€<sub>2011</sub> for 400 MW input reported by (Haarlemmer et al., 2012). For case 1.1, BtL and the hybrid process have equal NPC at an electricity price of around—22 €/MWh. For case 2.1, however, this has an adverse effect pushing the electricity price to below—50 €/MWh. This is due to the over-dimension BtL equipment in the EA mode.

Increasing the biomass price by +100% has a positive effect on the hybrid process. For case 1.1 and 2.1 it reduces the electricity price to around—30 €/MWh. Further, the electrolyzer investment costs reduction decreases the electricity price to around—10 €/MWh for case 1.1 and—20 €/MWh for case 2.1. The effect on case 1.1 is stronger, because in this case a larger AEL is required (cf. **Table 5**).

Overall, it can be seen that only a combination of the discussed parameter variations would increase the electricity price to a positive value. Seeing that negative electricity prices for half a year are not likely, it seems probable that a BtL plant is more economical than the presented hybrid process concept.

## CONCLUSION

In this study a techno-economic analysis is conducted for a hybrid operation concept of an electrolysis enhanced biomass-

to-liquid process. The electrolysis enhanced mode, which increases the overall product yield, is only activated when the prices on the Finnish day-ahead market for 2019 make it more profitable than feeding only biomass. To that end a cost calculation method for hybrid processes was applied within DLR's software tool TEPET. Eight process design cases are analyzed to study the economic impact of FT conversion, H<sub>2</sub>/CO ratio and the biomass feeding rate in the electrolysis enhanced mode. To do so a FT kinetic model was implemented in Aspen Plus. All cases are compared to the steady-state alternatives BtL or PBtL. To gain a broader understanding of the process concept, a sensitivity analysis over electricity price and share of operation hours in each mode as well as key economic parameters is conducted. Based on the results presented here, the following conclusions can be drawn:

- Production costs of 1.08 €<sub>2019</sub>/L for the hybrid concept compared to 0.66 €<sub>2019</sub>/L for BtL and 1 €<sub>2019</sub>/L for PBtL were found based on the Finnish day-ahead market for the base case.
  - Under these conditions, an overall carbon efficiency for the hybrid process of 53.5% is found compared to 35.4% for BtL and 61.1% for PBtL.
  - The production cost difference is mainly due to the lower capital investment requirement for the reference processes. Only 51% and 92% of the investment costs for the hybrid process are required for BtL and PBtL respectively.
- The lowest NPC and highest fuel efficiency are found for cases with low H<sub>2</sub>/CO ratio (1.6 instead of 2.05)
  - Fuel efficiency can be increased by +1% for BA/BtL and EA/PBtL for cases with equal H<sub>2</sub> conversion.
  - The NPC for the hybrid concept can be decreased by 0.07 €<sub>2019</sub>/L
- A 100 MW<sub>th</sub> biomass feed in the EA mode is sensible, if the process is predominantly operated in the BA mode.
- The BtL concept appears to be the most economic process alternative given the current renewable electricity price. However, changing economic conditions, i.e. power and biomass prices, and technology development like the reduction of electrolyzer investment cost could make the hybrid concept economically feasible in the future.

The following points should be investigated further to either validate the assumptions made in this study or improve the efficiency and profitability of the two processes: The H<sub>2</sub>/CO ratio and FT conversion can improve the overall process performance. However, a correlation between H<sub>2</sub>/CO ratio and the conversion limit was not presented in literature so far. An experimental study on this correlation would help to better assess the optimal yield for the FT reactor.

Further, the CO<sub>2</sub> recycling rate was not discussed in this study. With a higher recycling rate, the hydrogen demand of the process would be greater and a higher product yield can be expected. The amount of product yield can even be increased further when hydrogen is added to the reformer directly. This was simulated in (Hillestad et al., 2018). Finding the optimal amount of hydrogen to add to the process would be highly dependent upon the electricity price, electrolyzer investment and efficiency among other factors.

The FT recycle was assumed to have a recycle ratio of 95%. Increasing this value comes at the cost of accumulation of inert gas content in the syngas. However, it also leads to higher fuel yield. An upper limit to the recycling rate should be found experimentally.

## DATA AVAILABILITY STATEMENT

The original contributions presented in the study are included in the article/**Supplementary Material**, further inquiries can be directed to the corresponding author.

## REFERENCES

- Ail, S. S., and Dasappa, S. (2016). Biomass to Liquid Transportation Fuel via Fischer Tropsch Synthesis - Technology Review and Current Scenario. *Renew. Sustain. Energ. Rev.* 58, 267–286. doi:10.1016/j.rser.2015.12.143
- Albrecht, F. G., and Dietrich, R.-U. (2018). "Technical and Economic Optimization of Biomass-To-Liquid Processes Using Exergoeconomic Analysis," in 26th European Biomass Conference & Exhibition (EUBCE), Copenhagen, Denmark.
- Albrecht, F. G., König, D. H., Baucks, N., and Dietrich, R.-U. (2017). A Standardized Methodology for the Techno-Economic Evaluation of Alternative Fuels - A Case Study. *Fuel* 194, 511–526. doi:10.1016/j.fuel.2016.12.003
- Aspen Technology Inc (2013). *Aspen Physical Property System - Physical Property Methods*. Burlington, Massachusetts: Aspen Technology Inc.
- Bechtel (1998). *Aspen Process Flowsheet Simulation Model of a Battelle Biomass-Based Gasification, Fischer-Tropsch Liquefaction and Combined-Cycle Power Plant*. Pittsburgh, Pennsylvania: US Department of Energy (DOE Bechtel corporation).
- Blanco, H., and Faaij, A. (2018). A Review at the Role of Storage in Energy Systems with a Focus on Power to Gas and Long-Term Storage. *Renew. Sustain. Energ. Rev.* 81, 1049–1086. doi:10.1016/j.rser.2017.07.062
- Butera, G., Højgaard Jensen, S., Østergaard Gadsbøll, R., Ahrenfeldt, J., and Røngaard Clausen, L. (2020). Flexible Biomass Conversion to Methanol Integrating Solid Oxide Cells and Two-Stage Gasifier. *Fuel* 271, 117654. doi:10.1016/j.fuel.2020.117654
- Buttler, A., and Spliethoff, H. (2018). Current Status of Water Electrolysis for Energy Storage, Grid Balancing and Sector Coupling via Power-To-Gas and Power-To-Liquids: A Review. *Renew. Sustain. Energ. Rev.* 82, 2440–2454. doi:10.1016/j.rser.2017.09.003
- Clausen, L. R., Elmegaard, B., and Houbak, N. (2010). Technoeconomic Analysis of a Low CO<sub>2</sub> Emission Dimethyl Ether (DME) Plant Based on Gasification of Torrefied Biomass. *Energy* 35 (12), 4831–4842. doi:10.1016/j.energy.2010.09.004

## AUTHOR CONTRIBUTIONS

The study is based on EK process design as studied in the EU project FLEXCHX. Modeling, simulation and analysis was done by FH under the guidance of R-UD and EK. The software tool TEPET was provided by SM. The authors FH and SM prepared the manuscript. R-UD, EK, and SM discussed and commented the manuscript.

## FUNDING

This study is part of the FLEXCHX project, which has received funding from the European Union's Horizon 2020 research and innovation Programme under Grant Agreement No 763919.

## ACKNOWLEDGMENTS

Further, the authors would like to thank Julia Weyand, Moritz Raab and Dr. Marc Linder for their valuable inputs.

## SUPPLEMENTARY MATERIAL

The Supplementary Material for this article can be found online at: <https://www.frontiersin.org/articles/10.3389/fenrg.2021.723774/full#supplementary-material>

- European Commission (2020). Stepping up Europe's 2030 Climate Ambition Investing in a Climate-Neutral Future for the Benefit of Our People. [Online]. Available: <https://eur-lex.europa.eu/legal-content/EN/TXT/PDF/?uri=CELEX:52020DC0562&from=EN> (Accessed May 3, 2021).
- Haarlemmer, G., Boissonnet, G., Imbach, J., Setier, P.-A., and Peduzzi, E. (2012). Second Generation BtL Type Biofuels - a Production Cost Analysis. *Energy Environ. Sci.* 5 (9), 8445. doi:10.1039/c2ee21750c
- Hamelinck, C. N., and Faaij, A. P. C. (2006). Outlook for Advanced Biofuels. *Energy policy* 34 (17), 3268–3283. doi:10.1016/j.enpol.2005.06.012
- Hannula, I., and Kurkela, E. (2010). A Semi-empirical Model for Pressurised Air-Blown Fluidised-Bed Gasification of Biomass. *Bioresour. Technol.* 101 (12), 4608–4615. doi:10.1016/j.biortech.2010.01.072
- Hannula, I., and Reiner, D. M. (2019). Near-term Potential of Biofuels, Electrofuels, and Battery Electric Vehicles in Decarbonizing Road Transport. *Joule* 3 (10), 2390–2402. doi:10.1016/j.joule.2019.08.013
- Hannula, I. (2016). Hydrogen Enhancement Potential of Synthetic Biofuels Manufacture in the European Context: A Techno-Economic Assessment. *Energy* 104, 199–212. doi:10.1016/j.energy.2016.03.119
- Helen Oy (2021). *Confidential Deliverable Report D8.5 - Techno-Economic Assessment Report for the Finnish Case Studies*. Finland.
- Helin, K., Jaäskeläinen, J., and Syri, S. (2018). "Energy Security Impacts of Decreasing CHP Capacity in Finland," in 2018 15th International Conference on the European Energy Market (EEM): (IEEE), Piscataway, NJ, 1–5. doi:10.1109/eem.2018.8469786
- Hillestad, M., Ostadi, M., Alamo Serrano, G. d., Rytter, E., Austbø, B., Pharoah, J. G., et al. (2018). Improving Carbon Efficiency and Profitability of the Biomass to Liquid Process with Hydrogen from Renewable Power. *Fuel* 234, 1431–1451. doi:10.1016/j.fuel.2018.08.004
- HSV (2021). Sähkö Siirtohinnoista 110 kV -asiakkaille. [Online]. Available: <https://www.helensahkoverkko.fi/globalassets/hinnastot-ja-sopimusehdot/hsv/sahkon-siirtohinnoista-110kv.pdf> (Accessed May 2, 2021).
- Jenkins, S. (2020). 2019 Chemical Engineering Plant Cost Index Annual Average. [Online]. Available: <https://www.chemengonline.com/2019-chemical-engineering-plant-cost-index-annual-average/> (Accessed March 24, 2021).

- Kempegowda, R. S., del Alamo, G., Berstad, D., Bugge, M., Matas Güell, B., and Tran, K.-Q. (2015). CHP-integrated Fischer-Tropsch Biocrude Production under Norwegian Conditions: Techno-Economic Analysis. *Energy Fuels* 29 (2), 808–822. doi:10.1021/ef502326g
- Kotzur, L., Markewitz, P., Robinius, M., and Stolten, D. (2018). Time Series Aggregation for Energy System Design: Modeling Seasonal Storage. *Appl. Energ.* 213, 123–135. doi:10.1016/j.apenergy.2018.01.023
- Krebs, S. (2015). *Arbeitskosten Pro Stunde im Verarbeitenden Gewerbe*. Volkswirtschaft und Statistik. VDMA. Available at: <http://www.waterwastewater technology.info/documents/105628/778064/Internationaler%20Arbeitskostenvergleich%20Verarbeitendes%20Gewerbe/05a1a0bf-ea29-4a7a-b905-37ffec17957> (Accessed November 10, 2021).
- Kurkela, E., Ståhlberg, P., and Laatikainen, J. (1993). *Pressurized Fluidized-Bed Gasification Experiments with wood, Peat and Coal at VTT in 1991-1992: Part 1. Test Facilities and Gasification Experiments with Sawdust*. Espoo, Finland: VTT Technical Research Centre of Finland.
- Kurkela, E., Kurkela, M., Hiltunen, I. J. E. P., and Energy, S. (2014). The Effects of wood Particle Size and Different Process Variables on the Performance of Steam-oxygen Blown Circulating Fluidized-bed Gasifier. *Environ. Prog. Sustain.* 33 (3), 681–687. doi:10.1002/ep.12003
- Kurkela, E., Kurkela, M., Frilund, C., Hiltunen, I., Rollins, B., and Steele, A. (2020). Flexible Hybrid Process for Combined Production of Heat, Power and Renewable Feedstock for Refineries: Managing seasonal energy supply and demand for heat and power in Europe. *Johnson Matthey Technol. Rev.* 65 (2), 333–345.
- LeViness, S., Deshmukh, S. R., Richard, L. A., and Robota, H. J. (2014). Velocys Fischer-Tropsch Synthesis Technology—New Advances on State-Of-The-Art. *Top. Catal.* 57 (6-9), 518–525. doi:10.1007/s11244-013-0208-x
- LeViness, S. (2013). “Velocys Fischer-Tropsch Synthesis Technology—Comparison to Conventional FT Technologies,” in AICHE 2013 Spring Meeting, San Antonio, TX.
- Lillebø, A., Rytter, E., Blekkan, E. A., and Holmen, A. (2017). Fischer-Tropsch Synthesis at High Conversions on Al<sub>2</sub>O<sub>3</sub>-Supported Co Catalysts with Different H<sub>2</sub>/CO Levels. *Ind. Eng. Chem. Res.* 56 (45), 13281–13286. doi:10.1021/acs.iecr.7b01801
- Mathiesen, B. V., Lund, H., Connolly, D., Wenzel, H., Østergaard, P. A., Möller, B., et al. (2015). Smart Energy Systems for Coherent 100% Renewable Energy and Transport Solutions. *Appl. Energ.* 145, 139–154. doi:10.1016/j.apenergy.2015.01.075
- Molino, A., Chianese, S., and Musmarra, D. (2016). Biomass Gasification Technology: The State of the Art Overview. *J. Energ. Chem.* 25 (1), 10–25. doi:10.1016/j.jechem.2015.11.005
- Müller, S., Groß, P., Rauch, R., Zweiler, R., Aichernig, C., Fuchs, M., et al. (2018). Production of Diesel from Biomass and Wind Power—Energy Storage by the Use of the Fischer-Tropsch Process. *Biomass Convers. Biorefin.* 8 (2), 275–282. doi:10.1007/s13399-017-0287-1
- Nord Pool AS (2021). Finnish Day-Ahead Market Data 2019. [Online]. Available: <https://www.nordpoolgroup.com/Market-data1/Dayahead/Area-Prices/ALL1/Hourly1/?view=table> (Accessed May 6, 2021).
- Olofsson, I., Nordin, A., and Söderlind, U. (2005). *Initial Review and Evaluation of Process Technologies and Systems Suitable for Cost-Efficient Medium-Scale Gasification for Biomass to Liquid Fuels*. Umeå, Sweden: Umeå Universitet.
- Ostadi, M., and Hillestad, M. (2017). Enriched Air or Pure Oxygen as Oxidant for Gas-to-Liquid Process with Microchannel Reactors. *Chem. Eng. Technol.* 40 (10), 1946–1951. doi:10.1002/ceat.201700269
- Padurean, A., Cormos, C.-C., and Agachi, P.-S. (2012). Pre-combustion Carbon Dioxide Capture by Gas-Liquid Absorption for Integrated Gasification Combined Cycle Power Plants. *Int. J. Greenhouse Gas Control.* 7, 1–11. doi:10.1016/j.ijggc.2011.12.007
- Papaefthymiou, G., and Dragoon, K. (2016). Towards 100% Renewable Energy Systems: Uncapping Power System Flexibility. *Energy Policy* 92, 69–82. doi:10.1016/j.enpol.2016.01.025
- Peters, M. S., Timmerhaus, K. D., West, R. E., Timmerhaus, K., and West, R. (1968). *Plant Design and Economics for Chemical Engineers*. New York: McGraw-Hill.
- Piermartini, P., Boeltken, T., Selinsek, M., and Pfeifer, P. (2017). Influence of Channel Geometry on Fischer-Tropsch Synthesis in Microstructured Reactors. *Chem. Eng. J.* 313, 328–335. doi:10.1016/j.cej.2016.12.076
- Rytter, E., and Holmen, A. (2015). Deactivation and Regeneration of Commercial Type Fischer-Tropsch Co-catalysts—A Mini-Review. *Catalysts* 5 (2), 478–499. doi:10.3390/catal5020478
- Schanke, D., Lian, P., Eri, S., Rytter, E., Sannæs, B. H., and Kinnari, K. J. (2001). “Optimisation of Fischer-Tropsch Reactor Design and Operation in GTL Plants,” in *Studies in Surface Science and Catalysis* (Fogelsville: Elsevier), 239–244. doi:10.1016/s0167-2991(01)80310-4
- Schmidt, O., Gambhir, A., Staffell, I., Hawkes, A., Nelson, J., and Few, S. J. I. J. o. H. E. (2017). Future Cost and Performance of Water Electrolysis. *An Expert Elicitation study* 42 (52), 30470–30492. doi:10.1016/j.ijhydene.2017.10.045
- Schweitzer, J., and Viguié, J. (2009). Reactor Modeling of a Slurry Bubble Column for Fischer-Tropsch Synthesis. *Oil Gas Sci. Technol. Revue de l'IFP* 64 (1), 63–77. doi:10.2516/ogst/2009003
- Searle, S., and Malins, C. (2013). *Availability of Cellulosic Residues and Wastes in the EU*. Washington, DC, USA: International Council on Clean Transportation.
- Shen, Y., and Yoshikawa, K. (2013). Recent Progresses in Catalytic Tar Elimination during Biomass Gasification or Pyrolysis—A Review. *Renew. Sustain. Energ. Rev.* 21, 371–392. doi:10.1016/j.rser.2012.12.062
- Sigurjonsson, H. Æ., and Clausen, L. R. (2018). Solution for the Future Smart Energy System: A Polygeneration Plant Based on Reversible Solid Oxide Cells and Biomass Gasification Producing Either Electrofuel or Power. *Appl. Energ.* 216, 323–337. doi:10.1016/j.apenergy.2018.02.124
- Smith, A., and Klosek, J. (2001). A Review of Air Separation Technologies and Their Integration with Energy Conversion Processes. *Fuel Process. Technol.* 70 (2), 115–134. doi:10.1016/s0378-3820(01)00131-x
- Swanson, R. M., Platon, A., Satrio, J. A., and Brown, R. C. (2010). Techno-economic Analysis of Biomass-To-Liquids Production Based on Gasification. *Fuel* 89, S11–S19. doi:10.1016/j.fuel.2010.07.027
- Todic, B., Bhatelia, T., Froment, G. F., Ma, W., Jacobs, G., Davis, B. H., et al. (2013). Kinetic Model of Fischer-Tropsch Synthesis in a Slurry Reactor on Co-Re/Al<sub>2</sub>O<sub>3</sub> Catalyst. *Ind. Eng. Chem. Res.* 52 (2), 669–679. doi:10.1021/ie3028312
- Todic, B., Ma, W., Jacobs, G., Davis, B. H., and Bukur, D. B. (2014). Effect of Process Conditions on the Product Distribution of Fischer-Tropsch Synthesis over a Re-promoted Cobalt-Alumina Catalyst Using a Stirred Tank Slurry Reactor. *J. Catal.* 311, 325–338. doi:10.1016/j.jcat.2013.12.009
- Unde, R. B. (2012). *Kinetics and Reaction Engineering Aspects of Syngas Production by the Heterogeneously Catalysed Reverse Water Gas Shift Reaction*. Dissertation Universität Bayreuth.
- Van Der Laan, G. P., and Beenackers, A. A. C. M. (1999). Kinetics and Selectivity of the Fischer-Tropsch Synthesis: a Literature Review. *Catal. Rev.* 41 (3-4), 255–318. doi:10.1081/cr-100101170
- Verohallinto (2021). Tax Rates on Electricity and Certain Fuels. [Online]. Available: <https://www.vero.fi/en/businesses-and-corporations/taxes-and-charges/excise-taxation/sahko-ja-eraat-polttoaineet/Tax-rates-on-electricity-and-certain-fuels/> (Accessed March 2, 2021).
- Wang, J., You, S., Zong, Y., Træholt, C., Dong, Z. Y., and Zhou, Y. (2019). Flexibility of Combined Heat and Power Plants: A Review of Technologies and Operation Strategies. *Appl. Energ.* 252, 113445. doi:10.1016/j.apenergy.2019.113445
- Warnecke, R. (2000). Gasification of Biomass: Comparison of Fixed Bed and Fluidized Bed Gasifier. *Biomass Bioenergy* 18 (6), 489–497. doi:10.1016/s0961-9534(00)00009-x

**Conflict of Interest:** The author EK is employed by VTT Technical Research Centre of Finland Ltd.

The remaining authors declare that the research was conducted in the absence of any commercial or financial relationships that could be construed as a potential conflict of interest.

**Publisher's Note:** All claims expressed in this article are solely those of the authors and do not necessarily represent those of their affiliated organizations, or those of the publisher, the editors and the reviewers. Any product that may be evaluated in this article, or claim that may be made by its manufacturer, is not guaranteed or endorsed by the publisher.

Copyright © 2021 Habermeyer, Kurkela, Maier and Dietrich. This is an open-access article distributed under the terms of the Creative Commons Attribution License (CC BY). The use, distribution or reproduction in other forums is permitted, provided the original author(s) and the copyright owner(s) are credited and that the original publication in this journal is cited, in accordance with accepted academic practice. No use, distribution or reproduction is permitted which does not comply with these terms.

## Publication II

### **Power Biomass to Liquid – an option for Europe’s sustainable and independent aviation fuel production**

F. Habermeyer, J. Weyand, S. Maier, E. Kurkela and R.-U. Dietrich

Biomass Conversion and Biorefinery 2023

DOI: 10.1007/s13399-022-03671-y

#### **Author Contributions:**

The study is based on Esa Kurkela’s process design as studied in the EU project FLEXCHX. Modeling, simulation and analysis was done by Felix Habermeyer under the guidance of Ralph-Uwe Dietrich and Esa Kurkela. The GHG emission analysis was conducted by Julia Weyand. The software tool TEPET was provided by Simon Maier. The author Felix Habermeyer prepared the manuscript. Ralph-Uwe Dietrich, Esa Kurkela, Julia Weyand and Simon Maier discussed and commented the manuscript.



# Power Biomass to Liquid — an option for Europe's sustainable and independent aviation fuel production

Felix Habermeyer<sup>1</sup> · Julia Weyand<sup>1</sup> · Simon Maier<sup>1</sup> · Esa Kurkela<sup>2</sup> · Ralph-Uwe Dietrich<sup>1</sup>

Received: 12 October 2022 / Revised: 11 December 2022 / Accepted: 13 December 2022  
© The Author(s) 2023

## Abstract

The European Union guides its member states to a gradual uptake of sustainable aviation fuel (SAF) from 2% vol. in 2025 to 63% vol. by 2050 with the ReFuelEU proposal as part of the Fit-for-55 package. A promising production pathway for SAF presents itself in the Power Biomass to Liquid (PBtL) process, which converts non-crop-based biomass residue and renewable power via the Fischer–Tropsch route. In this study, a techno-economic and greenhouse gas (GHG) emission analysis of a small-scale (50 MW<sub>th</sub>) PBtL process concept, developed in the EU project FLEXCHX, is presented. The analysis is conducted with a thermodynamic process model implemented in Aspen Plus<sup>®</sup>, which relies on experimental project data. For the PBtL base case production costs of 1.09 €<sub>2020</sub>/l are estimated, whereby electricity and investment into the alkaline electrolyzer constitute the largest cost drivers. At low electricity prices (<39.2 €/MWh), the PBtL process is more cost effective than the reference process Biomass to Liquid (BtL). To identify improvements to the base case design, different design options are considered under varying economic boundary conditions: Solid oxide electrolysis is more economic than alkaline electrolysis at higher electricity prices due to its higher system efficiency. Maximizing the product yield by increased CO<sub>2</sub> recycling is only economically reasonable below an electricity price threshold, which is found at 20 €/MWh for the base case. Further, PBtL is heavily dependent upon the availability of low GHG electricity in order to produce SAF with a low carbon footprint. Assuming full utilization of the EU's non-crop-based biomass residues, the EU jet fuel demand for 2030 could be met with the PBtL process.

**Keywords** Power and Biomass to Liquid · Biomass to Liquid · Fischer–Tropsch · Techno-economic analysis · Alkaline electrolysis

## Abbreviations

ACC	Annual capital cost	HEFA	Hydrotreated ester and fatty acids
AEL	Alkaline electrolysis	HPS	High pressure steam
AR	Agricultural residue	HRSG	Heat recovery steam generation
ASU	Air separation unit	IR	Interest rate
BtL	Biomass to Liquid	LCA	Life-cycle assessment
CAPEX	Capital expenditures	LPS	Low pressure steam
CW	Cooling water	LR	Long recycle
DME	Dimethyl ether	MPS	Medium pressure steam
FCI	Fixed capital investment	NPC	Net production cost
FR	Forrest residue	OPEX	Operational expenditures
FT	Fischer-Tropsch	PBtL	Power Biomass to Liquid
		PEM	Proton exchange membrane
		PL	Plant lifetime
		PV	Photovoltaic
		RF	Refrigeration
		RWGS	Reverse water gas shift
		SAF	Sustainable aviation fuel
		SBCR	Slurry bubble column reactor
		SNG	Synthetic natural gas
		SOEC	Solid oxide electrolysis cell

✉ Felix Habermeyer  
felix.habermeyer@dlr.de

<sup>1</sup> DLR e.V., Deutsches Zentrum für Luft- und Raumfahrt, Stuttgart, Germany

<sup>2</sup> VTT Technical Research Centre of Finland Ltd., Teknologian Tutkimuskeskus VTT Oy, Espoo, Finland

SR	Short recycle
SRR	Short recycle with reformer
SXB	Staged fixed bed
WHSV	Weight hourly space velocity

### Symbols

R	Reaction rate
k	Kinetic constant
K	Equilibrium constant
$\alpha$	Chain growth probability
DENOM	Denominator
LHV	Lower heating value
HHV	Higher heating value
P	Price
AC	GHG abatement cost

## 1 Introduction

Towards its goal of reaching 55% GHG-emission reduction by 2030, the EU has passed the legislative package Fit-for-55 [1]. The package contains the ReFuelEU proposal introducing measures for GHG reduction in the aviation industry [2]. Along with other measures, ReFuelEU mandates a gradual ramp-up of sustainable aviation fuel (SAF) blending from 2% vol. in 2025 to 63% vol. by 2050. Similarly, the US government targets a SAF production increase to 3 billion gallons per year until 2030 [3]. SAF is currently the most promising option for replacing fossil jet fuel due to its high energy density compared to other forms of energy provision such as battery or hydrogen storage. Yet, an optimal SAF production route remains a topic of discussion as many aspects, including production cost, GHG-footprint or the possible production volume in the EU, have to be considered.

A variety of feedstock and process types have been proposed for the production of SAF. E-fuel routes convert CO<sub>2</sub> from industrial point sources or direct air capture to SAF. The advantage of biomass-based routes over e-fuels is the lower energy demand for the feedstock reduction. Besides biomass routes that rely on oils (HEFA), sugar or algae, lignocellulose biomass offers a comparatively large feedstock base, for which a number of conversion routes have been established [4]. The Fischer–Tropsch (FT) route is a mature process with many commercial plants running on coal today and several biomass based project plants [5]. In addition, the FT route is estimated to have lower production cost for large-scale plants than alternative lignocellulose biomass routes, such as alcohol to jet (AtJ) or the synthesized iso-paraffine (SiP) route [4]. Yet, the FT route, also referred to as Biomass to Liquid (BtL), is limited in its carbon conversion [6]. Accordingly, it has been argued that BtL can only contribute a fraction of the EU's SAF demand [7]. Here, relying on the conversion of renewable electricity and non-crop-based

biomass, the Power Biomass to Liquid (PBtL) process offers a promising solution for the large scale low-emission production of SAF. The addition of electrolytic hydrogen while recycling CO<sub>2</sub> generated in the process enables a nearly full conversion of the limited biogenic carbon to hydrocarbon chains [6].

Several techno-economic studies on the PBtL process have been published: Hillestad et al. [8] find production cost of 1.7 \$/l for a PBtL process with 435 MW<sub>th</sub> biomass input assuming an electricity price of 50 \$/MWh. Thereby, a carbon efficiency of 91% is reached by nearly full carbon recycling. Albrecht et al. estimate production costs of 2.15 €/l<sub>GasolineEquivalent</sub> at an electricity price of 105 €/MWh [6]. Here, the PBtL plant with an output of 240 kt/year has a carbon efficiency of 97.7%. Isaacs et al. assess local PBtL production costs for the eastern part of the USA based on local biomass prices and PV and wind availability [9]. For every location, an off-grid electrolysis and energy storage system is optimized to produce a constant hydrogen stream at minimal cost. For the year 2030, the most economic product quartile is estimated to have a minimum selling price of 2.40 \$<sub>2030</sub>/l for systems operated with PV and wind as their power sources.

Other PBtL studies aim to find process designs for optimal technical efficiency. Nielsen et al. simulate a novel PBtL process concept in which an SOEC is partially fed by FT off-gas [10]. Based on their detailed simulation of the SOEC unit, the PBtL process' energy efficiency is hypothesized to reach 90% at a carbon efficiency of 91%. Dossow et al. discuss different process designs for a PBtL concept operated with a PEM electrolyzer [11]. With a hydrogen addition of 0.24 t<sub>H<sub>2</sub></sub>/t<sub>fuel</sub>, the process is estimated to reach a carbon efficiency of 97%.

The principle of adding electrolytic hydrogen to biomass derived syngas can also be used for other products than Fischer–Tropsch fuel. Here, products like SNG [12, 13], methanol [14, 15] or methanol to gasoline [13], ethanol [14], and DME [16] can be found in literature.

A number of studies include an LCA in their discussion of the PBtL process. Bernical et al. perform a comparative study on PBtL and BtL considering GHG impact and production costs of both processes [17]. The PBtL concept producing hydrogen with a SOEC system is found to be the more efficient concept, with higher fuel yield and similar economics and emissions, when electricity with a GHG footprint lower than 150 g<sub>CO<sub>2</sub>,eq</sub>/kWh is available. Koponen and Hannula [18] conduct a comparative LCA study for the processes presented in Hannula [13]. Here, the outsized role of green electricity for the production of low GHG fuels is emphasized as well.

In the EU project FLEXCHX, a small-scale hybrid BtL-PBtL plant (50 MW<sub>th</sub>) has been investigated [19]. The project concept relies on the idea of the plant switching



operation mode between BtL and PBtL depending on the situation on the energy market. When inexpensive and low GHG electricity is available, an electrolysis unit is switched on to boost the fuel output of the system. Otherwise, the plant can be run in BtL mode, where the electrolyzer is turned off, and the oxygen for gasification is provided by an ASU. To facilitate the small-scale and hybrid operation, a staged fixed bed (SXB) gasifier [20] in combination with a novel syngas cleaning system [21] have been developed and experimentally analyzed in a 1 MW pilot plant throughout the project. Similarly, the Winddiesel project successfully showcased the operation of an 8 MW<sub>th</sub> PBtL plant with a dynamic H<sub>2</sub> hydrogen input [22]. Further, Shell has presented plans to build a PBtL plant at the Rhineland refinery. An already installed 10 MW<sub>e1</sub> PEM electrolyzer will be scaled up to 100 MW<sub>e1</sub> to provide the necessary hydrogen for this plant [23].

The aim of this study is to evaluate the possible role of PBtL for the EU aviation sector. To that end, production cost, GHG emissions and production capacity in the EU are estimated. The same analysis is conducted for the BtL process, which serves as a reference case. Both process models are derived from the 50 MW<sub>th</sub> steady-state FLEXCHX process concept. The unit models are based on experimental project data. In order to avoid an overestimation of the production cost, different PBtL process designs are discussed under varying economic boundary conditions. A similar comprehensive techno-economic and ecologic approach to this novel process scheme and the discussion of its process design options has not been published yet. With that, it can be shown how the key advantage of the PBtL process, its higher product yield, can be utilized for SAF provision in the EU depending on national economic boundary conditions.

## 2 Methodology

### 2.1 Power Biomass to Liquid

The super-structure flowsheet, as depicted in Fig. 1, includes all process units needed for the conversion of biomass to FT product. Additionally, the flowsheet contains all process

design options, which will be discussed in the following sections.

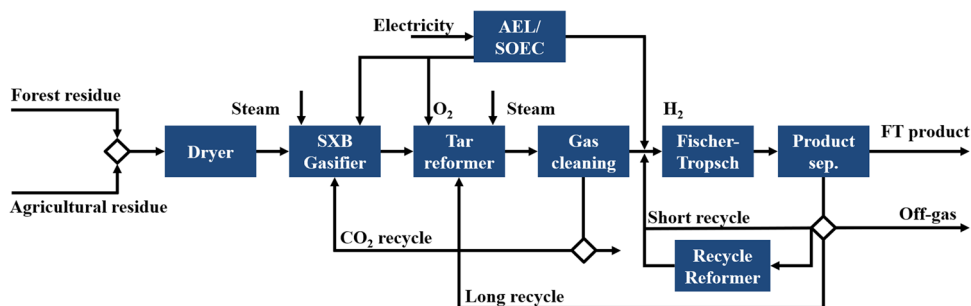
This flowsheet is conceptualized for a small-scale application with 50 MW<sub>th</sub> biomass input. Compared to larger plants that rely on the economy-of-scale effect for low production costs, this concept has mainly two advantages: small-scale biofuel production only requires a limited biomass transport radius. This leads to lower greenhouse gas emissions and lower cost for the biomass transport. Secondly, second generation biofuel plants are not in industrial use to date. This can be attributed to the high investment cost for a first-of-a-kind plant. To that end, small-scale plants can lower the financial risk for the initial investment [20]. However, lower total investment costs, lower material use for the plant construction, and a more seamless integration into the refinery infrastructure might persuade investors to switch to larger plant sizes later.

The initial wet biomass is introduced into an air dryer. Only low-grade heat is needed for air drying [24], which is readily available from the exothermal PBtL process. Therefore, air drying is preferred over steam drying in this study. Additional pre-treatment steps, such as torrefaction or pelleting [25], are not considered in this study, as they are not necessarily required for an SXB gasifier. These steps increase the biomass LHV and subsequently the process yield. This delta in yield would have to be weight against additional investment and operation costs for these pre-treatment steps.



The dried biomass is converted to syngas in a staged fixed bed gasifier (SXB). With the addition of steam, recycled CO<sub>2</sub> and oxygen, the complex biomass molecules can be cracked into a product gas phase containing mainly CO, H<sub>2</sub>, CO<sub>2</sub>, and steam as well as contaminant components such as tars, CH<sub>4</sub>, H<sub>2</sub>S, and NH<sub>3</sub>. For gasifier and reformer, all syngas components can be assumed to be in chemical equilibrium according to the water gas shift reaction in Eq. (1) [26]. The SXB gasifier technology is applied in this concept due to its lower capacity range compared to entrained flow and fluidized bed gasification, which are typically used for plants with > 100 MW<sub>th</sub> biomass input [20].

**Fig. 1** PBtL super-structure process flowsheet. Design options are signified by diamond shapes (◇)



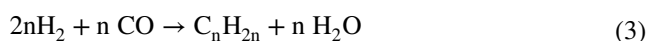
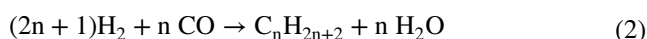
Tars formed in the gasifier have to be removed due to their detrimental effect to the subsequent process steps, especially the FT catalyst. Here, catalytic tar reforming is chosen for its higher H<sub>2</sub> and CO yield compared to thermal tar cracking. Thermal cracking requires higher temperatures (1100–1300 °C) than catalytic reforming (700–900 °C) [27]. For autothermal operation, higher temperatures can only be attained by oxidizing a larger part of the syngas and thereby losing fuel efficiency.

Not all contaminants that would act as catalyst poison in the FT reactor can be removed in the tar reformer. Therefore, additional gas cleaning steps are comprised in the gas cleaning section in Fig. 1. A novel adsorption-based gas cleaning system is studied here. This system is experimentally proven in conjunction with an SXB gasifier and an FT reactor [21]. Additionally, this technology is advantageous for small scale plants compared to conventional wet scrubbing technologies, such as Selexol or Rectisol, due to its simpler operation and reduced need for adsorbent replacement [21].

CO<sub>2</sub> removed from the syngas stream by a water scrubber is partly recycled to the SXB gasifier. This will improve the overall carbon conversion. Alternative measures to increase the process carbon conversion, e.g., the addition of hydrogen to gasifier or reformer stage [6, 8], are not studied here. The CO<sub>2</sub> recycling option appears to be most suitable for this concept because CO<sub>2</sub> can substitute steam as gasification medium [20].

Syngas from the gas cleaning section has a H<sub>2</sub>/CO ratio below the stoichiometric ratio of 2.1, especially when CO<sub>2</sub> is recycled. Hydrogen from the electrolyzer unit is added to the syngas prior to the FT reactor to attain the stoichiometric reactant ratio. Additionally, the electrolytically produced oxygen can be used in gasifier and reformer.

In the FT reaction, hydrogen and carbon monoxide are converted to long-chained hydrocarbons. The main reactions are the conversion to paraffine (Eq. 2) and olefin (Eq. 3) [28].



For this concept, a low temperature Fischer–Tropsch reaction over a cobalt catalyst is applied. Its high selectivity for the product fraction C<sub>5+</sub> sets it apart from the high temperature FT reaction [28]. The slurry bubble column reactor is selected as the reactor type rather than fixed bed or microreactor [5]. Advantages of the slurry bubble column are its high thermal stability and low investment cost [29].

The FT product is separated from short hydrocarbon molecules C<sub>1-4</sub>, unconverted reactants and the produced water. The hydrocarbon byproducts C<sub>1-4</sub> together with the unconverted reactants are recycled to the process in order to increase the product yield. In order to avoid inert gas

accumulation in the process, a fraction of the gas stream has to leave the process as off-gas. The off-gas is subsequently burned and considered in the heat integration.

## 2.2 Design options

### 2.2.1 Biomass feedstock

Biomass feedstock for the PBtL process can be broadly categorized into forestry and agricultural residue. First generation biofuels produced from food or animal feed crops are not included in this study. The advantage of focusing only on second generation biofuels is that their production is not in competition with food production [30].

The high availability of agricultural residue is a strong argument for its utilization for fuel production. In the EU, an annual availability of 139 Mt<sub>dry</sub> is estimated [31]. Whereas, forest residue has an annual potential of 40 Mt<sub>dry</sub> [31]. Yet, forest residue can be converted to fuel with less technical effort in the syngas cleaning section. The on average higher level of contaminants in agricultural biomass can only be reduced with a more energy-intense syngas cleaning in this process concept [20]. For both biomass types, continuous supply throughout the year is assumed.

The availability values used here can be seen as a rough benchmark. Studies on the biomass availability diverge in their estimated ranges. Searle and Marlins state a forest residue potential of 67 Mt<sub>dry</sub>/a. When considering biomass retention for soil quality, only 21.53 Mt<sub>dry</sub>/a remain [32]. Of the total agricultural residue of 315.9 Mt<sub>dry</sub>/a remain 119.8 Mt<sub>dry</sub>/a after subtracting the retention value [32]. Panoutsou and Maniatis find a forest residue availability of 41–68 Mt<sub>dry</sub>/a in 2030 [33].

### 2.2.2 Fischer–Tropsch off-gas recycle

An FT off-gas recycle is employed to increase the process product yield. Only a limited fraction of the hydrogen and carbon monoxide in the FT input stream can be converted to liquid product in a once-through operation [34]. A higher carbon conversion for the process can be attained by recycling the unconverted syngas. Here, different recycling options can be employed. In this work, three recycling options, as depicted in Fig. 1, are discussed.

The long recycle (LR) reintroduces the FT off-gas into the reformer. This allows the reforming of the short-chained hydrocarbon gas fraction C<sub>1-4</sub>. However, the long recycle needs to be heated up to the reformer temperature, typically 700–900 °C [27]. As an autothermal reformer is considered in this concept, energy for the temperature increase can only be provided by oxidizing part of the syngas stream. This, in turn, shifts the overall process yield from the product

towards CO<sub>2</sub> and steam. This option has been discussed in literature by several sources [35, 36].

The short recycle (SR) leads the off-gas stream to the FT inlet. Here, the recycle stream only needs to be heated up to the FT temperature, which in this concept is distinctly lower than the reformer temperature. In addition, the already clean FT off-gas stream does not have to be led through the syngas cleaning section. The short recycle has been studied in combination with a long recycle by Hillestad et al. [8].

For the short recycle reformer (SRR) option, an additional reforming stage is added in the short recycle loop. Thereby, the short-chained hydrocarbon gas fraction C<sub>1-4</sub> can be reformed while an unnecessary pass through the syngas cleaning section can be avoided. This saves capital and operational expenses in the gas cleaning section. Yet, these savings have to be weighed against the cost for the additional reformer.

### 2.2.3 Electrolysis technology

The electrolytic splitting of water into hydrogen and oxygen can be accomplished via different technology options. Here, the alkaline electrolysis (AEL) is compared with the solid oxide electrolysis cell (SOEC) technology.

The alkaline electrolysis has the highest technology readiness level of all currently available electrolysis technologies [37]. The largest AEL system currently installed has a reported capacity of 10 MW<sub>el</sub> [38]. Accordingly, investment costs for this technology are low compared to other electrolysis technology options [37, 39].

Although SOEC technology has the lowest technological development level, its high electric efficiency promises low operation costs. SOEC systems are commonly operated at a high temperature range of 700–900 °C, opposed to 60–90 °C for AEL. At this temperature range, a large part of the reaction enthalpy can be covered by thermal instead of electrical energy [37].

Both technologies have drawbacks in the context of high-pressure and highly dynamic applications. A proton exchange membrane (PEM) electrolyzer is more suitable for these operation conditions. Pressures up to 50 bar can be handled by a PEM electrolyzer, while the typical pressure range for AEL systems only operate up to 30 bar [37].

Similarly, its low start-up time and high load flexibility makes PEM the preferred technology over AEL and SOEC when operating the electrolyzer under flexible load [37].

### 2.2.4 CO<sub>2</sub> recycle rate

CO<sub>2</sub> is removed from the syngas stream in the gas cleaning section via a pressurized water scrubber [21]. The removed CO<sub>2</sub> can be reintroduced into the SXB gasifier. Here, CO<sub>2</sub> can replace steam as a dilution medium for oxygen [40]. A higher CO<sub>2</sub> recycle rate leads to a higher carbon conversion and, consequently, a higher total product yield. However, it also prompts a higher hydrogen demand to fix the H<sub>2</sub>/CO ratio to the stoichiometric value of 2.1. As a consequence, the higher product yield has to be weighed against the additional electricity demand for the electrolyzer.

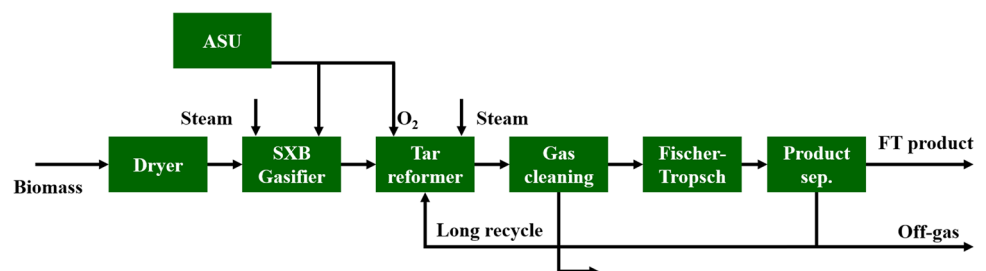
## 2.3 Biomass to Liquid

To have a reference case, the PBtL process is simulated alongside the BtL process [6]. In contrast to the PBtL process, no electrolyzer is utilized for the conversion of biomass to FT fuel in the BtL process. This lowers the product yield. Yet, investment for the electrolyzer and the connected electricity cost can be omitted.

The BtL process flowsheet can be taken from Fig. 2. The unit sequence from dryer to product separation relies on the same technology as the PBtL process, with two notable exceptions: Firstly, the BtL process has no CO<sub>2</sub> recycle. The stoichiometric H<sub>2</sub>/CO ratio for the FT reaction is adjusted by steam addition in the gasifier and reformer. Steam addition shifts the chemical equilibrium in the water gas shift reaction towards H<sub>2</sub> while depleting CO (cf. Equation 1). Secondly, the oxygen for reformer and gasifier has to be produced in an air separation unit (ASU) since no electrolyzer is used in the BtL process.

An ASU was chosen here, as it is the most mature technology for the separation of oxygen. Adsorption and chemisorption based solutions should be monitored as alternative solutions as their technical maturity increases [41]. Especially for applications with a low oxygen demand, these solutions can be favorable. Air separation units have an economic application range higher than 20 sTPD (short

Fig. 2 BtL flowsheet



tons per day sTPD) [41]. Yet, for this BtL process concept an oxygen production of 155 TPD (171 short tons per day sTPD) is required.

## 2.4 Process model

The process analysis is based on a flowsheet simulation implemented in Aspen Plus® (V10). A super-structure model containing the two paths, PBtL and BtL, along with the described process design options is modeled. DLR's software tool TEPET enables the selection of path and process design with a subsequent automated techno-economic-ecological process analysis [42]. More specifically, a set of simulation parameters are specified in TEPET. The program then runs simulations with the specified parameters and automatically retrieves the simulation results from Aspen Plus®. With the results, an automated utility integration is conducted before the techno-economic and GHG emission analysis can be performed. This allows for the rapid analysis of various process designs.

For the Aspen Plus flowsheet, the Soave–Redlich–Kwong equation of state is used [13], which is the recommended property method for hydrocarbon processes [43]. In the following sections, crucial modeling parameters are discussed in detail. Further assumptions can be found in the Supplementary Material.

All technical and economic modeling assumptions underlie different levels of uncertainty. Economic assumptions are almost all subject to price fluctuations, whereas technical parameters, such as the availability of biomass residues or the electrolyzer efficiency, are affected by macro-economic or technical developments. To ensure the validity of the statements derived from the simulation results, a sensitivity study is conducted for the most important parameters. To assess the uncertainty regarding the results further, methods such as the global sensitivity and uncertainty analysis could be applied in future work [44].

### 2.4.1 Feedstock model

To make a broader statement about the entire forest and agricultural residue, two representative feedstocks are chosen. Their respective properties can be found in Table 1. The total set of forest residue is represented by wood pellets as analyzed by Kurkela et al. [20]. Agricultural residues are simulated with the composition of sunflower husk [20].

### 2.4.2 Gasification and reforming section

The gasifier is operated at 5 bar and 850 °C. Steam and CO<sub>2</sub> function as the dilution medium for the gasifier's oxygen input. The mass flow of dilution medium is fixed to 1.3

**Table 1** Biomass feedstock compositions and thermodynamic properties as modeled in Aspen Plus [20]

Feedstock	Forest residue	Agricultural residue
Proximate analysis, wt. % dry basis		
Fixed carbon	17.1	22.2
Volatile matter	82.5	75
Ash	0.4	2.8
Ultimate analysis, wt. % dry basis		
Ash	0.4	2.8
C	49.8	52.1
H	6.3	5.8
N	0.13	0.7
S	0.01	0.14
O (difference)	43.36	38.46
Other properties		
HHV, MJ/kg <sub>db</sub> <sup>a</sup>	19.77	19.67
Initial moisture content, wt. %	50	50

<sup>a</sup>HHV calculation according to  $HHV = LHV_{dry} \cdot 0.02441 \cdot w_{H_2,db} \cdot (18.015/2.016)$

times the mass of oxygen input. These operation conditions represent set point 20/11B in the SXB test campaign [20].

The CO<sub>2</sub> and steam ratio in the dilution medium is variable in the simulation. The more CO<sub>2</sub> is recycled to the gasifier, the more steam can be replaced by CO<sub>2</sub> as dilution medium. For the base case, as defined in Sect. 2.5, CO<sub>2</sub> makes up 65% of the total dilution stream in accordance with set point 20/11B [20].

The SXB gasifier's hydrocarbon and tar formation, modeled as naphthalene and benzene, are fitted to the experimental results of operation point 20/11B [20]. In Aspen Plus, this is modeled with an RYield reactor. The molecule specific yield can be found in the Supplementary Material.

Syngas components H<sub>2</sub>, CO<sub>2</sub>, H<sub>2</sub>O, and CO react according to the water gas shift equilibrium (Eq. 1). Here, the reaction's equilibrium coefficient describes the ratio of H<sub>2</sub> and CO<sub>2</sub> to H<sub>2</sub>O and CO. A higher gasification temperature leads to a lower equilibrium coefficient. During the gasification experiments in the FLEXCHX project, the measured equilibrium coefficients were found to be lower than the theoretical values at the respective gasification temperature. To account for this effect in Aspen Plus, a second reactor stage is modeled using an RGibbs equilibrium reactor. The reactor temperature is set to 950 °C and subsequently cooled down to the actual gasification temperature of 850 °C.

Fly ash, formed in the gasification, is removed by a filter unit following the gasifier. At high temperatures, tar components form soot, which can lead to filter blinding [13, 20]. This is prevented by cooling the gasification syngas prior to the filter unit to 550 °C when agricultural residue serves

as feedstock. Forest residue, with its lower tar formation rate, can enter the filter with the unchanged temperature of 850 °C. Only for cases with a long FT off-gas recycle, a filter temperature of 700 °C is assumed, which accounts for the cooling effect of the recycle.

The autothermal reformer is operated at 750 °C for forest residues and 850 °C for agricultural residues. The higher temperature for agricultural residues is needed for a full conversion of the higher tar content in the syngas. At this temperature a conversion of 80% for CH<sub>4</sub>, NH<sub>3</sub>, and HCN is assumed [45]. The main components H<sub>2</sub>, CO<sub>2</sub>, H<sub>2</sub>O, and CO are brought into chemical equilibrium with an RGibbs reactor in Aspen Plus. The temperature is adjusted by iterating the oxygen input to the reformer. The oxygen has to be mixed with an equal mass flow of steam to provide the necessary oxygen dilution. For the BtL simulation, the steam addition is iterated to adjust the molar H<sub>2</sub>/CO ratio in the reformer product to 2.1. By adding steam to the water gas shift equilibrium (Eq. 1), CO is converted to CO<sub>2</sub> while the H<sub>2</sub> content is increased.

### 2.4.3 Fischer–Tropsch slurry bubble column reactor

The reaction kinetic by Todic et al. from 2017 is used to describe a continuous stirred tank reactor (CSTR) with Co/Re/γ-Al<sub>2</sub>O<sub>3</sub> catalyst loading [46]. The model is based on the carbide mechanism and fitted to experimental data for a temperature range of 478–503 K, a pressure range of 15–25 bar, an H<sub>2</sub>/CO ratio in the range of 1.4–2.1 and a weight hourly space velocity (WHSV) in the range of 1–22.5 l<sub>N</sub>/(g<sub>cat</sub> h). N-alkanes and primary alkenes with a carbon chain length up to 30 are considered as product. Equations 4 to 9 give the reaction rate expressions for the kinetic model [46]. Contrary to earlier work by the research group [47, 48], Todic et al. include Eqs. 8 and 9 to account for the secondary 1-olefin hydrogenation kinetic and the secondary pathway for methane formation [46]. Especially for a short recycle process design, the secondary 1-olefin hydrogenation is an important aspect to consider. Unreformed olefins can be re-adsorbed at the FT catalyst and their chain growth may continue. This effect leads to a higher product yield.

$$R_{C_nH_{2n+2}}^{prim} = \frac{k_7 K_2^{0.5} p_{H_2}^{0.5} \alpha_1 \prod_{i=3}^n \alpha_i}{DENOM^2} \quad n \geq 2 \quad (4)$$

$$R_{C_nH_{2n}}^{prim} = \frac{k_{8,0} e^{cn} \alpha_1 \alpha_1 \prod_{i=3}^n \alpha_i}{DENOM} \quad n \geq 3 \quad (5)$$

$$R_{C_2H_4}^{prim} = \frac{k_{8E,0} e^{c^2} \alpha_1 \alpha_1}{DENOM} \quad (6)$$

$$R_{CH_4}^{prim} = \frac{k_7 K_2^{0.5} p_{H_2}^{0.5} \alpha_1}{DENOM^2} \quad (7)$$

$$R_{CH_4}^{sec} = \frac{k_M^* P_{CO} P_{H_2}}{DENOM^{*2}} \quad (8)$$

$$R_{C_nH_{2n}}^{*,hyd} = \frac{k_{OH} P_{C_nH_{2n}} K_2^* P_{H_2}}{DENOM^{*2}} \quad n \geq 2 \quad (9)$$

The differential system of equations contains partial pressure expressions of H<sub>2</sub>, CO, H<sub>2</sub>O (in the denominator terms), and of all 1-olefins in the secondary hydrogenation term (Eq. 9). Therefore, an iterative solution is needed. Since no predefined reaction kinetic model in Aspen Plus fits this problem, a FORTRAN kinetic subroutine is used. The corresponding FORTRAN code can be found in the Supplementary Material. Additionally, a validation of the Aspen model with experimental results from [46] can be found in the Supplementary Material.

In Aspen Plus, the FT reactor is represented by an RCSTR block and operated at 230 °C and 25 bar. High pressure increases selectivity and reaction rate for the FT Co catalyst [28, 46]. Similarly, the highest catalyst activity can be found at high temperatures. Therefore, the highest temperature and pressure are chosen for which the model is still valid. At this operation point, the reactor is assumed to have a CO conversion of 55% [8]. The catalyst mass is iterated to find the defined CO conversion.

### 2.4.4 Electrolyzer

The two electrolyzer technologies, AEL and SOEC, are modeled with a splitter block operated at 25 bar. The AEL is operated at 60 °C with a system efficiency of 70.8%<sub>HHV</sub> [37]. For the SOEC technology, a system efficiency of 95%<sub>HHV</sub> is assumed in thermo-neutral operation [37]. The H<sub>2</sub> and O<sub>2</sub> product streams leave the electrolyzer at 230 °C after recuperation. Pressurized operation of an SOEC system is not technically feasible at the current state due to material restriction. However, it can be assumed that future technological development could make an operation at 25 bar possible [8]. As pressure level and system efficiency are optimistic assumptions, the result should be viewed as a best-case analysis for the SOEC technology.

## 2.5 Simulation case definition

Table 2 shows the process design configurations for the analyzed cases. A PBtL plant with an AEL, long recycle, and forest residue feedstock is chosen as the base case. This configuration is the most likely design for a first-of-a-kind PBtL plant: The long recycle (LR) is commonly

**Table 2** Case definition for the modeled process design options

Case	PBtL (base case)	PBtL-SR	PBtL-SRR	PBtL-SOEC	PBtL <sub>AR</sub>	BtL
Electrolyzer technology	AEL	AEL	AEL	SOEC	AEL	-
FT recycle	LR	SR	SRR	LR	LR	LR
Biomass type	FR	FR	FR	FR	AR	FR

used in literature not only for PBtL [8, 35, 49] but also for BtL [50] simulations. Secondly, alkaline electrolysis has the highest technology readiness level [37]. Thirdly, average forest residue requires less effort in the syngas cleaning section [20] and is therefore the preferred option over agricultural residue.

The two other FT off-gas recycling methods, short recycle (SR) and short recycle with reformer (SRR), are discussed with the simulation cases PBtL-SR and PBtL-SRR. Further, when cases with a SOEC system are discussed instead of an AEL, these cases are denoted as PBtL-SOEC. To signify the use of agricultural residues (AR) the index notation PBtL<sub>AR</sub> is used. Finally, the reference case Biomass to Liquid will be referred to with the abbreviation BtL. For all BtL simulations, a long recycle is modeled.

## 2.6 Techno-economic analysis

### 2.6.1 Technical analysis

In order to assess the process performance from a technical perspective, carbon efficiency  $\eta_C$ , fuel efficiency  $\eta_{Fuel}$ , and process efficiency  $\eta_{Process}$  are considered in this study. Whereby, in all equations the product is defined as the liquid Fischer–Tropsch fraction C<sub>5+</sub>. The carbon efficiency  $\eta_C$ , as defined in Eq. (10), shows the share of biomass' carbon atoms that can be converted to product carbon [6].

$$\eta_C = \frac{\dot{n}_{C,Prod}}{\dot{n}_{C,Biom}} \quad (10)$$

The energetic fuel efficiency is stated in Eq. (11). It shows the fraction of the input energy that can be converted to FT product. Here, the lower heating value LHV of the wet biomass and the process power requirement  $P_{El}$  are considered as energy inputs [6].

$$\eta_{Fuel} = \frac{\dot{m}_{Prod}LHV_{Prod}}{\dot{m}_{Biom}LHV_{Biom} + P_{El}} \quad (11)$$

For the process efficiency in Eq. 12, the process off-heat  $\dot{Q}_{Process}$  is included as an additional product. The calculation method for process off-heat and corresponding utility integration is automated in the software tool TEPET. The underlying methodology is described in [42].

$$\eta_{Process} = \frac{\dot{m}_{Prod}LHV_{Prod} + \dot{Q}_{Process}}{\dot{m}_{Biom}LHV_{Biom} + P_{El}} \quad (12)$$

For this study, a pinch temperature of 5 °C is assumed for the heat integration. Excess heat streams at a temperature level higher than 183 °C can be used for the production of high (35.5 bar), medium (20 bar), or low (10 bar) pressure steam. Here, a brown field site is assumed, where all steam types can be sold. The cooling demand for the process is provided by cooling water with an initial temperature of 15 °C and an outlet temperature of 20 °C. Cooling below 15 °C is accomplished with a refrigeration cycle with a refrigerant temperature of -10 °C. As an example, Fig. 3 shows the composite curve after utility integration for the base case. Here, no low-pressure steam is produced. Instead, the production of 8 MW<sub>th</sub> of high-pressure steam and 17 MW<sub>th</sub> of medium-pressure steam is prioritized, as these pressure levels generate higher revenue. In addition, a duty of 8 MW<sub>th</sub> for cooling and 0.5 MW<sub>th</sub> for refrigeration is required for the process.

### 2.6.2 Economic analysis

The economic analysis is based on the approach published by Peters, Timmerhaus, and West [51]. The calculation algorithm implemented in DLR's techno-economic software tool TEPET is described in [6, 42]. The aim of the economic analysis is to estimate the net production costs NPC. These are calculated, according to Eq. 13, as the ratio of all production cost divided by the product mass flow [42]. Annual capital cost ACC, indirect and direct operational expenditures OPEX and the hourly labor cost  $c_L$  multiplied with the number of workers per shift  $N_w$  contribute to the production cost. For all cases analyzed in this study, 7 workers per shift with hourly labor cost of 43.14 €/h [52] are assumed.

$$NPC = \frac{ACC + \sum OPEX_{ind} + \sum OPEX_{dir} + N_w c_L}{\dot{m}_{Product}} \quad (13)$$

Direct OPEX are calculated as the sum of all utility and feedstock costs and revenues for the byproducts. The corresponding utility prices can be found in Tables 3 and 6. Further, it is assumed that the plant can be operated for 8100 h per year in steady state mode, which is necessary for the economic operation especially of the electrolyzer [36]. Indirect

**Fig. 3** Composite curves including heat integration for the base case. Hot streams are depicted in red, cold streams in blue. Medium pressure (MPS), high pressure steam (HPS), cooling water (CW), and refrigeration (RF) utilities are marked in the plot

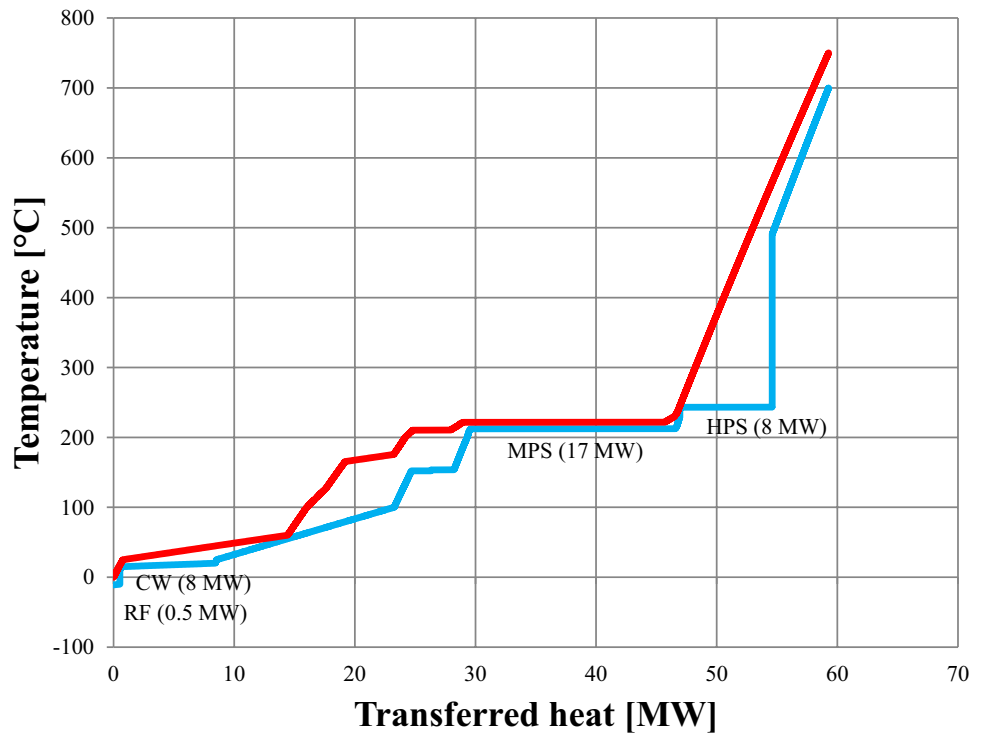


**Table 3** Utility and feedstock prices used for the production cost estimation. For electricity prices, please refer to Table 6

Utility	Prices	Source
Forest residue <sup>a</sup>	42.23 €/t	[53]
Agricultural residue <sup>a</sup>	40.01 €/t	[53]
Demineralized water for electrolysis	2 €/m <sup>3</sup>	[35]
Fresh water	0.426 €/m <sup>3</sup>	[54]
FT catalyst <sup>b</sup>	33 €/kg	[55]
Gas cleaning utilities	1.437 €/t	[56]
Waste water	0.907 €/m <sup>3</sup>	[51]
HPS	21.216 €/t	[57]
MPS	19.241 €/t	[57]
LPS	13.142 €/t	[57]
Cooling water	0.005 €/m <sup>3</sup>	[6]

<sup>a</sup>Price from ENSPRESO data base for FI 2020 for the MED scenario

<sup>b</sup>Catalyst lifetime of 5 years [58] with continuous replacement

OPEX account for additional production expenses such as maintenance, plant overhead or administration. The estimation algorithm for indirect OPEX can be taken from [6].

A plant’s annual capital cost *ACC* is calculated according to Eq. (14). Here, the capital cost is determined by the fixed capital investment *FCI*, the interest rate *IR*, 7% for all cases, and the plant lifetime *PL*, for which 20 years are assumed. Fixed capital investment *FCI*, Eq. (15) [6], represents the equipment cost for all plant equipment *E<sub>i</sub>* in combination

with their auxiliary cost, such as installation cost or cost for their instrumentation and controls. Auxiliary costs are estimated with Lang factors *F<sub>1-12</sub>* that may vary with the analyzed equipment type, cf. Table 4. A list of all Lang factor types can be found in the Supplementary Material.

$$ACC = FCI \cdot IR \left( \frac{(1 + IR)^{PL}}{(1 + IR)^{PL} - 1} + \frac{1}{9} \right) \tag{14}$$

$$FCI = \sum_{i=1}^m E_i \left( 1 + \sum_{j=1}^{10} F_{eco,i,j} \right) \left( 1 + \sum_{j=11}^{12} F_{eco,i,j} \right) \tag{15}$$

$$E_i = E_{ref,i} \left( \frac{S_i}{S_{ref}} \right)^k \left( \frac{CEPCI_{2020}}{CEPCI_{ref}} \right) \tag{16}$$

The equipment costs *E<sub>i</sub>*, follow from Eq. (16). Here, the cost for an equipment type is scaled up using a scaling exponent *k* from a reference unit, for which investment cost *E<sub>ref</sub>* and characteristic size *S<sub>ref</sub>* are known. The CEPCI term accounts for inflation from the reference year until 2020. A comprehensive list of all equipment cost functions can be found in Table 4.

### 2.7 GHG emission analysis

To assess the process’ greenhouse gas (GHG) emissions, an approach focusing on the two most impactful variables,

**Table 4** Equipment cost functions

Unit	$E_{ref}$	Currency	$S_{ref}$	Unit	$k$	Year	Source	Lang factors
Miscellaneous	3.5	M€	5.3	$kg_{biom,out}/s$	0.7	2019	[56]	E
Gas cleaning island	10.8	M€	8.25	$kg_{syng,in}/s$	0.7	2019	[56]	E
HRSG	6	M€	43.6	Transferred heat, [MW]	0.8	2010	[13]	C
ASU	13.8	M€	1.38	$kg_{O_2}/s$	0.7	2019	[56]	E
Syngas compressor	5	M€	10	Compression work, $MW_e$	0.67	2010	[13]	C
CO <sub>2</sub> compressor	5	M€	10	Compression work, $MW_e$	0.67	2010	[13]	C
Oxygen compressor	5.7	M€	10	Compression work, $MW_e$	0.67	2010	[13]	D
Gasification island <sup>d</sup>	31.6	M€	5.3	$kg_{biom,out}/s$	0.7	2019	[56]	E
Dryer & feedstock handling	7.5	M€	5.3	$kg_{biom,out}/s$	0.7	2019	[56]	E
Gas/liquid separator <sup>a</sup>	0.09	M€	10	Unit length, m	0.79	2014	[51]	A
Fischer–Tropsch SBCR <sup>c</sup>	2.025	M\$	341.3	Reactor volume, m <sup>3</sup>	0.67	1998	[59]	A
AEL <sup>b,c</sup>	1	M€	1	Electrical power input, $MW_e$	0.8	2019	[37]	E,B
SOEC <sup>b</sup>	2	M€	1	Electrical power input, $MW_e$	1	2019	[39]	E
Reformer (short recycle)	21.8	M€	2.037	Syngas, kmol/s	0.67	2010	[13]	C
Water scrubber (short recycle)	5.2	M€	1.446	Syngas input, kmol/s	0.67	2010	[60]	3

<sup>a</sup>Cost data for storage vessels were used. The cost function has three input parameters (vessel length, vessel diameter, pressure). The stated cost function is an example based on a horizontal storage vessel with a diameter of 2 m at pressure levels up to 10 bar [6]

<sup>b</sup>Maintenance cost 2% and 5% of stack investment for AEL and SOEC respectively [37]

<sup>c</sup>For exact costing method refer to [36]

<sup>d</sup>Includes gasifier, filter, and reformer

**Table 5** Impact factors on the process GHG footprint calculation

	Value	Source
Average biomass transport radius $r_{transport}$	100 km	[18]
Biomass transport emissions $GHG_{transport}$	69 $g_{CO_2,eq}/(t\ km)$	[61]
RED II fossil fuel comparator	94 $g_{CO_2,eq}/MJ$	[62]
GHG emission reduction for sustainable fuel	65%	[62]
AR harvesting $GHG_{harvest}$	0.27 MJ/kg <sub>AR</sub>	[63]
FR harvesting $GHG_{harvest}$	0.21 MJ/kg <sub>FR</sub>	[63]
Average crude oil price, Brent 2020	41.3 $\$/_{2020}/bbl$	[64]

biomass provision and electricity production [18], is taken. Assumptions for the biomass provision GHG calculation can be found in Table 5.

$$GHG_{process} = r_{transport}GHG_{transport} + GHG_{harvest} + P_{el}GHG_{el} \quad (17)$$

As shown in Eq. (17), total process emissions are calculated with transport  $GHG_{transport}$ , harvesting  $GHG_{harvest}$  and power production emissions  $GHG_{el}$ . Whereby, harvesting and transport are powered by fossil fuel. The biomass itself is regarded as carbon-neutral.

In this study, PBtL fuel falls under the definition of transport biofuel in the RED II directive [62]. The same classification for PBtL fuel is chosen in a recent study by the Policy Department for Structural and Cohesion Policies

[65]. At the same time, the GHG emission reduction limit for sustainable fuel for 2021 is used here. Although a different limit of 60% would apply for the studied year 2020, the 65% limit is used, as plants constructed in 2020 with a lifetime of 20 years would have to be designed according to the 65% limit.

The process is analyzed with different national grid electricity mixes, whereby the Finnish grid serves as the base case. Average carbon intensity and electricity prices are listed in Table 6. For the EU grid mix, average values for all 27 member states are taken into account.

When process GHG emissions and NPC are established, the GHG abatement cost  $AC$  can be calculated with Eq. 18. The abatement costs indicate how costly the GHG savings are when using an alternative fuel instead of fossil fuel. To that end, the additional cost for producing alternative fuel ( $NPC_{PBtL} - P_{crude\ oil}$ ) is divided by the amount of GHG savings expressed in CO<sub>2</sub> equivalents ( $GHG_{crude\ oil} - GHG_{PBtL}$ ). As the price for crude oil  $P_{crude\ oil}$  the average price for a barrel of Brent in 2020 is used. The fossil GHG emissions are calculated with the fossil fuel comparator defined in the RED II directive [68]. It should be noted that the RED II definition for fossil fuel includes the emissions during the burning process. These are not included for the alternative fuel, where only the production process has an impact on the GHG emissions. However, this assumption can be justified when considering their marginal combustion emissions [69].



**Table 6** Carbon intensity and electricity price for different European grid mixes

	Average grid electricity price [€ <sub>2020</sub> /MWh] [66]*	GHG footprint electrical power $GHG_{el}$ [kg <sub>CO2,eq</sub> /MWh] [67]
EU-27	59.3	230.7
Germany	64.3	311
Finland (base case)	45.9	68.6
Sweden	35.6	8.8
Norway	30.8	19
France	53.5	51.1

\*Prices for industrial consumers > 19 MW excluding VAT and other recoverable taxes and levies

$$AC_{PBtL} = \frac{NPC_{PBtL} - P_{crudeoil}}{GHG_{crudeoil} - GHG_{PBtL}} \quad (18)$$

potential production volume (Sect. 3.5). With that, conclusions about the possible fuel provision via the PBtL process for the EU aviation sector can be derived.

### 3 Results and discussion

After presenting the results for the different cases defined in the Sect. 3.1, a discussion of the design options under varying economic boundary conditions can be found in Sect. 3.2. The effect of selected process parameters on the base case results is shown in Sect. 3.3 with a sensitivity analysis. Finally, BtL and PBtL base case are compared in terms of their GHG abatement cost (Sect. 3.4) and their

#### 3.1 Techno-economic analysis

The results of the technical analysis can be taken from Table 7. The efficiency terms, as defined in Sect. 2.6.1, are displayed here along with key mass and energy flows. Similarly, economic results are shown in Table 8. For a discussion of the case studies, described in 2.5, refer to the following sections.

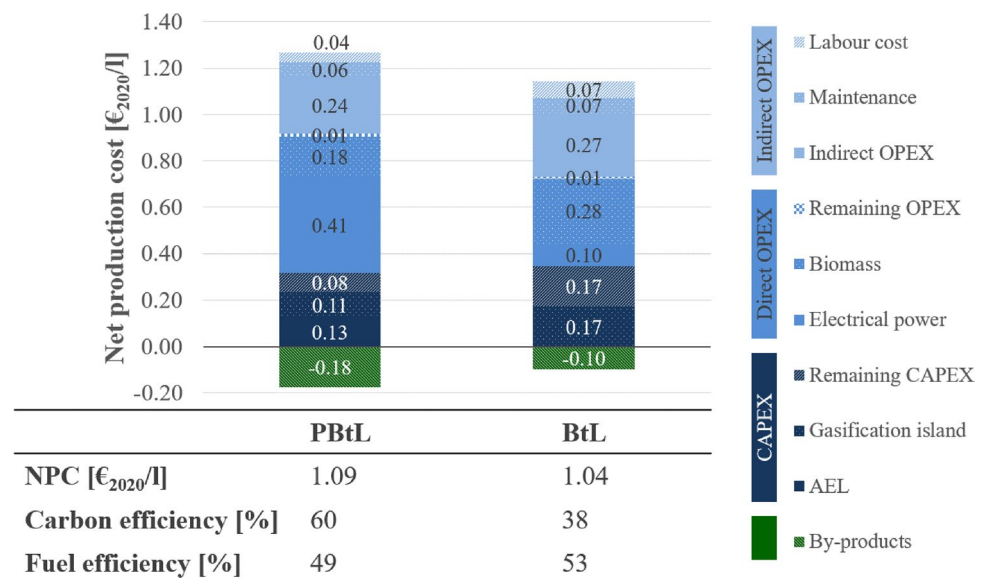
A breakdown of the NPC for the PBtL base case along with the BtL case is presented in Fig. 4. Whereby, the

**Table 7** Technical analysis: selected mass and energy flows for all cases

Case		PBtL	PBtL-SR	PBtL-SRR	PBtL-SOEC	PBtL <sub>AR</sub>	BtL
<i>Input</i>							
Wet biomass	kg/s	6.27	6.27	6.27	6.27	6.27	6.27
LHV wet biomass	MJ/kg	7.98	7.98	7.98	7.98	7.98	7.98
Total electrical power	MW <sub>el</sub>	48.8	35.4	62.1	38.2	61.8	7.18
Power electrolyzer	MW <sub>el</sub>	42.0	31.3	58.3	31.4	54.6	
H <sub>2</sub> production	kg/s	0.21	0.16	0.29	0.21	0.27	
<i>Product</i>							
Product output	kg/s	1.098	0.621	1.259	1.098	1.105	0.689
Product LHV	MJ/kg	44.0	44.2	44.0	44.0	44.0	44.0
<i>Alkanes</i>							
C5–10	kg/s	0.204	0.155	0.239	0.204	0.207	0.129
C11–20	kg/s	0.398	0.172	0.456	0.398	0.401	0.250
C21+	kg/s	0.359	0.095	0.401	0.359	0.358	0.223
<i>Alkenes</i>							
C5+	kg/s	0.136	0.199	0.163	0.136	0.139	0.087
<i>By-products</i>							
High pressure steam	MW <sub>th</sub>	7.65	6.34	8.91	4.66	15.2	7.84
Medium pressure steam	MW <sub>th</sub>	17.1	15.4	21.6	10.3	15.5	0
Low pressure steam	MW <sub>th</sub>	0	15.7	0	0	0	0
Process efficiency	%	73.9	75.9	76.6	71.7	71.0	66.7
Fuel efficiency	%	48.9	32.1	49.4	54.8	43.4	53.0
Carbon efficiency	%	59.8	33.8	68.5	59.8	57.4	37.5

**Table 8** Economic results for all simulation cases including largest OPEX and FCI cost items

Case		PBtL	PBtL-SR	PBtL-SRR	PBtL-SOEC	PBtL-AR	BtL
<i>OPEX</i>	M€ <sub>2020</sub> /a						
Electricity		18.1	13.2	23.1	14.2	23	2.7
Biomass		7.8	7.8	7.8	7.8	7.3	7.8
Other		0.5	0.9	0.6	0.6	0.6	0.3
Total		26.4	21.9	31.5	22.6	30.9	10.8
<i>Revenue by-product</i>	M€ <sub>2020</sub> /a	7.7	9.7	9.5	4.7	9.9	2.7
<i>FCI</i>	M€ <sub>2020</sub>						
Electrolyzer		53.9	41.1	72.9	60.4	68.7	0
Gasification island		46.2	46.2	46.2	46.2	46.2	46.2
Fischer–Tropsch reactor		11.7	38.2	13.7	11.7	11.9	8.3
Gas cleaning island		13.6	9.5	9.5	13.6	15.1	12.3
Recycle reformer		0	0	14	0	0	0
Other		10.6	6.9	11	10.6	11.7	26.2
Total		135.9	141.9	167.3	142.5	153.5	92.9
<i>Indirect OPEX</i>	M€ <sub>2020</sub> /a	10.6	10.9	12.2	10.9	11.5	8.4
<i>NPC</i>	€ <sub>2020</sub> /l	1.09	1.68	1.13	1.10	1.21	1.04

**Fig. 4** Comparison of PBtL and BtL base case including the breakdown of NPC in €<sub>2020</sub>/l by cost type

liquid FT product fraction has a density of 0.729 kg/l. Given the analyzed economic boundary conditions, production costs for PBtL are 0.05 €<sub>2020</sub>/l higher. Hereby, the largest NPC drivers for PBtL are the feedstock cost, electricity and biomass, and the electrolyzer investment cost.

Additionally, Fig. 4 shows carbon and fuel efficiency for both process types. Although the fuel efficiency is rather similar for BtL and PBtL, a large difference in carbon efficiency can be found. The higher carbon efficiency follows from the higher product output based on the same biomass input, which can be attributed to the CO<sub>2</sub> recycle. Yet, the recycle necessitates the electrolyzer to adjust the H<sub>2</sub>/CO ratio in the syngas to the stoichiometric value of 2.1. The

effects of an increased CO<sub>2</sub> recycling rate on NPC and carbon efficiency are further discussed in Sect. 3.2.

### 3.2 Discussion of design options under varying boundary conditions

The technical and economic results for the process design options under Finnish boundary conditions are presented in Sect. 3.1. To highlight the advantages of certain process design options, those are discussed under varying economic boundary conditions.

### 3.2.1 Electrolyzer choice and CO<sub>2</sub> recycling under variable electricity price

The electricity cost is the largest operation cost contributor to the PBtL process under Finnish conditions, as seen in Table 8. In Fig. 5, the electricity price is varied for BtL as well as PBtL with the two electrolyzer options, AEL and SOEC. Changing electricity prices have the largest effect on the PBtL-AEL NPC. This is due to the large power demand for the AEL compared to the other cases, as shown in Table 7.

Overall, the base case PBtL-AEL has the economic edge over BtL and PBtL-SOEC at electricity prices lower than 39.4 €/MWh. At higher prices, the BtL process is the preferable option. The advantage of the SOEC, its higher electrolytic efficiency, gains importance at higher electricity prices. Yet, the lower investment cost for the AEL system makes it the more cost effective technology choice at low electricity prices.

For the cases analyzed thus far, the CO<sub>2</sub> recycling is iterated to attain an oxygen dilution rate of 65% in the gasifier feed (cf. Section 2.4.2). This amounts to a CO<sub>2</sub> recycling ratio of 44% for the base case. In Fig. 6, the effect of

changing the CO<sub>2</sub> recycle rate is depicted. Here, the oxygen dilution is varied from 10 to 100% resulting in a CO<sub>2</sub> recycle rate of 7 to 70%.

As can be taken from the left plot in Fig. 6, the carbon efficiency and thereby the product yield of the process increases with the CO<sub>2</sub> recycling rate. This is to be expected, as more biogenic carbon leaves the gasification island as CO. Yet, the increased CO output leads to a reduction in the syngas' H<sub>2</sub>/CO ratio. In the analyzed CO<sub>2</sub> recycle range, the H<sub>2</sub>/CO ratio drops from 2.05 to 1.34. Subsequently, more electrical power is needed to adjust the H<sub>2</sub>/CO ratio to the stoichiometric value of 2.1. At the maximum CO<sub>2</sub> recycling rate, 80 MW<sub>el</sub> total energy input are required while only 8 MW<sub>el</sub> are needed for the minimal rate.

The right plot in Fig. 6 shows which effect a higher CO<sub>2</sub> recycling rate has on the NPC when assuming different electricity prices. For the Finnish electricity price in 2020 (45.9 €/MWh), increased recycling leads to higher NPC. Here, the additional electricity costs outweigh the cost benefits of a higher product output. Only for electricity prices lower than 20 €/MWh, a decrease in NPC can be expected. This parameter variation shows an example, how the optimal plant configuration is influenced by the local cost boundary

**Fig. 5** NPC over electricity price for the base case PBtL-AEL (dark blue), PBtL-SOEC (light blue), and BtL (green)

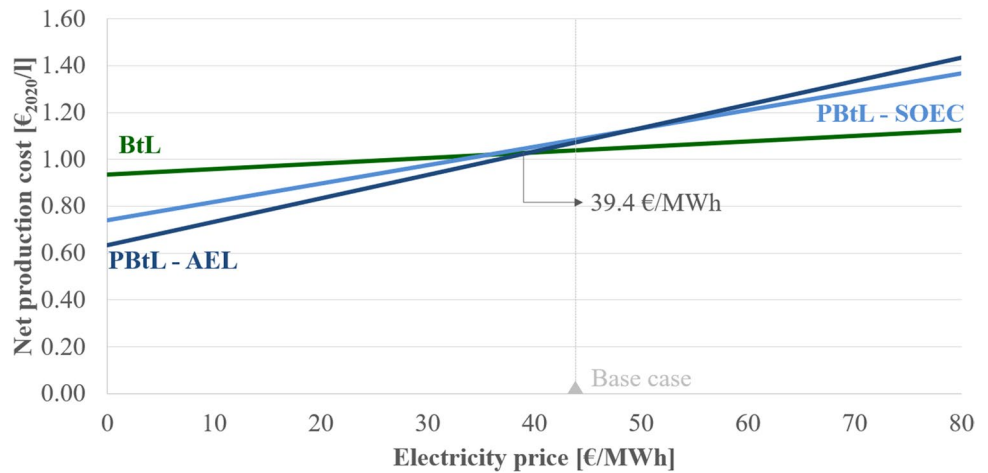
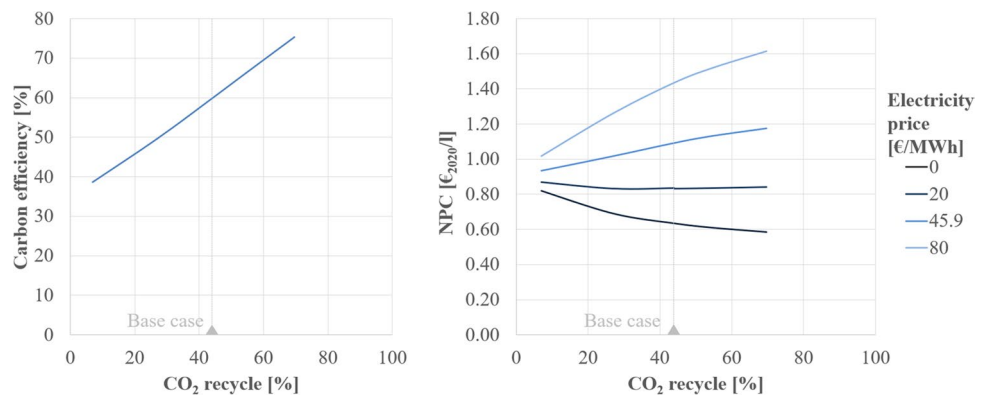


**Fig. 6** Effect of an increase in CO<sub>2</sub> recycle rate on carbon efficiency (left) and NPC (right) for the PBtL base case



conditions. An optimal CO<sub>2</sub> recycling rate can only be determined with a techno-economic assessment.

### 3.2.2 Recycle options and feedstock

Figure 7 compares NPC for the analyzed recycle options when using forest residue (FR) or agricultural residue (AR) as feedstock. It is apparent that for both biomass types SR results in the highest NPC: 1.68 €<sub>2020</sub>/l for FR and 2.16 €<sub>2020</sub>/l for AR. This suggests that reforming the recycled FT gas fraction C<sub>1-4</sub> is economically reasonable under the given economic constraints. As the SR option has the lowest power demand of all PBtL recycle options (cf. Table 7), an argument can be made for using the SR at high electricity prices.

A slight NPC advantage can be found for the LR over the SRR option for forest residue. Here, the base case PBtL<sub>FR</sub>-LR (1.09 €<sub>2020</sub>/l) has lower NPC than PBtL<sub>FR</sub>-SRR (1.13 €<sub>2020</sub>/l). Yet, the advantage is reversed when using agricultural residue, with 1.21 €<sub>2020</sub>/l for PBtL<sub>AR</sub>-LR against 1.20 €<sub>2020</sub>/l for PBtL<sub>AR</sub>-SRR. As shown in Table 7, a higher product yield is found for the SRR case which comes at the cost of a higher electrolysis power input. This results in

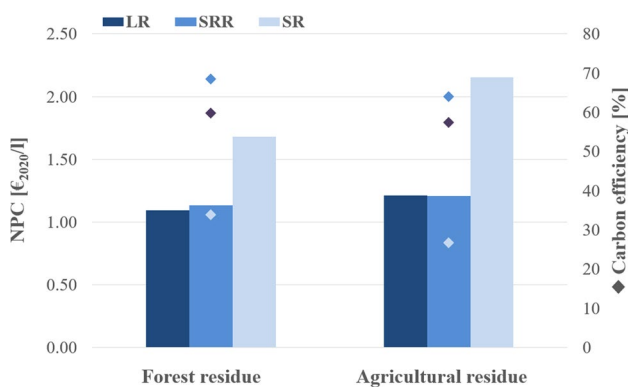
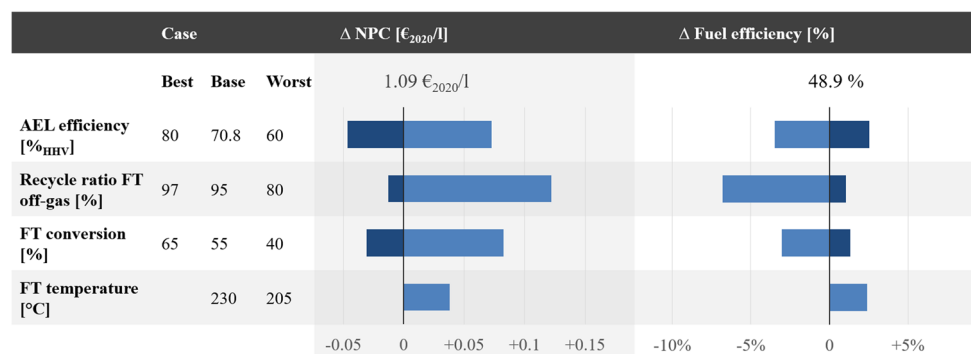


**Fig. 7** NPC shown with bars for short (SR), long (LR), and short recycle with reformer (SRR) using forest residue or agricultural residue. The carbon efficiency for all design options is indicated with diamond shapes referring to the right axis

**Fig. 8** Sensitivity of NPC and process efficiency to process parameters varied in the PBtL base case. Result for best (dark blue) and worst (light blue) case given as the absolute difference to the base case results



lower NPC for the LR case with FR at the base case electricity prices of 45.9 €<sub>2020</sub>/MWh. When using agricultural residue as feedstock, the filter temperature is decreased and reformer temperature increased compared to the forest residue case. This results in a higher electrolytic hydrogen demand. Therefore, a cost advantage can be found for the SRR option because the reformer recycle can be avoided. Overall, both options, SRR and LR, can be favorable options depending on the economic boundary conditions and should both be considered when designing a PBtL process.

The forest residue cases in Fig. 7 show consistently lower NPC and higher carbon efficiencies. This is due to the less intensive syngas treatment for forest residue. The lower tar formation rate allows for a syngas treatment with higher filter and lower reformer temperature compared to agricultural residues.

### 3.3 Base case sensitivity analysis

The effects of selected process parameters on NPC, carbon and fuel efficiency for the PBtL base case are displayed in Fig. 8. Here, the four parameters electrolyzer efficiency, recycle ratio, FT conversion, and temperature were chosen for their impact and uncertainty underlying their base case assumption.

The alkaline electrolyzer efficiency is simulated in the base case with a system efficiency of 70.8%<sub>HHV</sub>. In an expert elicitation study, Schmidt et al. [39] display system efficiency predictions that go as high as 80%<sub>HHV</sub>. Those predictions are connected to further development of the zero-gap AEL technology [70]. As a worst-case assumption, a system efficiency of 60%<sub>HHV</sub> is used.

The FT off-gas recycle rate is set to 95% in the base case. Although a higher recycling rate leads to increased overall syngas conversion, it is unclear how much off-gas can be recycled to the reformer. Inert gas components, such as N<sub>2</sub> formed in the gasifier, will accumulate in the recycle loop. Correspondingly, full recirculation is not possible. As a best-case assumption 97% is chosen. The worst-case is simulated with an 80% recycle.

To avoid the deactivation of the FT catalyst, the CO conversion should be limited [34]. Rytter and Holmen report a conversion limit of 65% for a slurry-bubble column reactor using cobalt catalyst [34]. Along with the base case assumption of 55% CO conversion [8], a worst-case of 40% is analyzed.

For low-temperature catalyst, the Fischer–Tropsch reactor operation temperature is typically given in the range of 190–240 °C [5]. The used reaction kinetic is based on experimental data in the range of 205–230 °C [46]. Therefore, worst and base case FT temperatures are chosen according to [46] as 205 °C and 230 °C.

Overall, a correlation of fuel efficiency and NPC can be observed in Fig. 8. Except for the FT temperature, higher fuel efficiency leads to lower NPC. This underlines the significance of low OPEX for the PBtL process. Higher NPC at low FT temperatures result from an increased capital expenditure for the FT reactor. Due to the lowered catalyst activity at 205 °C, more catalyst is needed to attain the same CO conversion. The higher product yield, a result of the higher product selectivity at low FT temperatures, cannot compensate for the higher FT reactor investment.

### 3.4 GHG abatement cost

The resulting fuel emissions, calculated according to the methodology described in Sect. 2.7, can be taken from the bar chart in Fig. 9. Here, it is assumed that the PBtL base case (blue) and the BtL reference case (green) are operated with different European national grid mixes. From fuel production emissions and NPC, the nation-specific abatement

costs can be calculated, which are depicted with diamond shapes referring to the right y-axis.

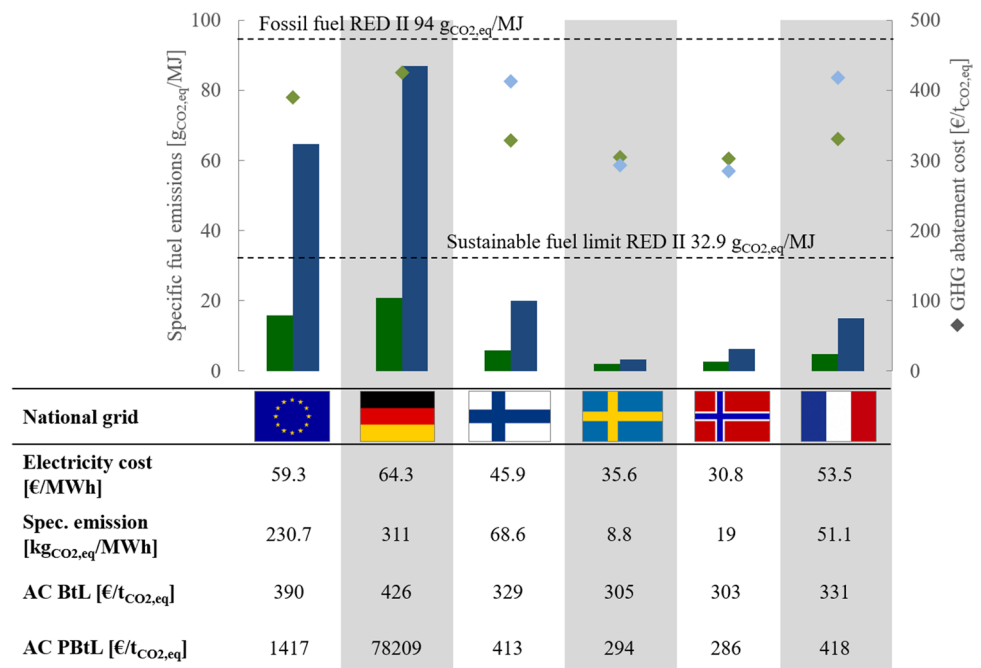
Using the PBtL base case configuration, only countries with low GHG footprint in their national grid can produce fuel that can be counted as sustainable according to the RED II directive in 2020 [62]. Here, a 65% reduction compared to fossil fuel has to be met for the sustainability limit, i.e., 32.9 g<sub>CO<sub>2,eq</sub></sub>/MJ. Using the German and EU-27 average electricity grid mix, this limit is exceeded. To stay under the limit, the electricity GHG footprint should not be higher than 116 kg<sub>CO<sub>2,eq</sub></sub>/MWh. All BtL cases, on the other hand, meet the sustainability limit due to their lower electricity demand.

Abatement costs scale with the electricity price and the electricity’s GHG footprint. For this reason, PBtL abatement costs for EU-27 and Germany are higher than 1000 €/t<sub>CO<sub>2,eq</sub></sub>, while Finland, Sweden, France, and Norway lie below 420 €/t<sub>CO<sub>2,eq</sub></sub>. As considerably less electricity is needed for the BtL process, GHG abatement cost range from 300 to 430 €/t<sub>CO<sub>2,eq</sub></sub> for the selected examples. Only for countries with relatively low electricity price and GHG footprint, such as Sweden or Norway, the PBtL GHG abatement costs lie below BtL. This underlines the importance of green and inexpensive electricity for the PBtL process.

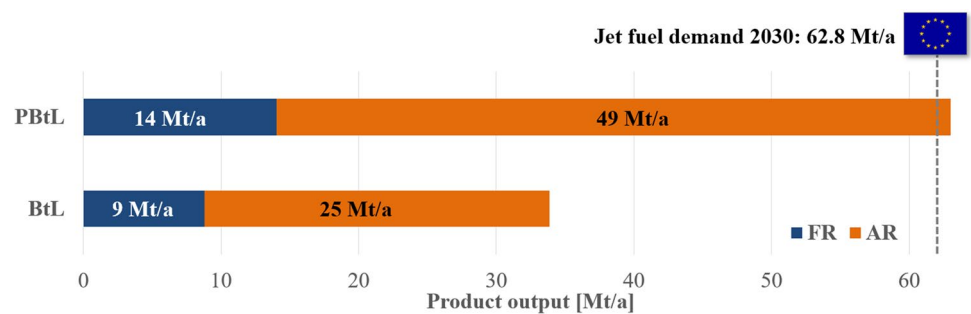
### 3.5 EU fuel potential analysis

Figure 10 shows the potential product output, if all currently available EU forest and agricultural residue is converted to fuel via the PBtL or the BtL route. The calculation is based on a total availability of 40 Mt<sub>dry</sub>/a forestry and 139 Mt<sub>dry</sub>/a agricultural residue in the EU [31]. The presented

**Fig. 9** Specific fuel production emissions indicated by bars and GHG abatement costs (AC) indicated by diamond shapes for the PBtL base case (blue) and BtL (green) using different national electricity grid mixes



**Fig. 10** Fuel production potential in the EU using forest residue (blue) and agricultural residue (orange) for BtL and PBtL (base case)



absolute product output values should be taken as an optimistic approximation. For one, only a part of the product fraction  $C_{5+}$  could actually be converted to SAF. Secondly, for a more exact estimation, local production conditions would have to be considered with locally varying biomass compositions and availability, as other sectors, such as heat and power production, compete for biomass residue as their feedstock. Still, the calculation allows for a comparison of BtL and PBtL because these optimistic assumptions affect both processes equally.

With the given assumptions, PBtL could produce around double the output (63 Mt/a) compared to BtL (34 Mt/a), whereby the agricultural residue makes up the bulk (~75%) of feedstock. The EU's jet fuel demand in 2030 of 62.8 Mt/a [7] could be met with PBtL when full biomass utilization is assumed. Yet, for this product output an installed AEL capacity of 101  $\text{GW}_{\text{el}}$  or 14.8 Mt/a of hydrogen would be required. Given that the European Commission only aims for a total  $\text{H}_2$  production rate of 10 Mt/a by 2030 [71], a substantial contribution the SAF production by the PBtL process can only be expected in later decades. Nevertheless, the results highlight the PBtL advantage over the BtL process of having a higher conversion rate of the limited biomass residue feedstock. This advantage could even be extended further with an increased  $\text{CO}_2$  recycling rate. Yet, the greater yield would have to be weight against the additional hydrogen demand as described in Sect. 3.2.1.

## 4 Conclusions

The Power and Biomass to Liquid (PBtL) process presents a promising pathway for the production of low GHG fuel. In this study, a techno-economic and GHG emission analysis has been conducted for a small-scale PBtL plant with a biomass input of 50  $\text{MW}_{\text{th}}$  and a 42  $\text{MW}_{\text{el}}$  alkaline electrolyzer producing 32 kt/a Fischer–Tropsch product. The analysis has been conducted on the basis of an Aspen Plus process model relying on experimental data from the EU project FLEXCHX as well as unit models from literature. Different process design options and a comparative Biomass to Liquid (BtL) case were assessed under varying economic boundary

conditions. Based on the findings in this study, the following assertions can be made:

- For the PBtL base case, net production costs (NPC) of 1.09  $\text{€}_{2020}/\text{l}$  have been estimated. Thereby, the cost for electrical power, biomass, and the AEL investment constitute the largest contributions to OPEX and CAPEX.
- The optimal process design and even the choice to use electrolytic hydrogen, largely depend on the local boundary conditions. A techno-economic analysis provides a good indication, which option to favor, but needs to be confirmed during the detailed design phase of any pursued project: The short recycle reformer (SRR) is advantageous at low electricity prices and when using feedstock requiring a high gas-cleaning effort. Short recycling (SR) should be avoided, if long recycle (LR) or SRR are feasible.
- Favoring an SOEC over an AEL electrolyzer is economically reasonable at high electricity prices. Here, the higher system efficiency can make up for the SOEC's higher investment costs.
- $\text{CO}_2$  recycling increases the carbon efficiency and, thereby, the product output. However, more hydrogen is required for the conversion. Therefore, NPC only fall with higher  $\text{CO}_2$  recycling rates, if the electricity price is below a certain threshold. For the base case, the price threshold is around 20  $\text{€}_{2020}/\text{MWh}$ .
- Generalizing from the two exemplary feedstocks analyzed in this study, it can be concluded that forest residue (FR) has a higher fuel efficiency and lower NPC than agricultural residue (AR). This is due to the on average lower tar formation rate for FR. Yet, in the EU more AR is available. The potential EU fuel output could be increased three-fold when utilizing AR in addition to FR.
- At low electricity prices ( $< 39.4 \text{ €}/\text{MWh}$ ), PBtL is the more cost-effective process option in comparison to BtL. In addition, a higher product output at similar fuel and process efficiencies can be expected. When converting the entire EU AR and FR potential, around double the fuel output would be generated with PBtL.
- Low GHG electricity is needed to produce sustainable fuel in accordance with the RED II directive: With the

German average 2020 grid mix of 311 g<sub>CO<sub>2</sub>,eq</sub>/MJ the RED II threshold of 32.9 g<sub>CO<sub>2</sub>,eq</sub>/MJ could not be met. For the base case, the electricity GHG footprint should not be higher than 116 kg<sub>CO<sub>2</sub>,eq</sub>/MWh. This is the case for countries like France, Finland, Sweden or Norway.

- For low GHG abatement costs green and inexpensive electricity is required: With the Norwegian or Swedish grid mix PBtL abatement costs below those of BtL can be reached.

The availability of green and inexpensive electricity is necessary for the production of fuel via the PBtL process. These conditions are not met in many countries in Europe. However, governments and industry are working on the reduction of GHG emissions from their national power production. In the opinion of the authors, fuel production in these countries should be ramped-up via the BtL process while this transition is under way. At a later stage, the process can be converted to PBtL by the addition of an electrolysis unit. This will increase the conversion of limited biomass residue.

**Supplementary information** The online version contains supplementary material available at <https://doi.org/10.1007/s13399-022-03671-y>.

**Acknowledgements** The authors would like to gratefully acknowledge the funding provided by the European Union's Horizon 2020 research and innovation program under Grant Agreement No 763919. Further, the authors would like to thank Julia Weyand, Moritz Raab, and for their valuable inputs.

**Author contribution** The study is based on Esa Kurkela process design as studied in the EU project FLEXCHX. Modeling, simulation, and analysis were done by Felix Habermeyer under the guidance of Ralph-Uwe Dietrich and Esa Kurkela. The GHG emission analysis was conducted by Julia Weyand. The software tool TEPET was provided by Simon Maier. The author Felix Habermeyer prepared the manuscript. Ralph-Uwe Dietrich, Esa Kurkela, Julia Weyand, and Simon Maier discussed and commented the manuscript.

**Funding** Open Access funding enabled and organized by Projekt DEAL. This study is part of the FLEXCHX project, which has received funding from the European Union's Horizon 2020 research and innovation Programme under Grant Agreement No 763919.

**Data availability** All data and materials as well as software application or custom code comply with field standards. Additional data is available in the Supporting Material.

## Declarations

**Ethical approval** Not applicable.

**Conflict of interest** The authors declare no competing interests.

**Open Access** This article is licensed under a Creative Commons Attribution 4.0 International License, which permits use, sharing, adaptation, distribution and reproduction in any medium or format, as long as you give appropriate credit to the original author(s) and the source, provide a link to the Creative Commons licence, and indicate if changes

were made. The images or other third party material in this article are included in the article's Creative Commons licence, unless indicated otherwise in a credit line to the material. If material is not included in the article's Creative Commons licence and your intended use is not permitted by statutory regulation or exceeds the permitted use, you will need to obtain permission directly from the copyright holder. To view a copy of this licence, visit <http://creativecommons.org/licenses/by/4.0/>.

## References

1. European Commission (2019) The European green deal. [https://eur-lex.europa.eu/resource.html?uri=cellar:b828d165-1c22-11ea-8c1f-01aa75ed71a1.0002.02/DOC\\_1&format=PDF](https://eur-lex.europa.eu/resource.html?uri=cellar:b828d165-1c22-11ea-8c1f-01aa75ed71a1.0002.02/DOC_1&format=PDF). Accessed 17 Jan 2023
2. European Commission (2021) Proposal for a regulation of the European parliament and of the council on ensuring a level playing field for sustainable air transport. [https://ec.europa.eu/info/sites/default/files/refuelev\\_aviation\\_-\\_sustainable\\_aviation\\_fuels.pdf](https://ec.europa.eu/info/sites/default/files/refuelev_aviation_-_sustainable_aviation_fuels.pdf). Accessed 17 Jan 2023
3. The White House (2021) Biden administration advances the future of sustainable fuels in American aviation. <https://www.whitehouse.gov/briefing-room/statements-releases/2021/09/09/fact-sheet-biden-administration-advances-the-future-of-sustainable-fuels-in-american-aviation/#:~:text=Current%20levels%20of%20domestic%20SAF,driving%20domestic%20innovation%20and%20deployment>. Accessed 17 Jan 2023
4. Shahriar MF, Khanal A (2022) The current techno-economic, environmental, policy status and perspectives of sustainable aviation fuel (SAF). *Fuel* 325. <https://doi.org/10.1016/j.fuel.2022.124905>
5. Ail SS, Dasappa S (2016) Biomass to liquid transportation fuel via Fischer Tropsch synthesis—technology review and current scenario. *Renew Sust Energy Rev* 58:267–286
6. Albrecht FG, König DH, Bauks N, Dietrich R-U (2017) A standardized methodology for the techno-economic evaluation of alternative fuels—a case study. *Fuel* 194:511–526. <https://doi.org/10.1016/j.fuel.2016.12.003>
7. O'malley J, Pavlenko N, Searle S (2021) Estimating sustainable aviation fuel feedstock availability to meet growing European Union demand. International Council on Clean Transportation. <https://theicct.org/publication/estimating-sustainable-aviation-fuel-feedstock-availability-to-meet-growing-european-union-demand/>. Accessed 17 Jan 2023
8. Hillestad M, Ostadi M, Serrano GA, Rytter E, Austbø B, Pharoah J, Burheim OS (2018) Improving carbon efficiency and profitability of the biomass to liquid process with hydrogen from renewable power. *Fuel* 234:1431–1451
9. Isaacs SA, Staples MD, Allroggen F, Mallapragada DS, Falter CP, Barrett SR (2021) Environmental and economic performance of hybrid power-to-liquid and biomass-to-liquid fuel production in the United States. *Environ Sci Technol* 55:8247–8257
10. Nielsen AS, Ostadi M, Austbø B, Hillestad M, del Alamo G, Burheim O (2022) Enhancing the efficiency of power-and biomass-to-liquid fuel processes using fuel-assisted solid oxide electrolysis cells. *Fuel* 321:123987
11. Dossow M, Dieterich V, Hanel A, Spliethoff H, Fendt S (2021) Improving carbon efficiency for an advanced biomass-to-liquid process using hydrogen and oxygen from electrolysis. *Renew Sustain Energy Rev* 152:111670
12. Clausen LR (2017) Energy efficient thermochemical conversion of very wet biomass to biofuels by integration of steam drying, steam electrolysis and gasification. *Energy* 125:327–336

13. Hannula I (2016) Hydrogen enhancement potential of synthetic biofuels manufacture in the European context: a techno-economic assessment. *Energy* 104:199–212. <https://doi.org/10.1016/j.energy.2016.03.119>
14. Menin L, Benedetti V, Patuzzi F, Baratieri M (2020) Techno-economic modeling of an integrated biomethane-biomethanol production process via biomass gasification, electrolysis, biomethanation, and catalytic methanol synthesis. *Biomass Conversion and Biorefinery* 13:1–22. <https://doi.org/10.1007/s13399-020-01178-y>
15. Poluzzi A, Guandalini G, Guffanti S, Elsidio C, Moioli S, Huttenhuis P, Rexwinkel G, Martelli E, Groppi G, Romano MC (2022) Flexible power & biomass-to-methanol plants: design optimization and economic viability of the electrolysis integration. *Fuel* 310:122113
16. Zhang H, Wang L, Maréchal F, Desideri U (2020) Techno-economic evaluation of biomass-to-fuels with solid-oxide electrolyzer. *Appl Energy* 270:115113
17. Bernical Q, Joulia X, Noirot-Le Borgne I, Floquet P, Baurens P, Boissonnet G (2013) Sustainability assessment of an integrated high temperature steam electrolysis-enhanced biomass to liquid fuel process. *Ind Eng Chem Res* 52:7189–7195
18. Koponen K, Hannula I (2017) GHG emission balances and prospects of hydrogen enhanced synthetic biofuels from solid biomass in the European context. *Appl Energy* 200:106–118
19. Kurkela E, Kurkela M, Frilund C, Hiltunen I, Rollins B, Steele A (2021) Flexible hybrid process for combined production of heat, power and renewable feedstock for refineries. *Johnson Matthey Technology Review* 65:333–345. <https://doi.org/10.1595/205651321X16013744201583>
20. Kurkela E, Kurkela M, Hiltunen I (2021) Pilot-scale development of pressurized fixed-bed gasification for synthesis gas production from biomass residues. *Biomass Conversion and Biorefinery* 1–22. <https://doi.org/10.1007/s13399-021-01554-2>
21. Frilund C, Tuomi S, Kurkela E, Simell P (2021) Small- to medium-scale deep syngas purification: Biomass-to-liquids multi-contaminant removal demonstration. *Biomass Bioenergy* 148:106031. <https://doi.org/10.1016/j.biombioe.2021.106031>
22. Müller S, Groß P, Rauch R, Zweiler R, Aichernig C, Fuchs M, Hofbauer H (2018) Production of diesel from biomass and wind power–energy storage by the use of the Fischer-Tropsch process. *Biomass Convers Biorefinery* 8:275–282
23. Shell Global (2021) Shell starts up Europe’s largest PEM green hydrogen electrolyser. <https://www.shell.com/media/news-and-media-releases/2021/shell-starts-up-europes-largest-pem-green-hydrogen-electrolyser.html>. Accessed 18 Aug 2021
24. Violidakis I, Drosatos P, Nikolopoulos N (2017) Critical review of current industrial scale lignite drying technologies. *Low-Rank Coals for Power Generation, Fuel Chemical Production* 41–71. <https://doi.org/10.1016/B978-0-08-100895-9.00003-6>
25. Peduzzi E, Boissonnet G, Haarlemmer G, Maréchal F (2018) Thermo-economic analysis and multi-objective optimisation of lignocellulosic biomass conversion to Fischer-Tropsch fuels. *Sustain Energy Fuels* 2:1069–1084
26. Bajirao UR (2012) Kinetics and reaction engineering aspects of syngas production by the heterogeneously catalysed reverse water gas shift reaction. Dissertation, Universität Bayreuth
27. Sikarwar VS, Zhao M, Fennell PS, Shah N, Anthony EJ (2017) Progress in biofuel production from gasification. *Prog Energy Combust Sci* 61:189–248. <https://doi.org/10.1016/j.pecs.2017.04.001>
28. Van Der Laan GP, Beenackers AACM (1999) Kinetics and selectivity of the Fischer-Tropsch synthesis: a literature review. *Catal Rev* 41:255–318
29. LeViness S (2013) Velocys Fischer-Tropsch synthesis technology—comparison to conventional FT technologies. In: AIChE 2013 Spring Meeting, San Antonio, Texas
30. Jeswani HK, Chilvers A, Azapagic A (2020) Environmental sustainability of biofuels: a review. *Proc Math Phys Eng Sci* 476:20200351. <https://doi.org/10.1098/rspa.2020.0351>
31. MMalins C, Searle S, Baral A, Turley D, Hopwood L (2014) Wasted: Europe's untapped resource: an assessment of advanced biofuels from wastes and residues. International Council on Clean Transportation. <https://theicct.org/wp-content/uploads/2021/06/WASTED-final.pdf>. Accessed 17 Jan 2023
32. Searle SY, Malins CJ (2016) Waste and residue availability for advanced biofuel production in EU Member States. *Biomass Bioenergy* 89:2–10. <https://doi.org/10.1016/j.biombioe.2016.01.008>
33. Panoutsou C, Maniatis K (2021) Sustainable biomass availability in the EU, to 2050. Concawe. [https://www.fuelseurope.eu/uploads/files/modules/publications/1661417357\\_Sustainable-Biomass-Availability-in-the-EU-Part-I-and-II-final-version.pdf](https://www.fuelseurope.eu/uploads/files/modules/publications/1661417357_Sustainable-Biomass-Availability-in-the-EU-Part-I-and-II-final-version.pdf). Accessed 17 Jan 2023
34. Rytter E, Holmen A (2017) Perspectives on the effect of water in cobalt Fischer-Tropsch synthesis. *ACS Catal* 7:5321–5328
35. Albrecht FG, Dietrich R-U (2018) Technical and economic optimization of Biomass-to-Liquid processes using exergoeconomic analysis. In: 26th European Biomass Conference & Exhibition (EUBCE), Copenhagen
36. Habermeyer F, Kurkela E, Maier S, Dietrich R-U (2021) Techno-economic analysis of a flexible process concept for the production of transport fuels and heat from biomass and renewable electricity. *Frontiers in Energy Research* 9:684. <https://doi.org/10.3389/fenrg.2021.723774>
37. Buttler A, Spliethoff H (2018) Current status of water electrolysis for energy storage, grid balancing and sector coupling via power-to-gas and power-to-liquids: a review. *Renew Sustain Energy Rev* 82:2440–2454
38. AsahiKasei (2020) <https://www.asahi-kasei.com/news/2020/ze200403.html>. Accessed 10 Aug 2021
39. Schmidt O, Gambhir A, Staffell I, Hawkes A, Nelson J, Few S (2017) Future cost and performance of water electrolysis: an expert elicitation study. *Int J Hydrogen Energy* 42:30470–30492. <https://doi.org/10.1016/j.ijhydene.2017.10.045>
40. Gao X, Zhang Y, Li B, Zhao Y, Jiang B (2016) Determination of the intrinsic reactivities for carbon dioxide gasification of rice husk chars through using random pore model. *Bioresour Technol* 218:1073–1081. <https://doi.org/10.1016/j.biortech.2016.07.057>
41. Smith A, Klosek J (2001) A review of air separation technologies and their integration with energy conversion processes. *Fuel Process Technol* 70:115–134
42. Maier S, Tuomi S, Kihlman J, Kurkela E, Dietrich R-U (2021) Techno-economically-driven identification of ideal plant configurations for a new biomass-to-liquid process – A case study for Central-Europe. *Energ Convers Manage* 247:114651. <https://doi.org/10.1016/j.enconman.2021.114651>
43. Aspen Technology Inc. (2013) Aspen physical property system - physical property methods. <https://docplayer.net/51476064-Aspen-physical-property-system-physical-property-models.html>. Accessed 17 Jan 2023
44. Adelung S (2022) Global sensitivity and uncertainty analysis of a Fischer-Tropsch based power-to-liquid process. *J CO2 Utilization* 65:102171
45. VTT (2020) Design and performance report for the reformer and final gas cleaning. Confidential FLEXCHX deliverable report D4.3
46. Todić B, Ma W, Jacobs G, Nikacević N, Davis BH, Bukur D (2017) Kinetic modeling of secondary methane formation and



- 1-olefin hydrogenation in Fischer-Tropsch synthesis over a cobalt catalyst. *Int J Chem Kinet* 49:859–874
47. Todic B, Ma W, Jacobs G, Davis BH, Bukur DB (2014) CO-insertion mechanism based kinetic model of the Fischer-Tropsch synthesis reaction over Re-promoted Co catalyst. *Catal Today* 228:32–39. <https://doi.org/10.1016/j.cattod.2013.08.008>
48. Todic B, Bhatelia T, Froment GF, Ma W, Jacobs G, Davis BH, Bukur DB (2013) Kinetic model of Fischer-Tropsch synthesis in a slurry reactor on Co-Re/Al<sub>2</sub>O<sub>3</sub> catalyst. *Ind Eng Chem Res* 52:669–679
49. Ostadi M, Rytter E, Hillestad M (2019) Boosting carbon efficiency of the biomass to liquid process with hydrogen from power: the effect of H<sub>2</sub>/CO ratio to the Fischer-Tropsch reactors on the production and power consumption. *Biomass Bioenerg* 127:105282. <https://doi.org/10.1016/j.biombioe.2019.105282>
50. Haarlemmer G, Boissonnet G, Imbach J, Setier P-A, Peduzzi E (2012) Second generation BTL type biofuels – a production cost analysis. *Energ Environ Sci* 5:8445. <https://doi.org/10.1039/C2EE21750C>
51. Peters MS, Timmerhaus KD, West RE, Timmerhaus K, West R (1968) Plant design and economics for chemical engineers. McGraw-Hill, New York
52. Krebs S (2015) Arbeitskosten pro Stunde im Verarbeitenden Gewerbe (2015). *Volkswirtschaft und Statistik, VDMA*. <https://www.vdma.org/documents/105628/778064/Internationaler%20Arbeitskostenvergleich%20Verarbeitendes%20Gewerbe/05a1a0bf-ea29-4a7a-b905-37ffec17957>. Accessed 16 Nov 2020
53. Ruiz P, Nijis W, Tarvydas D, Sgobbi A, Zucker A, Pilli R, Jonsson R, Camia A, Thiel C, Hoyer-Klick C (2019) ENSPRESO—an open, EU-28 wide, transparent and coherent database of wind, solar and biomass energy potentials. *Energ Strat Rev* 26:100379
54. Kempegowda RS, del Alamo G, Berstad D, Bugge M, Matas Güell B, Tran K-Q (2015) CHP-integrated fischer-tropsch biocrude production under norwegian conditions: techno-economic analysis. *Energy Fuels* 29:808–822
55. Swanson RM, Platon A, Satrio JA, Brown RC (2010) Techno-economic analysis of biomass-to-liquids production based on gasification. *Fuel* 89:S11–S19
56. VTT (2020) Gasification process design and performance report. Confidential FLEXCHX deliverable report D3.3.
57. Eurostat (2016) Gas prices for industrial consumers. [https://ec.europa.eu/eurostat/web/products-datasets/-/NRG\\_PC\\_203](https://ec.europa.eu/eurostat/web/products-datasets/-/NRG_PC_203). Accessed 17 Jan 2023
58. De Klerk A (2012) Fischer-tropsch refining. John Wiley & Sons
59. Bechtel (1998) Aspen process flowsheet simulation model of a battelle biomass-based gasification, Fischer-Tropsch liquefaction and combined-cycle power plant. US Department of Energy (DOE) Pittsburgh, Pennsylvania. <https://www.osti.gov/servlets/purl/1395>. Accessed 17 Jan 2023
60. Hannula I (2015) Co-production of synthetic fuels and district heat from biomass residues, carbon dioxide and electricity: performance and cost analysis. *Biomass Bioenerg* 74:26–46
61. NTM (2021) Road cargo transport baselines Europe. <https://www.transportmeasures.org/en/wiki/evaluation-transport-suppliers/road-transport-baselines-2020/>. Accessed 10 June 2022
62. European Parliament Council of the European Union (2018) Directive (EU) 2018/2001 of the European Parliament and of the Council of 11 December 2018 on the promotion of the use of energy from renewable sources. <http://data.europa.eu/eli/dir/2018/2001/oj>. Accessed 17 Jan 2023
63. Karlsson H, Börjesson P, Hansson P-A, Ahlgren S (2014) Ethanol production in biorefineries using lignocellulosic feedstock—GHG performance, energy balance and implications of life cycle calculation methodology. *J Clean Prod* 83:420–427
64. Index Mundi (2022) Crude oil (petroleum) monthly price - US dollars per barrel. <https://www.indexmundi.com/commodities/?commodity=crude-oil&months=60>. Accessed 10 Jun 2022
65. Gerard F, Gorner M, Lemoine P, Moerenhout J, De Haas V, Cazzola P (2022) Assessment of the potential of sustainable fuels in transport in the context of the Ukraine/Russia crisis. [https://www.europarl.europa.eu/RegData/etudes/IDAN/2022/699650/IPOL\\_IDA\(2022\)699650\\_EN.pdf](https://www.europarl.europa.eu/RegData/etudes/IDAN/2022/699650/IPOL_IDA(2022)699650_EN.pdf). Accessed 17 Jan 2023
66. Eurostat (2021) Electricity prices for non-household consumers - bi-annual data. <http://appsso.eurostat.ec.europa.eu/nui/submitViewTableAction.do>. Accessed 31 Jan 2022
67. Agency EE (2022) Greenhouse gas emission intensity of electricity generation by country [https://www.eea.europa.eu/data-and-maps/daviz/co2-emission-intensity-9/#tab-googlechartid\\_googlechartid\\_googlechartid\\_chart\\_1111](https://www.eea.europa.eu/data-and-maps/daviz/co2-emission-intensity-9/#tab-googlechartid_googlechartid_googlechartid_chart_1111). Accessed 31 Jan 2022
68. Commission E (2018) Renewable Energy – Recast to 2030 (RED II). [https://joint-research-centre.ec.europa.eu/welcome-jec-website/reference-regulatory-framework/renewable-energy-recast-2030-red-ii\\_en](https://joint-research-centre.ec.europa.eu/welcome-jec-website/reference-regulatory-framework/renewable-energy-recast-2030-red-ii_en). Accessed 24 Mar 2022
69. De Jong S, Antonissen K, Hoefnagels R, Lonza L, Wang M, Faaïj A, Junginger M (2017) Life-cycle analysis of greenhouse gas emissions from renewable jet fuel production. *Biotechnol Biofuels* 10:64. <https://doi.org/10.1186/s13068-017-0739-7>
70. Phillips R, Dunnill Charles W (2016) Zero gap alkaline electrolysis cell design for renewable energy storage as hydrogen gas. *RSC Adv* 6:100643–100651. <https://doi.org/10.1039/c6ra22242k>
71. European Commission (2022) Hydrogen: commission supports industry commitment to boost by tenfold electrolyser manufacturing capacities in the EU [https://ec.europa.eu/commission/press-corner/detail/en/ip\\_22\\_2829](https://ec.europa.eu/commission/press-corner/detail/en/ip_22_2829). Accessed 8 Dec 2022

**Publisher's note** Springer Nature remains neutral with regard to jurisdictional claims in published maps and institutional affiliations.

## Publication III

### **Sustainable aviation fuel from forestry residue and hydrogen – a techno-economic and environmental analysis for an immediate deployment of the PBtL process in Europe**

F. Habermeyer, V. Papantoni, U. Brand-Daniels and R.-U. Dietrich

Sustainable Energy & Fuels

DOI: 10.1039/D3SE00358B

#### **Author Contributions:**

Conceptualization, F.H., V.P., R.-U. D., U.B.; Data curation, F.H., V.P.; Formal analysis, F.H., V.P.; Funding acquisition, R.-U. D., U.B.; Investigation, F.H., V.P.; Methodology, F.H., V.P.; Project administration, F.H.; Resources, R.-U. D., U.B.; Software, F.H., V.P.; Supervision, R.-U. D., U.B.; Validation, F.H., V.P.; Visualization, F.H., V.P.; Writing – original draft, F.H., V.P.; Writing – review & editing, F.H., V.P., R.-U. D., U.B.

## PAPER



Cite this: *Sustainable Energy Fuels*,  
2023, 7, 4229

# Sustainable aviation fuel from forestry residue and hydrogen – a techno-economic and environmental analysis for an immediate deployment of the PBtL process in Europe†

Felix Habermeyer,<sup>a</sup> Veatriki Papantoni,<sup>b</sup> Urte Brand-Daniels<sup>b</sup>  
and Ralph-Uwe Dietrich<sup>a</sup>

Sustainable aviation fuels offer the opportunity to reduce the climate impact of air transport while avoiding a complete overhaul of the existing fleet. For Europe, the domestic production of sustainable aviation fuel would even lead to a reduced dependency on energy imports. Biomass-based fuel production in Europe is limited by the availability of sustainable biomass. This limitation can be alleviated by the Power and Biomass to Liquid (PBtL) process, which attains near full biogenic carbon conversion to Fischer–Tropsch fuel by the addition of electrolytic hydrogen. This study evaluates the economic feasibility and environmental impact of the sustainable aviation fuel production from European forest residue based on a region-specific analysis. As of 2020, only a few sweet spots, such as Norway or Sweden, could serve as production sites for sustainable PBtL fuel when the electrical energy for the electrolysis is supplied by the national grid. The grid mix for many other countries is too carbon intensive to justify producing PBtL fuel there. Yet, with the direct usage of renewable electricity sources, a fuel output of 25 Mt a<sup>-1</sup> can be reached assuming 33% of all forest residue can be used for fuel production. Under these conditions, the EU goal of providing 32% of the total aviation fuel demand with sustainable aviation fuel in 2040 could be met.

Received 17th March 2023  
Accepted 13th July 2023

DOI: 10.1039/d3se00358b  
[rsc.li/sustainable-energy](https://doi.org/10.1039/d3se00358b)

## 1. Introduction

The European aviation industry faces two challenges today. First, as a net contributor of 3.8% to the total European CO<sub>2</sub> emissions,<sup>10</sup> the aviation industry is poised to reduce its carbon emissions to net-zero by 2050.<sup>13</sup> Sustainable aviation fuel (SAF) offers an immediate solution for emission reduction that does not require a complete technology overhaul of the existing fleet by switching to alternative energy carriers or propulsion systems<sup>17</sup> as with hydrogen or battery-electric aircrafts. Accordingly, the European Union aims to increase the SAF share in the fuel mix to 63%<sub>vol.</sub> by 2050 with its ReFuelEU Aviation initiative.<sup>22</sup> Secondly, the aviation industry is faced with the uncertainty related to energy imports. As currently seen with gas imports<sup>24</sup> or the oil crises of the 1970s, energy imports have an inherent default risk.

The Power and Biomass to Liquid (PBtL) process offers a solution for both challenges, as low greenhouse gas (GHG) SAF can be produced within Europe. The PBtL process converts

biomass feedstock *via* gasification to syngas. With the addition of electrolytic hydrogen, syngas reacts to hydrocarbon chains *via* the Fischer–Tropsch (FT) route. The product is then refined to FT synthetic paraffinic kerosene (FT-SPK), which is certified as a 50% drop-in fuel.<sup>11</sup> PBtL is not the only route to convert biomass to SAF. Alcohol to jet (AtJ), the synthesised iso-paraffine (SIP), and other Fischer–Tropsch routes without the addition of electrolytic hydrogen (Biomass to Liquid – BtL<sup>9</sup>) are also certified as drop-in fuels.<sup>30,31</sup> The PBtL process stands out from its alternatives due to its high carbon conversion. In general, SAF production processes convert a carbon source with low energy content (*e.g.* CO<sub>2</sub> 0 MJ<sub>LHV</sub> kg<sup>-1</sup> or dry biomass 19 MJ<sub>LHV</sub> kg<sup>-1</sup>) to a highly energy-dense fuel (43 MJ<sub>LHV</sub> kg<sup>-1</sup>). A full conversion of the carbon is only possible with an additional energy input.<sup>3</sup> The energy input *via* electrolytic hydrogen addition in the PBtL process leads to a higher carbon conversion compared to the BtL process. However, the additional product output has to be weighed against additional cost and global warming potential (GWP) for the hydrogen production.

To evaluate whether the PBtL process is a suitable solution for the production of SAF in Europe, three criteria have to be met. First, the European aviation sector will have an annual estimated fuel demand of 63 Mt a<sup>-1</sup> by 2030.<sup>21</sup> Can the PBtL process cover a significant amount of this SAF demand given the limited biomass feedstock in Europe? Secondly, the

<sup>a</sup>Institute of Engineering Thermodynamics, German Aerospace Centre (DLR), 70569 Stuttgart, Germany. E-mail: [Ralph-Uwe.Dietrich@dlr.de](mailto:Ralph-Uwe.Dietrich@dlr.de)

<sup>b</sup>Institute of Networked Energy Systems, German Aerospace Centre (DLR), 26129 Oldenburg, Germany

† Electronic supplementary information (ESI) available. See DOI: <https://doi.org/10.1039/d3se00358b>

environmental impact of the production chain has to be analysed. GHG emissions of sustainable fuel should be reduced by 65% compared to fossil fuel, *i.e.* less than  $32.9 \text{ g}_{\text{CO}_2, \text{eq}} \text{ MJ}_{\text{fuel}}^{-1}$ , as defined in the RED II directive.<sup>11</sup> Third, a cost analysis has to be conducted to understand whether the fuel can be produced at a reasonably low price.

### 1.1. Literature review

An overview of studies related to SAF production *via* the PBtL process shown in Table 1. The PBtL process has been the subject of several techno-economic analyses (TEA). Hillestad *et al.* find net production costs (NPC) of 1.7 \$<sub>2017</sub> per l for a PBtL process with 435 MW<sub>th</sub> biomass input assuming an electricity price of 50 \$ per MW per h.<sup>3</sup> Thereby, near full carbon recycling leads to a carbon efficiency of 91%. Albrecht *et al.* estimate production costs of 2.15 €<sub>2014</sub> per l<sub>gasoline equivalent</sub> at an electricity price of 105 € per MW per h.<sup>9</sup> The simulated PBtL plant with an output of 240 kt per year has a carbon efficiency of 97.7%. Isaacs *et al.* estimate local production costs for PBtL plants in the eastern part of the USA based on local biomass prices and PV and wind availability.<sup>12</sup> For every location, an off-grid electrolysis and hydrogen storage system is designed to produce a constant hydrogen stream at minimal cost. For the year 2030, the most inexpensive product quartile has a minimum selling price of 2.40 \$<sub>2030</sub> per l for systems operated with PV and wind input.

Studies regarding the environmental impact assessment of synthetic fuels focus on jet fuel *via* gasification of forestry residues and FT-synthesis (BtL pathway)<sup>35,36</sup> or *via* water electrolysis, direct air capture, and FT-synthesis (PtL pathway).<sup>37,38</sup> Bernical *et al.* investigate the combination of the BtL process with additional hydrogen sources (namely high-temperature steam and alkaline electrolysis) in order to benefit from the higher carbon conversion rate of such a hybrid process.<sup>16</sup> Apart from a techno-economic analysis, they also evaluate the GHG emissions of the hybrid pathway and demonstrate that it can only result in fuels compatible with EU requirements when electricity sources with very low fossil carbon intensity are used for electrolysis. Isaacs *et al.* also conduct an LCA of the PBtL

pathway in the USA for various biomass feedstocks (corn stover, switchgrass or willow) accounting for regional availability and compare it to the PtL and BtL pathways.<sup>12</sup> The study focuses on the impact of fuel production on climate change in terms of GWP and confirms the high sensitivity of the result to the electricity's emission intensity.

O'Malley *et al.* estimate the SAF production from forest residue *via* the BtL route to be 0.22 Mt a<sup>-1</sup> in Europe by 2030.<sup>21</sup> The authors account for feedstock availability, sustainable harvesting limits, utilisation competition for those materials, and SAF conversion yields. Yet, only the conversion *via* the BtL route is considered. This inevitably leads to lower SAF yields compared with PBtL. Furthermore, Prussi *et al.* claim that GHG neutrality in the European aviation industry can be achieved with the FT BtL route.<sup>23</sup> However, this statement is based on rough calculations assuming all possible feedstock, biomass from forestry and agriculture as well as municipal waste, is used for the production of aviation fuel.<sup>23</sup> Throughout literature no study on the SAF production potential of the PBtL process in Europe was found.

The aim of this study is to assess the economic feasibility and ecological impact of sustainable aviation fuel production *via* the PBtL process in Europe. The novelty in this approach lies in the combination of fuel production potential estimation, LCA and TEA, which take the local European boundary conditions into consideration. The analysis is based on a flowsheet simulation of a fixed size PBtL plant implemented in Aspen Plus®. To account for the production conditions within Europe, such as biomass and electricity price or GHG footprint of the local electricity production, an individual TEA and GHG emission calculation is conducted for around 300 European NUTS2 regions. Grid power, PV and wind energy are considered as energy sources for the PBtL process in separate scenarios. With this analysis, this study gives a unique insight into the PBtL process' SAF production volume, cost and GWP within Europe, as so far only studies for single locations have been published. A similar region-specific analysis has been conducted for the USA. However, this study also omits discussing the amount of SAF that can be produced within the analysed region.

Table 1 Studies on the production of SAF from biomass and electrolytic hydrogen

Study	Study type	Main finding	Reference year	Geographical		Plant size
				scope	Key assumptions	
Hillestad <i>et al.</i> <sup>3</sup>	TEA	NPC 1.7 \$ per l	2014	Norway	50 \$ per MW per h (grid)	435 MW <sub>th</sub> biomass input
Albrecht <i>et al.</i> <sup>9</sup>	TEA	NPC 2.15 € per l	2014	Germany	105 € per MW per h (grid)	240 kt a <sup>-1</sup> product output
Isaacs <i>et al.</i> <sup>12</sup>	TEA, GWP focused LCA	Grid: NPC <sub>2016</sub> 1.84 \$ per l, GWP <sub>2016</sub> 187 g <sub>CO<sub>2</sub>,eq</sub> MJ <sub>fuel</sub> <sup>-1</sup>	2016, 2030 and 2050	USA	67.3 \$ per MW per h (grid)	1000 t <sub>dry</sub> d <sup>-1</sup> (~200 MW <sub>th,dry</sub> )
Bernical <i>et al.</i> <sup>16</sup>	TEA, GWP focused LCA	NPC 1.5 € per l, GWP 41 g <sub>CO<sub>2</sub>,eq</sub> kW <sup>-1</sup> h <sub>fuel</sub> <sup>-1</sup>	2011	France	70 € per MW per h 55 g <sub>CO<sub>2</sub>,eq</sub> kW <sup>-1</sup> h <sub>grid</sub> <sup>-1</sup> (grid)	500 MW <sub>th</sub> biomass input
O'Malley <i>et al.</i> <sup>21</sup>	Fuel potential	0.22 Mt <sub>SAF</sub> a <sup>-1</sup> from forest residue (fr)	2030	EU	BtL route (5.1 Mt <sub>fr</sub> a <sup>-1</sup> , 39% utilization, 0.22 g <sub>FT</sub> g <sub>fr</sub> <sup>-1</sup> , 0.5 g <sub>SAF</sub> g <sub>fr</sub> <sup>-1</sup> )	BtL route
Prussi <i>et al.</i> <sup>23</sup>	Fuel potential	Enough biomass potential to completely cover SAF demand	2019	EU28	BtL route	

## 2. Methodology

### 2.1. Process description

Fig. 1 depicts the process flowsheet including all selected technology options. The base case is simulated with a biomass input of 400 MW<sub>th</sub>. This has been shown to be a feasible size for processes with forest residue as feedstock.<sup>39</sup> It might be beneficial for future individual production sites, to adapt the plant size to the local availability of unused biomass and renewable electricity. Yet, for this calculation the size is kept constant.

This study focuses on forest residues omitting agricultural residues or municipal and industrial waste, which could also serve as feedstock for an FT process.<sup>21</sup> Agricultural residues, especially, have a larger potential compared to forest residues.<sup>21,40</sup> Yet, syngas production from forest residue appears to be less energy- and capital-intensive, as other feedstocks tend to have a higher contaminant content.<sup>41</sup>

A circulating fluidised bed (CFB) gasifier is selected for its low capital cost, broad spectrum of biomass feedstock and low oxygen demand.<sup>42,43</sup> The CFB gasifier uses CO<sub>2</sub> recycled from the syngas cleaning section as a dilution medium for the oxygen provided by the electrolyser. This type of gasification can be referred to as CO<sub>2</sub> gasification.<sup>44</sup> Ash from the gasifier is removed *via* a filter unit.

Biomass drying is accomplished with a belt dryer using air as drying medium. Air is used here instead of steam because the PBtL process is exothermic. Thus, the low temperature heat for air drying can be supplied by the process itself.

The syngas' tar concentration is reduced with a catalytic tar reformer. The reformation reaction decomposes large tar components into light gases.<sup>41,45</sup> Recycled CO<sub>2</sub> is used as

a dilution medium for the reformer oxygen feed as well. Additionally, this reactor partially reforms methane and ammonia. Compared to high temperature cracking, catalytic tar cracking requires less oxygen to reach its lower operation temperature.<sup>42</sup> Thereby, more H<sub>2</sub> and CO can be retained.

The removal of syngas contaminants, which can act as catalyst poison on the Fischer–Tropsch catalyst, is accomplished with cold gas cleaning steps. A heat recovery steam generation unit (HRSG) makes use of the syngas heat before feeding it into a water scrubber. The scrubber reduces the water content along with other gas contaminants such as ammonia.<sup>42</sup> CO<sub>2</sub> and H<sub>2</sub>S are removed in a Selexol scrubber.<sup>46</sup> Selexol was shown to have the lowest energy requirement for CO<sub>2</sub> removal compared to alternative removal technologies.<sup>46</sup> Before entering the Selexol scrubber, the syngas stream is compressed. Higher pressure levels are also beneficial for ab- and adsorption processes in the subsequent cleaning steps. Finally, trace contaminants such as alkali compounds are removed in a guard bed.<sup>42</sup>

The slurry bubble column (SBCR) is chosen as the Fischer–Tropsch reactor for its low investment costs at large scale<sup>47</sup> compared to micro-channel reactors and its relatively high CO conversion per pass compared to fixed bed reactors.<sup>48</sup>

Hydrogen and oxygen for the process are provided by an alkaline electrolysis (AEL) system, as the technology has the lowest current investment costs and the highest technological maturity.<sup>34</sup> AEL systems are even capable of operating with a flexible load due to their nominal load ramp speed of around 2% s<sup>-1</sup>.<sup>49</sup> In addition, no rare material is needed for the AEL production as opposed to the PEM technology, whose iridium demand might prove to be a bottleneck in the future.<sup>50</sup>

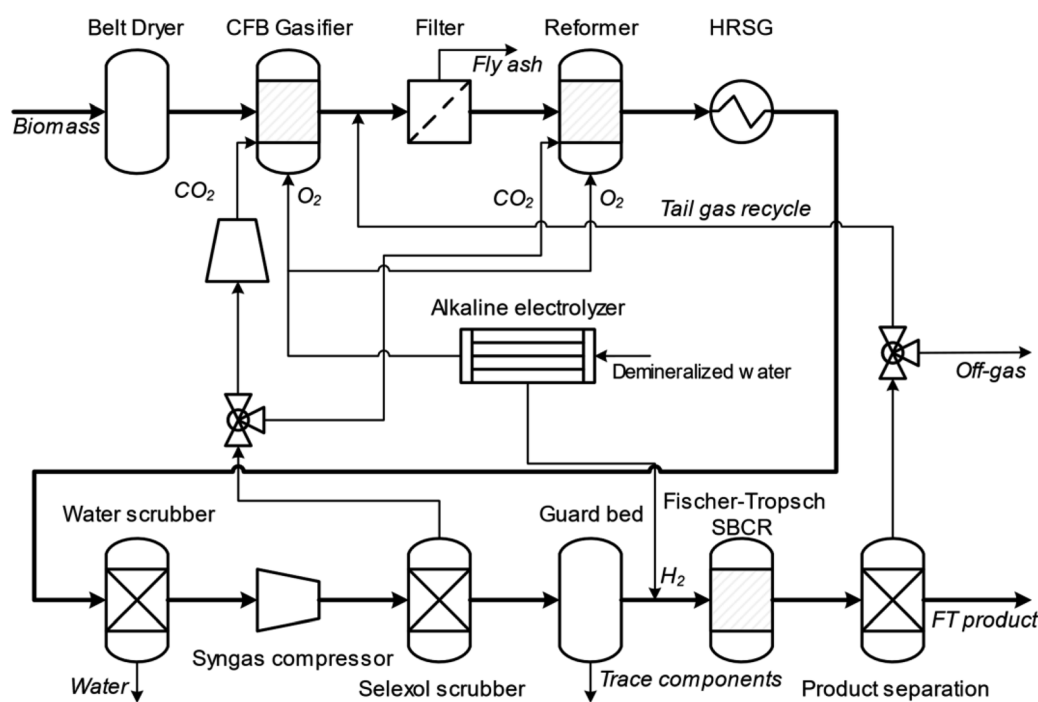


Fig. 1 Power Biomass to Liquid (PBtL) flowsheet showing all major process components.

In summary, that process was tested and validated in many research and demonstration projects in the past<sup>51,52</sup> and still lacks full-size proof of operation. However, current engineering knowledge provides enough confidence for a simulation of a full-size plant.

## 2.2. Process model

The process model is implemented in the commercial simulation software Aspen Plus® (V10). For the Aspen Plus® flowsheet, the Soave–Redlich–Kwong equation of state is used,<sup>5</sup> which is the recommended property method for hydrocarbon processes.<sup>53</sup> In the following sections, crucial modelling parameters are discussed in detail. Further assumptions can be found in the ESI.† A more detailed description of the modelling assumptions can be found in Habermeyer *et al.*<sup>4</sup>

**2.2.1. Feedstock.** As feedstock for the process, forest residue is chosen. The corresponding composition and higher heating value (HHV) are listed in Table 2. The initial moisture content before drying is assumed to be 50 wt%.<sup>5</sup> Before introducing biomass to the gasifier, the moisture content is decreased to 12 wt%<sup>5</sup> in the belt dryer.

**2.2.2. Gasification and reformer.** The circulating fluidised bed gasifier is operated at 850 °C and 4 bar.<sup>4,5</sup> The main syngas components are brought into chemical equilibrium at 900 °C using a RGibbs reactor. The yield functions for all other gasification products can be found in the ESI.† The oxygen input is iterated in order to attain a heat loss of 1% of the biomass feed's LHV. Recycled CO<sub>2</sub> is used in gasifier and autothermal reformer as dilution medium, whereby the gasifier has an equal feed mass ratio of oxygen to CO<sub>2</sub>. All remaining CO<sub>2</sub> is recycled to the reformer, which is simulated as an adiabatic equilibrium stage at 850 °C.<sup>4</sup> For this stage a CH<sub>4</sub> conversion of 35% is assumed.<sup>4</sup>

**2.2.3. Fischer–Tropsch.** The Fischer–Tropsch SBCR reactor is simulated with the kinetic reaction model developed by Todic *et al.*<sup>54</sup> The corresponding implementation in a FORTRAN

subroutine is documented in Habermeyer *et al.*<sup>4</sup> The CO conversion of 55%<sup>48</sup> at a fixed operation point of 220 °C and 25 bar is attained by iterating the catalyst mass in the FT reactor. In this study, the Fischer–Tropsch fraction C<sub>5+</sub> is considered as the final product of the process and subsequently regarded as SAF. Additional cost and conversion losses in the refining process are therefore not within the scope of this study. The pressure for the FT reactor is selected to maximise the selectivity for the product fraction C<sub>5+</sub> within the model's validity boundaries. The FT temperature of 220 °C is assumed to simulate a realistic product output. During operation, the FT reactor temperature is continually increased to counteract reversible catalyst degradation, thereby keeping the CO conversion constant. Therefore, selecting a temperature in the middle of the model's valid range (205–230 °C) reflects a typical reactor operation.

**2.2.4. Electrolyser.** The AEL is operated at the FT pressure level of 25 bar, whereby the H<sub>2</sub> output is iterated to achieve an H<sub>2</sub>/CO ratio in the FT feed. The system efficiency is assumed to be 70.8%<sub>HHV</sub>.<sup>34</sup>

**2.2.5. Heat integration.** The heat integration procedure determines the quantity of utilities supplied to or produced in the process. Net cooling demand and net heat generation are calculated in DLR's software tool TEPET by balancing the process' heat streams. The exact heat integration algorithm can be taken from Maier *et al.*<sup>55</sup> In this study, it is assumed that steam can be sold at three pressure levels: 10 bar at 183 °C (low pressure steam, LPS), 20 bar at 215 °C (medium pressure steam, MPS) and 35.5 bar at 245 °C (high pressure steam, HPS). Heat below the temperature of 183 °C, that is not used to heat up cold process streams, has to be cooled using cooling water at 25 °C. For the FT product separation at a temperature of 0 °C a refrigeration cycle is considered.

## 2.3. Technical process evaluation

Mass and energy balances are retrieved from the Aspen Plus® process simulation. Based on the resulting balances, the following four process performance indicators can be calculated. The carbon conversion denotes the percentage of biomass carbon that can be transformed to FT product.

$$X_C = \frac{\dot{m}_{C,prod}}{\dot{m}_{C,biom}} \quad (1)$$

The biomass conversion sets the total product mass in relation to the wet biomass input. As biomass consists of components that cannot be converted to FT product, the biomass conversion value is inevitably lower than 100%.

$$X_{biom} = \frac{\dot{m}_{prod}}{\dot{m}_{biom,wet}} \quad (2)$$

The energy fraction converted to product from biomass and electrical power input is represented by fuel efficiency.

$$\eta_{fuel} = \frac{\dot{m}_{prod} LHV_{prod}}{\dot{m}_{biom} LHV_{biom} + P_{el,input}} \quad (3)$$

Table 2 Forest residue properties<sup>30</sup>

	wt% dry basis
<b>Proximate analysis</b>	
Fixed carbon	25.3
Volatile matter	70.8
Ash	3.9
<b>Ultimate analysis</b>	
Ash	3.9
C	53.2
H	5.5
N	0.3
Cl	0
S	0.04
O (difference)	37.06
<b>Other properties</b>	
HHV, MJ kg <sup>-1</sup>	20.67
LHV, MJ kg <sup>-1</sup>	19.34
Initial moisture content, wt%	50

The process efficiency additionally includes by-products, in this case steam, at different pressure levels. Here, only the evaporation enthalpy  $\Delta H_v$  is considered.

$$\eta_{\text{process}} = \frac{\dot{m}_{\text{prod}} \text{LHV}_{\text{prod}} + \sum \dot{m}_{\text{byprod}} \Delta H_v}{\dot{m}_{\text{biom}} \text{LHV}_{\text{biom}} + P_{\text{el,input}}} \quad (4)$$

#### 2.4. Production cost estimation

The cost estimation methodology used in this study is described in Peters *et al.*<sup>26</sup> This methodology can be considered a current standard methodology on this field and is therefore used in many recent techno-economic studies.<sup>56–58</sup> The plant's net production cost (NPC) is comprised of the annuity for the capital expenditure (CAPEX), the direct operation expenditure (OPEX), including feedstock and utility cost, and the indirect operation cost, accounting for cost factors like insurance. The cost estimation is conducted with the software tool TEPET, as described by Albrecht *et al.*<sup>9</sup> and Maier *et al.*<sup>55</sup>

The capital expenditure is estimated based on equipment cost as well as indirect capital cost, such as the cost of installation. The equipment cost functions used for this study are given in Table 3. Here, a unit's equipment cost  $E$  follows from cost ( $E_{\text{ref}}$ ) and size ( $S_{\text{ref}}$ ) of a reference unit as a function of the unit's size  $S$  and a scaling exponent  $k$ . The cost estimation is conducted for the year 2020. The CEPCI index method is used to account for inflation when cost functions from older sources are used.<sup>26</sup> Further, the exchange rate to euro is considered by using the yearly average exchange rate.<sup>59</sup>

$$E = E_{\text{ref}} \left( \frac{S}{S_{\text{ref}}} \right)^k \quad (5)$$

Indirect capital costs are estimated by multiplying the equipment costs with the factors defined in the corresponding FCI method. These factors defined in Table 3 can be found in the ESI.<sup>†</sup> The sum of direct and indirect investments is referred to as fixed capital investment (FCI). The plant annuity, which accounts for the plant's depreciation, is then calculated assuming the plant can be operated for 20 years with an interest rate of 7%.<sup>55</sup>

Direct operation costs are calculated with the prices given in Table 4. For the base case, typical electricity and biomass prices for Finland<sup>9</sup> are considered. Indirect operation costs, such as maintenance and insurance, are estimated with the factors given in the ESI.<sup>†</sup> The cost of operating supervision for example is estimated as 15% of the operating labour. Here, the operating labour for the plant is estimated as 80 000 h a<sup>-1</sup> with average labour costs of 43.14 € per h.<sup>9</sup>

#### 2.5. Environmental impact assessment

Various environmental analysis methods have been developed over time, including procedural ones, such as Environmental Impact Assessment (EIA) or Strategic Impact Assessment (SIA), and analytical ones, such as Life Cycle Assessment, Material Flow Analysis and Environmental Risk Assessment.<sup>60</sup> The procedural methods EIA and SIA are usually applied to large projects in order to assist authorities or companies in their decision-making process. Analytical methods are more common in the assessment of products. LCA is used for environmental assessment in this study, as it allows to quantify the environmental impacts of a product, in this case sustainable aviation fuel, in different categories and provides insights into the contributions of single life cycle stages and processes to the overall impact.

According to the guidelines introduced in DIN EN 14040/44 (ref. 61) the LCA consists of four phases being: the goal and

Table 3 Equipment cost functions

Unit	$E_{\text{ref}}$	Currency	$S_{\text{ref}}$	Unit	$k$	Year	Source	FCI method <sup>d</sup>
Belt dryer and feedstock handling	24.8	M€	10.22	Evaporated water, kg s <sup>-1</sup>	0.7	2019	4	5
Ceramic hot gas filter	6.8	M€	1.466	Syngas input, kmol s <sup>-1</sup>	0.67	2010	5	3
Guard bed	6	M€	260	Syngas, MW <sub>th</sub>	0.85	2010	5	4
Selexol scrubber	54.1	M\$	9909	CO <sub>2</sub> feed, kmol h <sup>-1</sup>	0.7	2001	18	5
Water scrubber	5.2	M€	1.446	Syngas input, kmol s <sup>-1</sup>	0.67	2010	5	3
Pressurised O <sub>2</sub> CFB gasifier	37.7	M€	37.7	Dry biomass, kg s <sup>-1</sup>	0.75	2010	5	4
HRSG	6	M€	43.6	Transferred heat, [MW]	0.8	2010	5	3
Syngas compressor	5	M€	10	Compression work, MW <sub>e</sub>	0.67	2010	5	3
CO <sub>2</sub> compressor	5	M€	10	Compression work, MW <sub>e</sub>	0.67	2010	5	3
Catalytic reformer	21.8	M€	2.037	Syngas, kmol s <sup>-1</sup>	0.67	2010	5	3
Gas/liquid separator <sup>a</sup>	0.09	M€	10	Unit length, m	0.79	2014	26	1
Fischer-Tropsch SBCR <sup>b</sup>	2.025	M\$	341.3	Reactor volume, m <sup>3</sup>	0.67	1998	33	1
AEL <sup>c</sup>	1	M€	1	Electrical power input, MW <sub>e</sub>	0.8	2019	34	5
Refrigeration system	1976	\$	1	Refrigeration capacity, kW	0.67	2002	26	1

<sup>a</sup> Cost data for storage vessels were used. The cost function has three input parameters (vessel length, vessel diameter, pressure). The stated cost function is an example based on a horizontal storage vessel with a diameter of 2 m at pressure levels up to 10 bar.<sup>9</sup> <sup>b</sup> The reactor volume  $V$  is calculated assuming a catalyst loading of 140 kg m<sup>-3</sup>.<sup>33</sup> The specific cost for the cobalt catalyst (cobalt + support) is calculated with 33.07 \$<sub>2007</sub> per kg.<sup>20</sup> <sup>c</sup> It is assumed that 80% of the equipment cost can be attributed to the AEL stack and 20% to the peripheral equipment. For the FCI estimation, stack costs are assumed to be turn key (method 5). 2% of the stack FCI has to be spent annually on maintenance. The peripheral equipment FCI is estimated with method 2. The costing method is based on a correspondence with an AEL supplier. <sup>d</sup> Fixed capital investment FCI calculation methods described in the ESI.

Table 4 Base case utility prices

Utility	Prices	Source
Wet biomass	42.232 € per t <sub>50% moist.</sub>	5
Electricity	50.4 € per MW per h	5
Demineralised water for electrolysis	2 € per m <sup>3</sup>	14
Cooling water	0.005 € per l	9
FT catalyst <sup>a</sup>	33 € per kg	20
Selexol <sup>b</sup>	4.395 € per kg	9
Waste water	0.918 € per m <sup>3</sup>	26
HPS	17.706 € per t	27
MPS	16.057 € per t	27
LPS	13.142 € per t	27

<sup>a</sup> Catalyst lifetime 2 years.<sup>32</sup> <sup>b</sup> Selexol makeup 0.00018 kg<sub>makeup</sub> kmol<sub>syngas</sub><sup>-1</sup>.

scope definition of the analysis, the inventory analysis, where the data describing the inputs and outputs of the product system is collected, the impact assessment, where the impact of the inventory processes is evaluated in specific environmental impact categories, and the interpretation that reflects the results of the analysis considering the defined goal and scope.

In order to calculate the environmental impacts of the PBtL production, an attributional LCA is conducted following the principles introduced in DIN EN 14040/44 (ref. 61) using the open-source software brightway2.<sup>62</sup> The process depicted in the PBtL process flowsheet in Fig. 1 as well as the collection of the biomass feedstock, transport of the biomass to the plant, and construction of the plant are included within the system boundaries. Environmental impacts of refining the FT product are not considered in this study. This system definition corresponds to the one used for the economic assessment.

The functional unit (“quantified performance of a product system for use as a reference unit”<sup>63</sup>) is 1 MJ<sub>LHV</sub> of produced FT product following the described PBtL pathway in Europe in the timeframe from 2020 to 2050.

The Aspen Plus® simulation of the PBtL process, as described in Section 2.1, and the corresponding mass and energy balance data (see ESI†) serve as basis for the life cycle inventory (LCI). This data is used to model the system processes (activities) in brightway2 using the ecoinvent life cycle inventory database v3.7.1 (system model “allocation, cut-off by classification”)<sup>63</sup> as a background database.

Regarding the life cycle inventory for the PBtL process, the following assumptions are made: the forestry residue feedstock is modelled by adapting the ecoinvent process “market for wood chips, wet, measured as dry mass, Europe without Switzerland” to exclude wood chips coming from sawmilling plants and the respective transport. This adaptation is done as it is assumed that all biomass for the PBtL production consists of primary residues harvested directly in forests and does not include secondary residues. Other variabilities in forestry practices, wood characteristics or carbon uptake by different tree species (e.g., spruce vs. oak) are not considered due to the lack of data. The harvested wood chips are assumed to be transported by trucks over a distance of 100 km, corresponding to a typical transport radius (see Section 2.7.1). Regarding the PBtL

production, the material compositions for the reformer catalyst and the active material of the guard bed are based on data from the FLEXCHX project,<sup>64</sup> while the FT catalyst data is based on the publication by Todic *et al.*<sup>54</sup> The amounts of catalysts (also considering their lifetimes) are derived from the Aspen Plus® model and data from the FLEXCHX project. A general land-filling process from the ecoinvent database is used for the disposal of the spent catalysts after their end of life due to the lack of more specific data. The material composition for Selexol is based on Schakel *et al.*<sup>65</sup> Regarding the PBtL plant construction, the inventory data for the construction of the electrolyser is based on Wulf and Kaltschmitt<sup>66</sup> and Delpierre *et al.*,<sup>67</sup> while the construction of the other components of the PBtL plant is based on the ecoinvent process “synthetic gas factory construction, CH” that describes a biomass gasification plant in Switzerland, and the process “petroleum refinery construction, Europe” as a proxy for the syngas cleaning and FT-reactor facilities. All mentioned plant construction inventories are scaled to match the requirements of the studied PBtL plant. As to the output flows of the PBtL production, the resulting wood ash is assumed to be treated using the European “market for wood ash mixture, pure” process of ecoinvent. All other output flows (except for the by-product steam) are assumed to be emitted to the environment (air or water) without further treatment in order to quantify the burdens for the environment without alteration. Treatment of the resulting wastewater in a suitably designed treatment plant would be possible, however it is not modelled here due to the lack of more specific data. More details on the LCI can be found in the ESI.†

The economic assessment considers the excess steam produced by the PBtL plant as a by-product that creates revenue (see Section 2.2.5). Thus, the system is assumed to have two products: the FT product and steam. In order to solve this multifunctionality and for consistency with the economic assessment, an economic allocation using the prices employed in the economic assessment is applied.

The impact categories chosen for the LCA are listed in the ESI.† The corresponding LCA methods follow the methodology and characterisation factors recommended by the International Reference Life Cycle Data System (ILCD 2.0 2018/EF 2.0). According to the ILCD recommendations, the results of the impact categories ecotoxicity (freshwater), land use, water scarcity, resource use/minerals and metals, and resource use/energy carriers need to be viewed with caution.<sup>68</sup>

In order to better understand the impact of each step along the process chain, the PBtL production process is subdivided into partial processes, such as electricity, biomass transport, *etc.* The corresponding LCIs are provided in the ESI.† These partial processes form the basis of a contribution analysis using the functions of the bw2calc package of brightway2.

## 2.6. Biomass potential analysis

One goal of this study is to evaluate the potential for fuel production *via* the PBtL pathway from European forest residue. For the purposes of this analysis, the ENSPRESO (ENergy System Potentials for Renewable Energy SOURces) dataset<sup>69,70</sup> is



used. It is an open-access dataset containing renewable energy potentials with different levels of geographic disaggregation (NUTS0 and NUTS2 levels) for the period between 2010 and 2050 for the EU-28 countries (and some additional European countries).

Three scenarios (high, medium and low bioenergy availability) with different assumptions regarding land use, forestry practices, and sustainability limitations are defined in the ENSPRESO dataset. The scenarios also include assumptions regarding the competition from non-energy sectors (*e.g.*, material use, bio-based products) and consider this in the resulting biomass potentials.<sup>69</sup> For the purposes of this analysis only the medium and low bioenergy availability are considered, as some assumptions in the high availability scenario do not comply with the sustainability criteria defined by the European Commission's revised Renewable Energy Directive 2018/2001/EU (RED II) (*"Member States shall grant no support for the use of saw logs, veneer logs, stumps and roots to produce energy"*).<sup>11</sup> Additionally, this analysis only considers primary forestry residues (ENSPRESO dataset codes MINBIOFSR1 and MINBIOFSR1a) and excludes secondary residues *e.g.*, from the wood processing industry, thus complying with the assumptions made in the techno-economic and environmental analysis (Sections 2.3 and 2.5).

The biomass potentials for energy purposes, as contained in the ENSPRESO dataset, are mainly distributed among electricity generation, use for heating, and biofuels production. The biomass distribution between these three applications differs in the literature on the topic. In most studies, the largest part of the biomass for energy purposes is used for heating and typically makes up around 65 to 70% of the available biomass.<sup>71,72</sup> The biomass used for electricity generation makes up around 15%.<sup>71,72</sup> Consequently, around 15 to 20% of the biomass potential is used for the production of biofuels, which are again distributed among the different transportation sectors, with aviation and shipping being the main recipients after 2040. To our knowledge, there are currently no studies that disaggregate the different sources of biomass, such as forestry residues, to the different applications. Thus, we assume for this analysis that 33% of the forest residue biomass potential is used for aviation biofuels.

## 2.7. Process analysis under local boundary conditions

To evaluate PBtL production costs and GHG emissions under local European boundary conditions, a techno-economic and emission analysis on a NUTS2 level was performed. A region's economic attractiveness as a PBtL plant site is determined by local biomass prices, labour costs and electricity price. The local emissions are dependent on the location-specific biomass transport radius and the GHG footprint for the electricity production. Here, NUTS2-specific PV, on-shore wind and the national grid are considered as sources for electricity.

**2.7.1. Local production cost.** National electricity prices are taken from the Eurostat database<sup>73</sup> for large scale consumers (>150 GW h) in the first half of the year 2020 excluding VAT and other recoverable taxes and levies. Where no data is available for

2020, prices for past years are used. If no prices are listed in this category, the calculation relies on price data from consumers from 70 GW h to 150 GW h. Labour costs are taken from the Eurostat dataset.<sup>74</sup> The used national values for electricity price and labour cost can be found in the ESI.<sup>†</sup>

To estimate the levelised cost of electricity (LCOE) for renewable energy sources, maintenance and investment cost are considered in eqn (6). For both PV and onshore wind capital expenditure (CAPEX) are considered as shown in Table 5,<sup>6</sup> whereby a lifetime  $t$  of 25 years is assumed for both technologies. With the maintenance factor  $mf$  annual maintenance costs are estimated as 1.5% (PV) or 2.5% (wind) of the investment.<sup>6</sup> With the capacity factor  $cf$  of the number of full load hours per year can be accounted for.

LCOE [€ per MW per h]

$$= \frac{\text{CAPEX} [\text{€ per MW}] + \text{CAPEX} [\text{€ per MW}] mf [\% \text{ a}^{-1}]}{t [\text{a}] \cdot cf8760 [\text{h a}^{-1}]} \quad (6)$$

The capacity factors  $cf$  for all European NUTS2 regions are taken from the ENSPRESO dataset.<sup>70</sup> In this study, the capacity factor for the average top 50% wind spots is used. For PV, global ground irradiation values are used to determine the  $cf$ .

The local biomass cost is calculated as the sum of feedstock and transport costs. The local biomass feedstock price for forest residue is calculated as the average of its subcategories, wood residue, chip and pellets, and landscaping residues, for the medium availability scenario in the ENSPRESO dataset.<sup>69,70</sup> The biomass transport cost is found as a function of the transport distance to the plant. The local biomass density  $\rho$  determines the feedstock sourcing area  $A$ , which is required for a 400 MW<sub>th</sub> biomass input  $W$ . The average transport radius  $r^*$  follows from eqn (8). The biomass transport cost is obtained by multiplying local transport cost, as documented in the ESI,<sup>†</sup> with the average transport radius  $r^*$ .

$$A = \frac{W}{\rho} \quad (7)$$

$$r^* = \sqrt{\frac{A}{2\pi}} \quad (8)$$

in cases where the NUTS2 area doesn't supply enough biomass for a 400 MW<sub>th</sub> plant, *i.e.* 13 PJ a<sup>-1</sup>, it is assumed that biomass can be imported at the area's own transport and feedstock costs from neighbouring NUTS2 areas. For the calculation of the

Table 5 Investment cost for hydrogen generation units<sup>6,7</sup>

CAPEX	M€ per MW
Onshore wind	1.53
PV	0.86
AEL	1

transport radius no availability limitations, as described in 2.6, are considered.

**2.7.2. Local GHG emissions.** The carbon intensity for all considered national grid mixes can be found in the ESI.<sup>†1</sup> PV and wind emissions are calculated based on their local capacity factor. Wind energy is considered to have a footprint of  $7.9 \text{ g}_{\text{CO}_2,\text{eq}} \text{ kW}^{-1} \text{ h}^{-1}$  at  $3600 \text{ h a}^{-1}$  and PV  $47 \text{ g}_{\text{CO}_2,\text{eq}} \text{ kW}^{-1} \text{ h}^{-1}$  at  $1200 \text{ h a}^{-1}$ .<sup>75</sup>

Emissions from biomass transport are scaled by the transport radius. The base case transport radius of 100 km has emissions of  $2.3 \text{ g}_{\text{CO}_2,\text{eq}} \text{ MJ}^{-1}$  as calculated in the ESI.<sup>†</sup>

Based on emissions and production cost, NUTS2 specific GHG abatement costs are determined. This value represents the premium of producing green SAF instead of using fossil fuels.

For the GHG abatement costs calculation according to eqn (9), a crude oil price of 75 \$ per barrel,<sup>76</sup> *i.e.*, 0.42 € per l, and GHG emissions from fossil fuel  $m_{\text{CO}_2,\text{eq,crude oil}}$  of  $94 \text{ g}_{\text{CO}_2,\text{eq}} \text{ MJ}^{-1}$  (ref. 77) are assumed.

$$\begin{aligned} \text{GHG abatement cost} [\text{€ per } t_{\text{CO}_2}] \\ = \frac{\text{price}_{\text{PBtL}} - \text{price}_{\text{crude oil}}}{m_{\text{CO}_2,\text{eq,crude oil}} - m_{\text{CO}_2,\text{eq,PBtL}}} \end{aligned} \quad (9)$$

### 2.7.3. Integration scenarios for fluctuating energy sources.

A continuous  $\text{H}_2$  supply from the electrolyser is required for a steady-state operation of the PBtL plant. To accomplish this for the fluctuating renewable resources, wind and PV, two idealised scenarios are considered in this study, as displayed in Fig. 2:

(1) Virtual grid scenario: the fluctuating energy input is turned into a stationary profile by a virtual grid. As no additional costs are associated with the virtual grid, this can be regarded as an optimistic scenario.

(2) Hydrogen storage scenario: the electrolyser is operated flexibly. The resulting fluctuating hydrogen output is then stored in hydrogen tanks or suitable cavern storage with a constant output. To match the hydrogen demand of the process, the electrolyser has to be over-dimensioned entailing additional investment cost. The electrolyser size increases with decreasing capacity factor of the energy source. The additional cost for hydrogen storage is not considered here.

## 2.8. Limitations of the analysis methodology

All presented technical, economic and ecologic assumptions underlie different levels of uncertainty. The uncertainty for any basic process design cost study is typically given within the range of  $\pm 30\%$ .<sup>9</sup> To make the uncertainty in the economic

results more transparent, a sensitivity analysis for the most impactful economic parameters in the base case is performed. Similarly, the ecological impact is discussed with a sensitivity analysis. Here, the GWP of PBtL production is discussed as a function of the GWP of the used electrical power.

For the local analysis, a number of assumptions on top of the base case analysis have to be highlighted for their uncertainty. The availability of forest residue for fuel production is assumed to be 33% NUTS2 regions. These percentages will be determined by political or economic processes in the future and are therefore hard to predict. Additionally, it is assumed that it will be possible to construct PBtL plants in all NUTS2 regions. This neglects the possibility that certain factors, such as lacking social acceptance, might make it impossible to produce fuel in these regions. Also, the availability of all required in process units is assumed. Nevertheless, the availability of enough electrolyzer units might prove to be a bottleneck for the process roll-out.<sup>78</sup> Further, the simplified approach for the integration scenarios, as described in Section 2.7.3, should only be understood as an approximation of the actual costs for the integration of fluctuating renewable energy sources. A more accurate process design would include a cost-optimised design of the power production system (mix of wind and PV), the electrolyzer and the hydrogen storage system depending on local boundary conditions.

Regarding the LCA, the current study uses the ecoinvent version 3.7.1 and the impact assessment methods as implemented in this version to model and assess the PBtL pathway. At the time of publication however, a newer ecoinvent version with updated datasets and LCIA methods has been made available. Even though this does not affect the foreground modelling, the final results of the analysis using the newest ecoinvent version are expected to be slightly different from the ones presented here due to the updates in the background processes. The updated EF 3.0 methods should also be used in place of the ILCD 2.0 2018/EF 2.0 methods used in this study.

Finally, another limitation lies in the lack of regional data for the LCA of the PBtL pathway. Should such data become available in the future, it is highly recommended to adapt the analysis to correspond to the regional circumstances of the system under evaluation.

## 3. Results and discussion

In this section, an analysis of the base case is presented, including a techno-economic analysis and a life cycle assessment. Based on the results, the impact of important process parameters on the process performance is discussed with a sensitivity analysis. Secondly, the results of the Europe-wide location-specific techno-economic and GHG emission analysis are shown. Their implications for the European SAF production are discussed assuming different integration scenarios for various electrical energy sources.

### 3.1. Base case evaluation

**3.1.1. Technical process evaluation.** Mass and energy balances derived from the Aspen Plus® model are displayed in

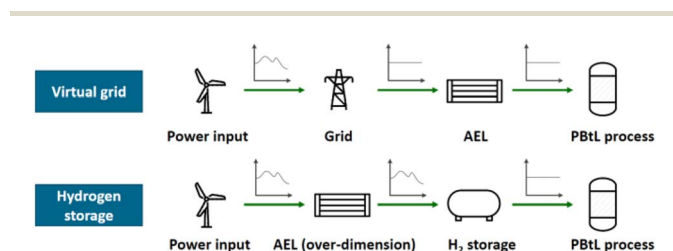


Fig. 2 Schematic flowsheet detailing integration scenarios for fluctuating power input.

Table 6. A more detailed version of the balances can be found in the ESI† along with the T–H diagram showing the process heat integration. The corresponding process performance indicators can be taken from Table 6 as well. Here, the relatively high carbon conversion of 92% is due to full CO<sub>2</sub> and high FT off-gas recycling. Around 45% of the energy input can be converted to fuel and another 25% to steam.

**3.1.2. Production cost estimation.** For the base case, location-specific economic boundary conditions typical for Finland are considered<sup>5</sup> as defined in Section 2.4. Overall, net production cost (NPC) of 1.75 €<sub>2020</sub> per kg are found for the base case. This amounts to 1.32 €<sub>2020</sub> per l or 39.9 €<sub>2020</sub> per GJ. Fig. 3 shows the production cost split by the contributing cost fractions. Operational expenditures (OPEX), in green, represent the largest cost share. It is apparent that OPEX are dominated by costs for the electrical power followed by the biomass cost. Similarly, investment costs, depicted in blue, are dominated by the electrolyser cost.

**3.1.3. Life cycle assessment.** The LCA results for the base case following the methodology introduced in Section 2.5 are discussed here.

As already mentioned, an economic allocation was applied to account for the revenues of the by-products. The resulting allocation factors are listed in the ESI.† Approximately 90% of the resulting environmental impacts are allocated to the FT product.

It must be noted that the biogenic carbon that is captured during forest growth was not considered in the life cycle inventories. This has to be considered when modelling the entire life cycle of the fuel. In a simplified model the CO<sub>2</sub> captured by the biomass is emitted again during combustion of

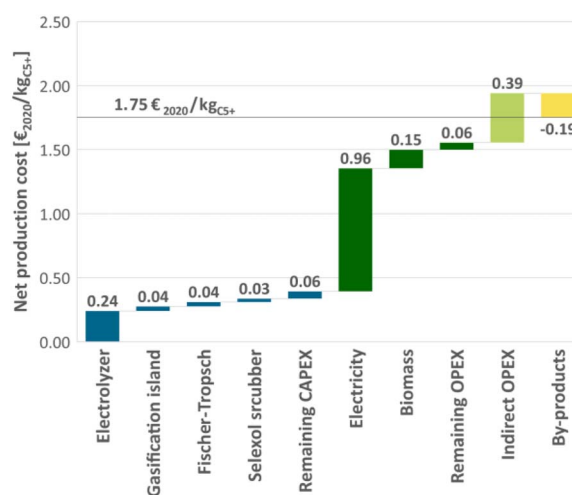


Fig. 3 Net production cost break-down for the base case economic boundary conditions. CAPEX (blue), direct OPEX (green), indirect OPEX (light green) and the revenue from by products (yellow) yield net production cost of 1.75 € per kg<sub>C<sub>5+</sub></sub>.

the PbTL fuel thus resulting in a net zero CO<sub>2</sub> emission when the fuel is used. This simplified assumption of biogenic carbon neutrality does not consider carbon stock changes in the forest. For a more accurate estimation of the GHG emission savings, all relevant forest carbon pools need to be considered in the analysis as well as their evolution within relevant time horizons.<sup>79</sup> Moreover, the evaluation in terms of climate change impact of the entire lifecycle of the fuels (including combustion) when used in aviation needs to consider the non-CO<sub>2</sub> effects of inflight emissions in the atmosphere (mostly due to the positive radiative forcing of contrails).<sup>80</sup> These effects are, however, not discussed here since the scope of the analysis is restricted to the fuel production.

Fig. 4 illustrates the relative contribution analysis of the different steps involved in the PbTL production for the case of electricity from wind turbines used for the production of PbTL. In more detail, a high percentage of the contribution to acidification (AP) stems from the emissions during PbTL production (mostly ammonia from the Selexol scrubbing step). Around half of the contribution to the use of fossil energy carriers (ECF) originates from the fossil resources needed for the construction of wind turbines for electricity. The majority of the remaining impact in this category is caused by the fossil fuels used during transportation and provision of the biomass. In the category of freshwater eutrophication (FEP), the main burdens can be attributed to the treatment of wood ash, which is for example used in landfarming (modelled as part of the emissions of the PbTL process). The construction of wind turbines (mainly steel production) and the wastewater emissions during the production of oils used in the forestry machines for biomass provision also contribute to this category. In the category of freshwater ecotoxicity (FETP), the main impacts can be attributed to the treatment of wood ash and the burdens from steel needed to manufacture wind turbines (contained in the category electricity). The contributions in the category of Global Warming

Table 6 Mass and energy balances for the PbTL process and resulting efficiency values

Input	
Biomass [MW <sub>LHV</sub> ]	400
Biomass 50% <sub>moist.</sub> mass flow [kg <sub>wet</sub> s <sup>-1</sup> ]	47.36
LHV 50% <sub>moist.</sub> [MJ kg <sup>-1</sup> ]	8.45
Total el. power [MW <sub>el</sub> ]	943.6
Power input electrolyser [MW <sub>el</sub> ]	890.1
Total power input [MW]	1343.6
Output	
Product [MW <sub>LHV</sub> ]	602.4
Product mass flow [kg <sub>C<sub>5+</sub></sub> s <sup>-1</sup> ]	13.72
Carbon content [% <sub>wt</sub> ]	85
Product LHV [MW <sub>LHV</sub> ]	43.91
Low pressure steam [MW <sub>LHV</sub> ]	179
Medium pressure stream [MW <sub>LHV</sub> ]	57.4
High pressure steam [MW <sub>LHV</sub> ]	95.3
Total power output [MW]	934.2
Process efficiency	
Carbon conversion X <sub>C</sub> [%]	92
Biomass conversion X <sub>biom</sub> [%]	29
Fuel efficiency η <sub>fuel</sub> [%]	45
Process efficiency η <sub>process</sub> [%]	70

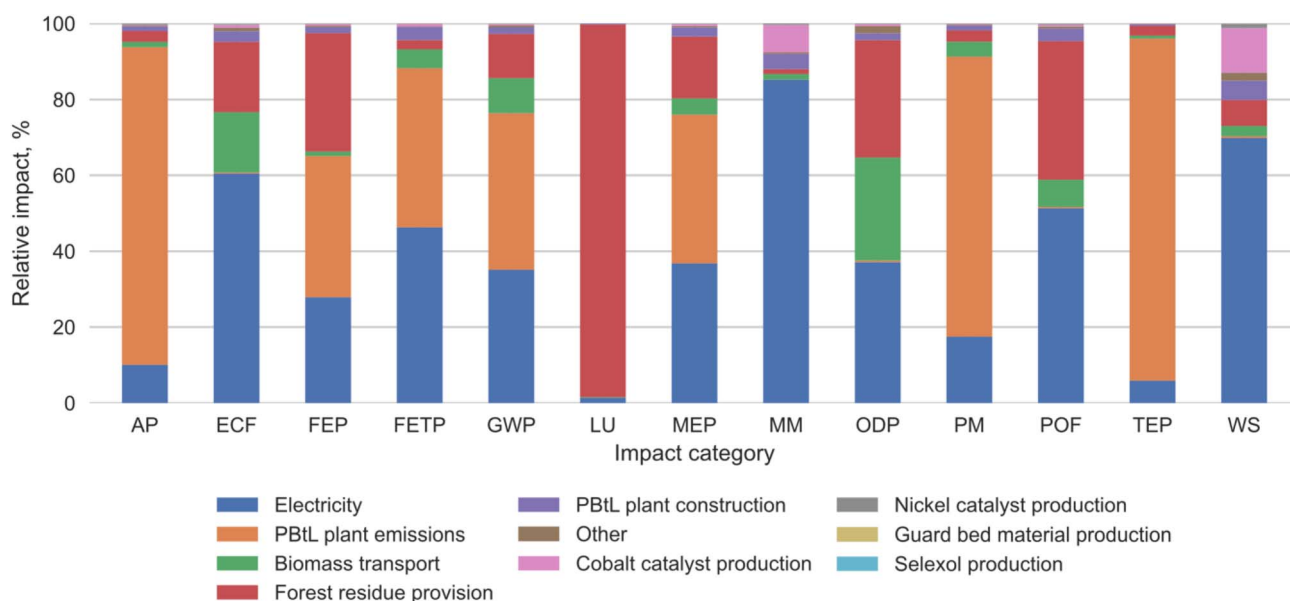


Fig. 4 Relative environmental impacts of the PBtL production processes in different impact categories for the case of electricity from wind turbines. (AP: acidification; ECF: energy carriers, fossil; FEP: eutrophication, aquatic freshwater; FETP: ecotoxicity (freshwater); GWP: global warming potential; LU: land use; MEP: eutrophication, aquatic marine; MM: minerals and metals; ODP: ozone depletion; PM: particulate matter/respiratory inorganics; POF: photochemical ozone formation; TEP: eutrophication, terrestrial; WS: water scarcity).

Potential (GWP) are distributed mainly among the burdens from the construction of wind turbines, the emissions of the PBtL production process itself (predominantly off-gas emissions), the biomass transport, and the biomass provision. Here, the biogenic as well as the fossil carbon emissions are included in the model. In the category of land use (LU), the main contribution stems from the biomass provision. In terms of marine eutrophication (MEP), the impacts result from the ammonia emitted during the PBtL production process itself, as well as the nitrogen oxides and ammonia emitted both during wind turbine construction and to a smaller extent from the biomass provision and transportation. In the category of minerals and metals (MM), the main contribution originates from the copper needed for electricity generation and transmission. Smaller contributions stem from the cobalt catalyst and the PBtL plant construction. The ozone depletion (ODP) is a result of gases emitted during the production of petroleum, which is mainly used for biomass transport and biomass provision (forestry equipment) in the PBtL process chain as well as in the construction of wind turbines. The impact on human health from particulate matter (PM) mainly stems from the ammonia emitted during PBtL production and particulates emitted in processes involved in the construction of wind turbines or during the biomass transport. The photochemical ozone formation (POF) can be attributed mainly to the nitrogen oxides and non-methane volatile organic compounds (NMVOCs) emitted in processes involved in the construction of wind turbines or during transport of biomass and biomass provision (*e.g.*, power sawing). The main contribution to terrestrial eutrophication (TEP) can be attributed to the emission of ammonia during PBtL production. Finally, the impact

on water scarcity mainly stems from the water dissipated in the processes involved in the construction of wind turbines.

For a better notion of the magnitude of the environmental impacts in absolute terms, Fig. 5 depicts the results of the production of PBtL according to the base case with electricity from wind turbines or photovoltaic panels and compares these two cases to the production of kerosene from fossil fuels. The latter was taken from theecoinvent database (“kerosene production, petroleum refinery operation in Europe without Switzerland”). It should be noted that all impacts of the kerosene burning process are not included, which are significant *e.g.* for the GWP category. Due to the higher burdens associated with the production of photovoltaic panels compared to wind turbines, the PBtL from solar energy performs worse than the PBtL from wind energy in all selected impact categories. In many categories the PBtL fuel has a significantly higher impact compared to fossil kerosene, *e.g.*, in the resource category minerals and metals as well as water scarcity, because of the high amounts of metals and water needed for renewable electricity production, respectively. The impact on land use is also significantly higher due to the provision of biomass.

A better management of the gaseous and wastewater emissions of the PBtL plant should result in a reduction of the impacts of the PBtL process, especially in the categories AP, TEP, PM, GWP, and MEP. A further increase in efficiency of renewable energy sources in combination with the use of recycled materials in the production of wind turbines and photovoltaic panels may further reduce the impacts in the categories where electricity has a high contribution. Finally, should more sustainable fuels be used in the transport and provision of biomass in the future, a reduction of these impacts in the relevant categories could be achieved.

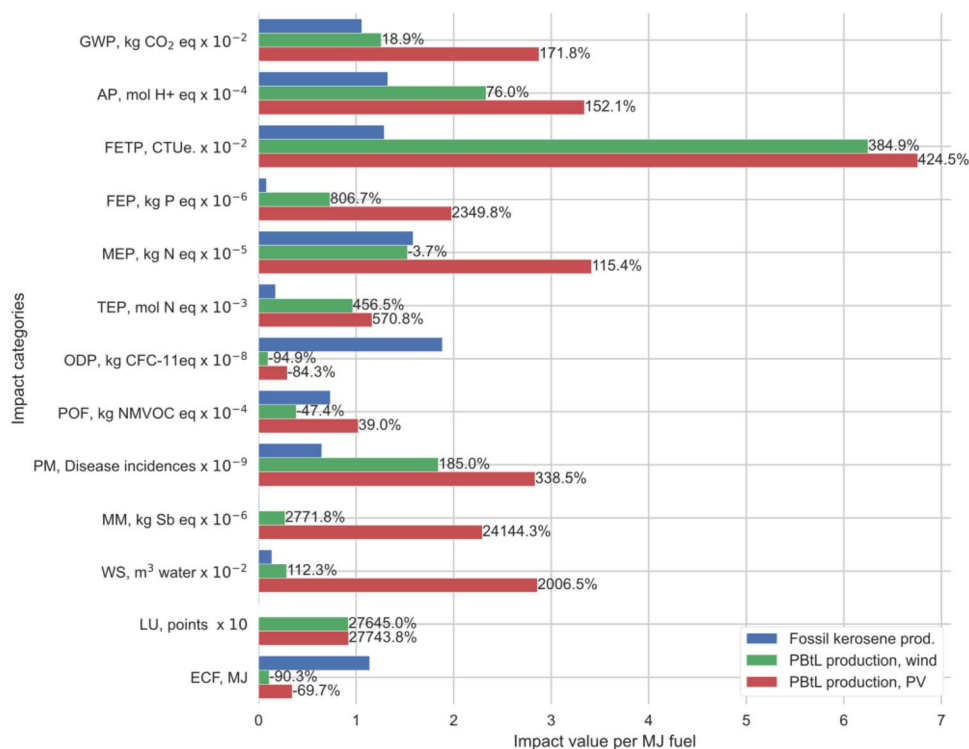


Fig. 5 Absolute environmental impacts from PBtL production using renewable energy from wind turbines or photovoltaic panels compared to the fossil kerosene production. (AP: acidification; ECF: energy carriers, fossil; FEP: eutrophication, aquatic freshwater; FETP: ecotoxicity (freshwater); GWP: global warming potential; LU: land use; MEP: eutrophication, aquatic marine; MM: minerals and metals; ODP: ozone depletion; PM: particulate matter/respiratory inorganics; POF: photochemical ozone formation; TEP: eutrophication, terrestrial; WS: water scarcity).

**3.1.4. Sensitivity analysis.** The presented cost estimates and LCA results are based on a number of assumptions that may vary depending on location and time of analysis. To account for this, biomass and electricity price, as the two most important OPEX factors (*cf.* Fig. 3), are subjected to a sensitivity analysis. A realistic range for forest residue biomass can be stated as 20.3 to 102.5 € per t.<sup>39</sup> The ENSPRESO dataset, which was used to estimate local production costs in Section 3.2.2, reports biomass prices in the range of 16.6 to 64.8 € per t<sub>50% moist.</sub> (ref. 69) for Europe. Similarly, grid electricity prices can range from 30.8 € per MW per h<sub>el</sub> in Norway to 136.1 € per MW per h<sub>el</sub> in the UK.<sup>73</sup>

Fig. 6 depicts the impact of both commodity prices on the PBtL process's production costs. The outsized impact of the electricity price can be seen here: a 20% reduction in electricity price reduces production cost by 0.21 € per kg<sub>C<sub>5+</sub></sub>. A 20% decrease in the price of biomass, on the other hand, only results in a 0.03 € per kg<sub>C<sub>5+</sub></sub> reduction in production cost.

As previously shown in Fig. 4, the contribution to the FT fuel's GWP of the electricity production is substantial, even when on-shore wind production with a footprint of 11.3 g<sub>CO<sub>2</sub></sub> kW<sup>-1</sup> h<sub>el</sub><sup>-1</sup> is considered. The full range of the electricity GWP impact on the fuel GWP is shown in Fig. 7. Here, the fuel GWP is represented by the blue line referring to the left y-axis. The fuel's GWP rises linearly with the carbon intensity of the electricity production. With an electricity GWP of 214 g<sub>CO<sub>2</sub></sub>eq kW<sup>-1</sup> h<sub>el</sub><sup>-1</sup>, FT fuel has the same GWP as fossil fuel (94 g<sub>CO<sub>2</sub></sub>eq MJ<sup>-1</sup>).<sup>11</sup> Consequently, PBtL fuel produced with the German or

European average grid mix of the year 2020 has a stronger climate effect than fossil fuel combustion. To qualify as sustainable fuel according to the RED II directive<sup>11</sup> (<32.9 g<sub>CO<sub>2</sub></sub>eq MJ<sup>-1</sup>), the electricity GWP must be lower than 63 g<sub>CO<sub>2</sub></sub>eq kW<sup>-1</sup> h<sub>el</sub><sup>-1</sup> under the assumed boundary conditions. As a result, only countries with a less carbon-intensive electricity grid mix, such as France or Sweden,<sup>1</sup> should be considered as production sites for grid-connected PBtL production.

In Fig. 7 the GWP intensity range found for PV and wind power in all NUTS2 regions is displayed. PBtL fuel produced

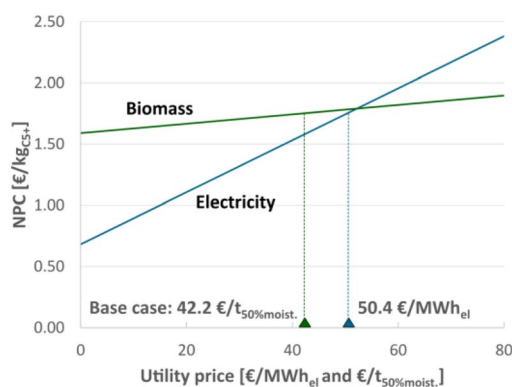


Fig. 6 Parameter variation showing the effect of electricity and biomass prices on the PBtL production cost.

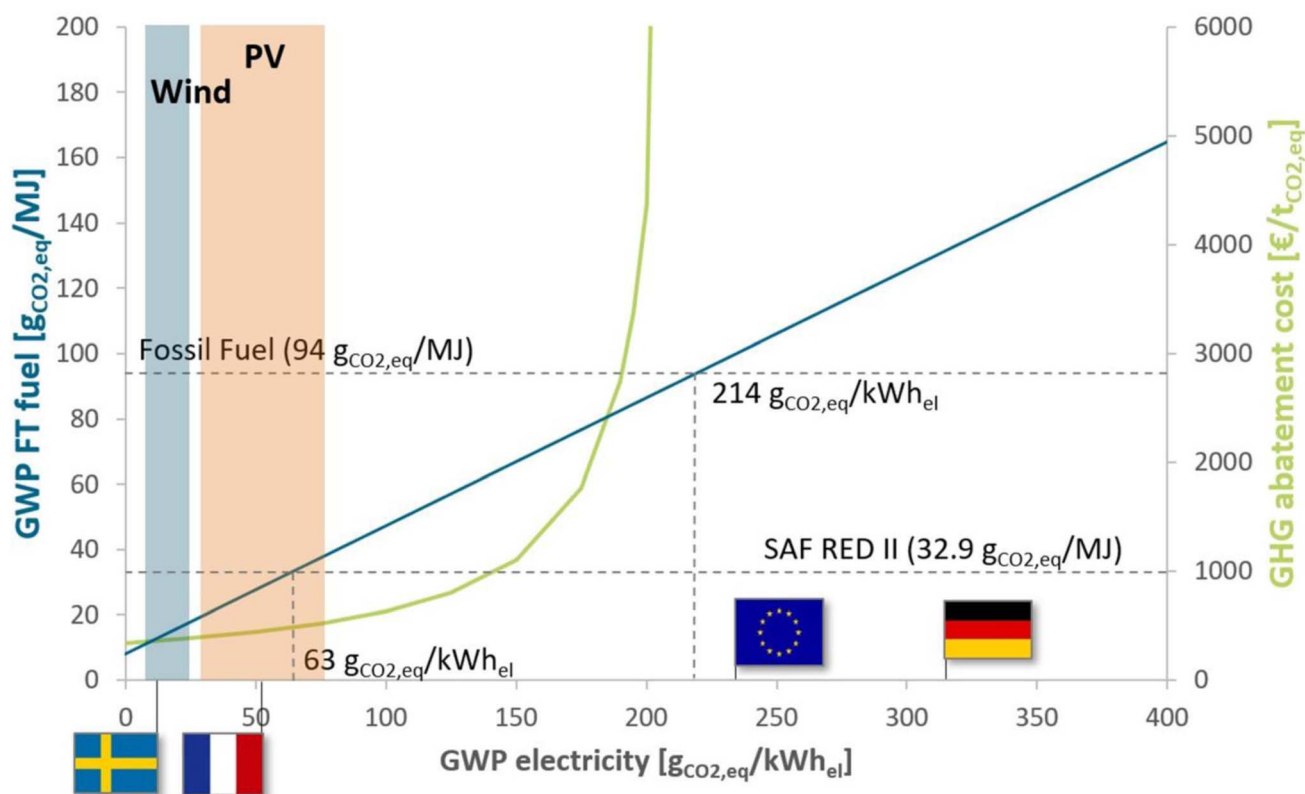


Fig. 7 Effect of the electricity GWP on fuel GWP (left axis) and GHG abatement cost (right axis). National grid GWP in Sweden ( $9 \text{ g}_{\text{CO}_2,\text{eq}} \text{ kW}^{-1} \text{ h}_{\text{el}}^{-1}$ ), France ( $51 \text{ g}_{\text{CO}_2,\text{eq}} \text{ kW}^{-1} \text{ h}_{\text{el}}^{-1}$ ), EU-27 ( $231 \text{ g}_{\text{CO}_2,\text{eq}} \text{ kW}^{-1} \text{ h}_{\text{el}}^{-1}$ ) and Germany ( $311 \text{ g}_{\text{CO}_2,\text{eq}} \text{ kW}^{-1} \text{ h}_{\text{el}}^{-1}$ ) are shown alongside the calculated GWP range for PV (orange:  $7\text{--}24 \text{ g}_{\text{CO}_2,\text{eq}} \text{ kW}^{-1} \text{ h}_{\text{el}}^{-1}$ ) and on-shore wind (blue:  $29\text{--}77 \text{ g}_{\text{CO}_2,\text{eq}} \text{ kW}^{-1} \text{ h}_{\text{el}}^{-1}$ ).<sup>6</sup> As reference the GWP of fossil fuel ( $94 \text{ g}_{\text{CO}_2,\text{eq}} \text{ MJ}^{-1}$ ) and the GWP limit for SAF as defined in the RED II directive ( $32.9 \text{ g}_{\text{CO}_2,\text{eq}} \text{ MJ}^{-1}$ )<sup>11</sup> are also shown. Base case electricity and biomass price are used to calculate the GHG abatement cost.

with wind power can be counted as SAF according to the RED II without any exceptions. Yet, PV production in northern European NUTS2 regions can exceed this limit.

The GHG abatement cost, as defined in eqn (9), is depicted in Fig. 7 with the green line referring to the right y-axis. The abatement cost increases exponentially with the electricity's GWP and approaches infinity when the FT fuel has the same GWP as fossil fuel at  $214 \text{ g}_{\text{CO}_2,\text{eq}} \text{ kW}^{-1} \text{ h}_{\text{el}}^{-1}$ . On the lower end, the abatement costs approach  $339 \text{ € per t}_{\text{CO}_2,\text{eq}}$  when assuming the base case electricity and biomass price.

### 3.2. European SAF production potential

A NUTS2-specific analysis was performed to estimate the potential amount and production cost of SAF that can be produced from European forest residue. Section 3.2.1 provides an overview of Europe's forestry residue potential. Based on that, the region-specific production costs for grid-connected PBT operation are discussed. Subsequently, results for renewable fluctuating energy sources are presented, whereby it is distinguished between the two integration scenarios, virtual grid and hydrogen storage, described in Section 2.7.3. Finally, the fuel's GWP footprint and GHG abatement cost for every NUTS2 region is shown.

**3.2.1. European biomass potential from forestry residues.** The local distribution of forestry residue for the ENSPRESO

MED scenario can be taken from Fig. 8. It is apparent that especially northern European and Baltic NUTS2 regions have a large forest residue potential.

The resulting total biomass potential from primary forestry residues available for energy uses as extracted from the ENSPRESO database can be seen in Table 7. It can be seen that in the medium bioenergy availability scenario (MED) the potential is assumed as almost constant between 2030 and

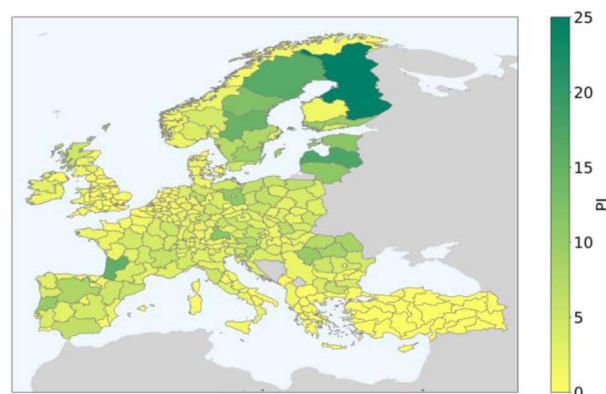


Fig. 8 Biomass potential for ENSPRESO MED scenario assuming 33% availability for SAF production.

**Table 7** Biomass potential from primary forestry residues for energy uses in Europe as calculated in this analysis and compared to literature (harmonised to primary residues expressed in EJ a<sup>-1</sup>)

Source	Potential	Year	Comment
This study, LOW scenario	1.12 EJ a <sup>-1</sup>	2030	
This study, MED scenario	2.24 EJ a <sup>-1</sup>	2030	
Searle and Malins, 2013 (ref. 2)	0.76 EJ a <sup>-1</sup>	2030	Only EU (derived from 40 Mt with 19 GJ t <sup>-1</sup> )
BRE, 2015 (ref. 8)	2.2 EJ a <sup>-1</sup>	2030	EU, technical-energy (TE) potential
BRE, 2015 (ref. 8)	0.44 EJ a <sup>-1</sup>	2030	EU, sustainable (S) potential
Searle and Malins, 2015 (ref. 15)	0.41 EJ a <sup>-1</sup>	2030	Forestry residues w/o amount retained for soil quality
Imperial College London Consultants, 2021 (ref. 19)	0.71 EJ a <sup>-1</sup>	2030	Primary forestry residues, low scenario
Imperial College London Consultants, 2021 (ref. 19)	1.13 EJ a <sup>-1</sup>	2030	Primary forestry residues, high scenario
This study, LOW scenario	0.56 EJ a <sup>-1</sup>	2050	
This study, MED scenario	2.24 EJ a <sup>-1</sup>	2050	
Smeets <i>et al.</i> , 2007 (ref. 25)	1 EJ a <sup>-1</sup>	2050	Wood harvest residues, West & East Europe
Haberl <i>et al.</i> , 2010 (ref. 28)	2 EJ a <sup>-1</sup>	2050	Mean value only considering primary residues
Lauri <i>et al.</i> , 2014 (ref. 29)	ca. 1.5 EJ a <sup>-1</sup>	2050	EU27 (derived from Fig. 6 with 7.2 GJ m <sup>-3</sup> )
Imperial College London Consultants, 2021 (ref. 19)	1.13 EJ a <sup>-1</sup>	2030	Primary forestry residues, high scenario

2050. In the low availability scenario (LOW) on the other hand, the potential is expected to decrease in the future. A comparison to other studies is also shown in Table 7. The highest predicted biomass potentials in other studies fall within the same range as the ones from the ENSPRESO dataset. Some of the other studies forecast lower potentials, which can be explained with stricter sustainability limitations assumed in their scenarios. It must also be noted that some discrepancies in the data from the various studies may stem from different definitions of primary forestry residues (*e.g.*, wood harvest residues) or from slightly different geographical scopes (*e.g.*, EU vs. Europe). Due to the unavailability of more detailed data, it was however not possible to eliminate these inconsistencies between the different datasets. The electricity demand for Europe wide PBtL production would amount to around 5.3 EJ a<sup>-1</sup> in 2030 and 2050 assuming

full utilization of the forest residue in the MED scenario. According to the ENSPRESO database, the PV (40 EJ a<sup>-1</sup>) and wind (30 EJ a<sup>-1</sup>) potential in Europe indicate that forest residue is the limiting resource for the PBtL process.<sup>79</sup> Other technical constraints could also prove to be the bottleneck for a European PBtL roll-out. The total electrolyser capacity, for instance, is aimed to be ramped up to only 1.2 EJ a<sup>-1</sup> hydrogen output by 2030.<sup>81</sup> Nevertheless, in this study only forest residue is treated as the limiting factor.

**3.2.2. Region-specific production cost.** Grid-connected local NPC for Europe on a NUTS2 level can be taken from Fig. 9. The production costs are in a range from 1.5 to 4 €<sub>2020</sub> per kg of Fischer-Tropsch product. The best conditions for the PBtL plant can be found in Northern European countries and parts of Belgium and Bulgaria. As shown in Section 3.1.3, the electricity

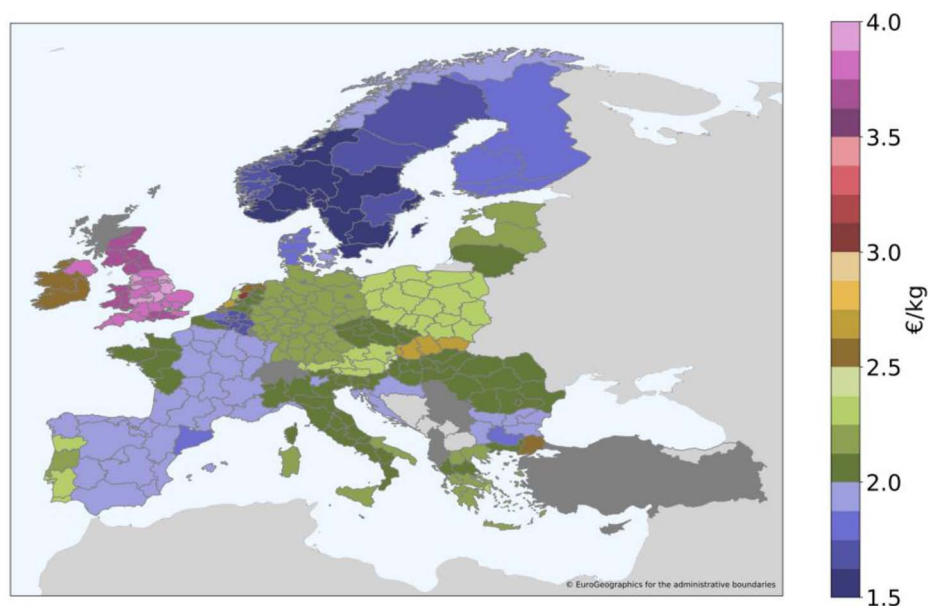


**Fig. 9** NPC for on-shore wind connected PBtL plants in the hydrogen storage scenario. Production cost > 4 €<sub>2020</sub> per kg<sub>C<sub>5+</sub></sub> are lumped in the highest price category.

price plays a dominant role for the NPC. Accordingly, the lowest NPC can be found in Norway, 1.47 €<sub>2020</sub> per kg<sub>C<sub>5+</sub></sub>, having the most inexpensive grid power at 30.8 € per MW per h<sub>el</sub>.<sup>73</sup>

Fig. 10 and 11 show local production costs for PBtL plants operated with on-shore wind and PV energy. In both figures the results for the hydrogen storage scenario are displayed (cf. Section 2.7.3). In this integration scenario for renewable fluctuating energy sources, the electrolyser is over-dimensioned according to the capacity factor of the analysed NUTS2 region and a steady state H<sub>2</sub> output is attained with a buffer tank. The lowest production costs are 1.60 €<sub>2020</sub> per kg<sub>C<sub>5+</sub></sub> for on-shore wind energy and 2.50 €<sub>2020</sub> per kg<sub>C<sub>5+</sub></sub> for PV.

In the optimistic virtual grid scenario, the fluctuating energy input is assumed to be converted to a steady power input for the electrolyzer without any additional cost. In this scenario, production costs as low as 1.23 €<sub>2020</sub> per kg<sub>C<sub>5+</sub></sub> for wind and 1.22 €<sub>2020</sub> per kg<sub>C<sub>5+</sub></sub> for PV were found. The price discrepancy between the scenarios is due to the additional cost for the over-dimensioned electrolyser.

For both scenarios, the production costs are highly dependent on the local capacity factor. Accordingly, the lowest

production cost for wind energy can be found in coastal regions in Northern and Western Europe. PV has the strongest prospect in Southern Europe.

**3.2.3. Local GHG abatement cost.** For many countries in Europe abating GHG emissions with PBtL production is impossible due to the emission intensity of their national grid mix. In all dark red NUTS2 regions in Fig. 12, the production of PBtL fuel leads to higher emissions than fossil fuel. Even countries with promising NPC, such as Bulgaria with under 2 €<sub>2020</sub> per kg<sub>C<sub>5+</sub></sub>, produce with a higher GWP than fossil fuel. Only countries with low-GHG and in-expensive electricity reach fairly low GHG abatement cost. The lowest abatement cost is found in Norway with 288 €<sub>2020</sub> per t<sub>CO<sub>2</sub>,eq</sub>. As of the year 2020, only PBtL fuel produced in France, Norway, Sweden and Lithuania has a GWP footprint lower than the 32.9 g<sub>CO<sub>2</sub>,eq</sub> MJ<sup>-1</sup> necessary for SAF production according to the RED II directive.<sup>11</sup> This might change in the future as many countries are in the process of decarbonizing their national grid mix.

The PBtL production in the hydrogen storage scenario with on-shore wind turbines yields an abatement cost as low as 337 €<sub>2020</sub> per t<sub>CO<sub>2</sub>,eq</sub> and 662 €<sub>2020</sub> per t<sub>CO<sub>2</sub>,eq</sub> for PV production. In the virtual grid scenarios, the lowest abatement cost is found at 208 €<sub>2020</sub> per t<sub>CO<sub>2</sub>,eq</sub> for wind and 237 €<sub>2020</sub> per t<sub>CO<sub>2</sub>,eq</sub> for PV. Abatement cost maps for all discussed cases can be found in the ESI.† No NUTS2 region has higher GWP emissions than fossil fuel. But, for a few Northern European regions PV powered production leads to a higher footprint than defined in the RED II directive.

**3.2.4. Aggregated PBtL SAF production potential.** The combined potential SAF production volume over all NUTS2 regions with a GWP under the RED II limit of 32.9 g<sub>CO<sub>2</sub>,eq</sub> MJ<sub>fuel</sub><sup>-1</sup> is shown in Fig. 13. Here, it is assumed that 33% of forest residues can be used for SAF production. In addition, the aggregated fuel potential is sorted by production cost categories. All PBtL production scenarios can be compared to the Biomass to Liquid (BtL) production route, for which a biomass conversion of 19.9% is assumed.

The high GWP grid mix in many countries makes PBtL fuel production under the RED II directive currently impossible as shown in Section 3.2.3. The BtL process, which requires only a marginal electrical power input, is not reliant upon low-GWP electricity. Thus, grid connected PBtL has a lower SAF potential than BtL.

With the renewable energy sources wind and PV, a fuel output of around 25 Mt a<sup>-1</sup> can be reached. The PV output is slightly lower as some Northern European NUTS2 regions exceed the REDII limit due to their low capacity factor. However, the production volume suffices for the 2040 ReFuel EU goal of 20.1 Mt a<sup>-1</sup>,<sup>22</sup> i.e., 32% of the estimated 2030 European fuel demand of 62.8 Mt a<sup>-1</sup>.<sup>21</sup> For the 2050 goal of 63% either a higher share of forest residue for fuel production or the use of additional renewable feedstocks, such as agricultural residues or municipal waste, are required.

The renewable energy integration scenario is crucial for the production cost. While the bulk of the product can be produced for under 2 €<sub>2020</sub> per kg<sub>C<sub>5+</sub></sub> with the virtual grid (VG), the

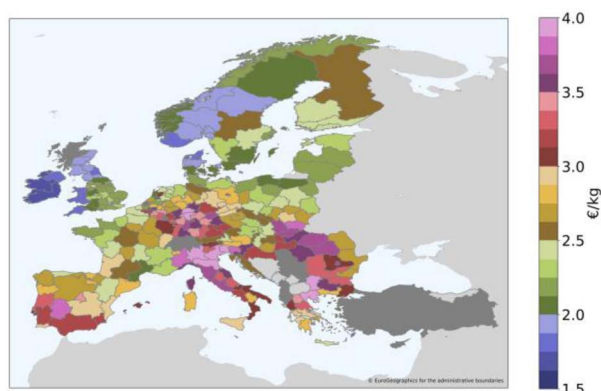


Fig. 10 Net production cost in €<sub>2020</sub> per kg for PBtL syncrude based on forest residue in EU on a NUTS2 level assuming operation with grid electricity. Regions with missing biomass price or energy density information are coloured in light and dark grey, respectively.

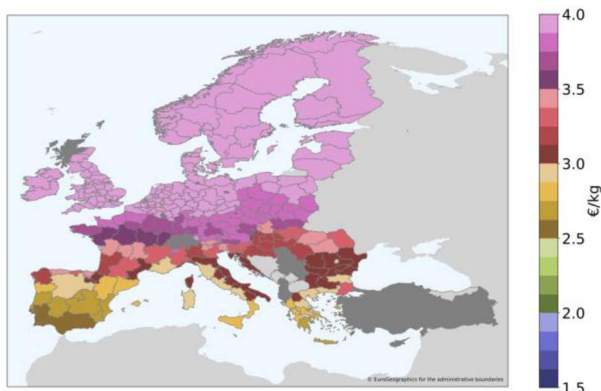


Fig. 11 NPC for PV connected PBtL plants in the hydrogen storage scenario. Production cost > 4 €<sub>2020</sub> per kg<sub>C<sub>5+</sub></sub> are lumped in the highest price category.



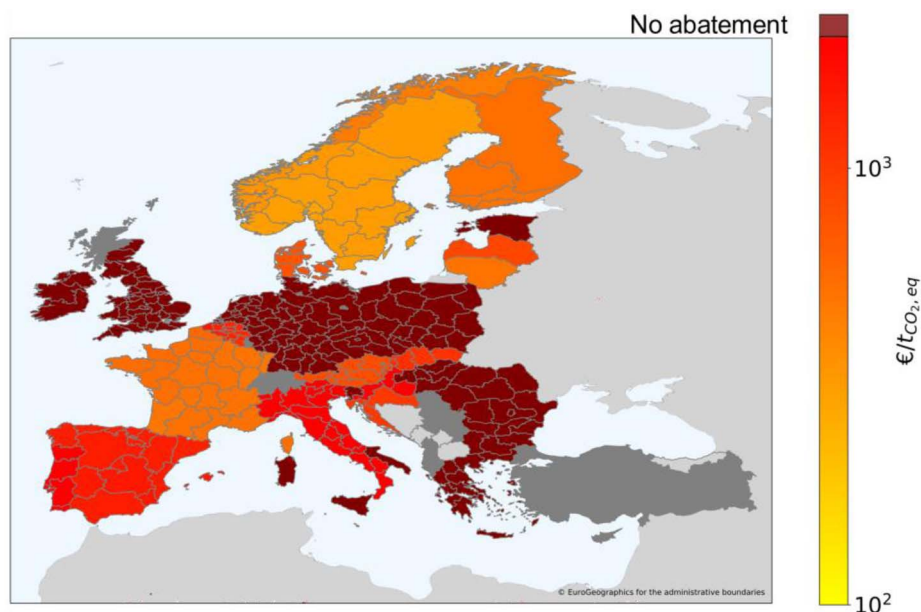


Fig. 12 GHG abatement cost map for a grid connected PBtL process. NUTS2 regions with no abatement are marked in dark red.

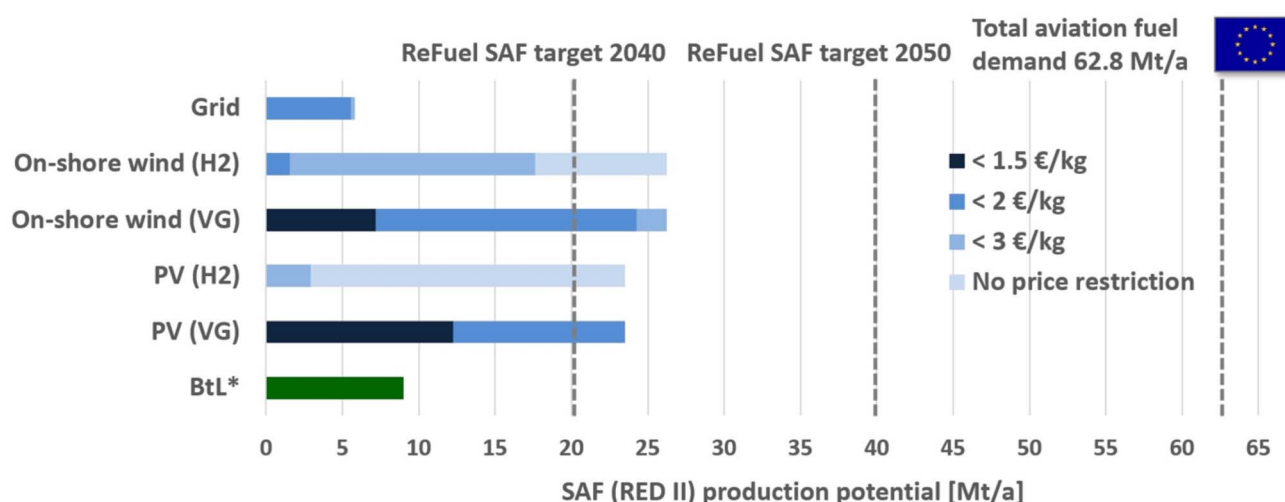


Fig. 13 European SAF production potential with a GWP under  $32.9 \text{ g}_{\text{CO}_2, \text{eq}} \text{ MJ}_{\text{fuel}}^{-1}$ . The potentials are calculated with the assumption that 33% of all forest residue can be used for fuel production. The different power integration scenarios grid, hydrogen storage ( $\text{H}_2$ ) and virtual grid (VG) are compared with a biomass to liquid (BtL) process, which has a biomass conversion of 19.9%. The ReFuel EU blending targets of 32% in 2040 and 63% in 2050 are applied to the 2030 European aviation fuel demand of  $62.8 \text{ Mt a}^{-1}$ .

hydrogen storage scenario ( $\text{H}_2$ ) results in production costs over  $2 \text{ €}_{2020}$  per  $\text{kg}_{\text{C}_{5+}}$ .

## 4. Conclusions

In this study, sustainable aviation fuel (SAF) production *via* the Power Biomass to Liquid (PBtL) route was evaluated in terms of an immediate European deployment. A techno-economic analysis and life cycle assessment (LCA) of a  $900 \text{ MW}_{\text{el}}$  and  $400 \text{ MW}_{\text{th}}$  PBtL process producing  $0.4 \text{ Mt a}^{-1}$  FT fuel have been conducted based on an Aspen Plus® flowsheet simulation. The national grid, on-shore wind and PV have been considered as

power sources. To account for region-specific utility costs, forest residue potentials and the GWP of regionally available electricity in Europe, a techno-economic and environmental analysis methodology has been applied in around 300 European NUTS2 regions. The results of this study show how much and at what cost SAF can be produced in Europe *via* the PBtL route.

Green and inexpensive electricity is essential for economic and sustainable fuel production *via* the PBtL process. Only a few national grid mixes currently have a GWP low enough to achieve a 65% GWP reduction for SAF compared to fossil fuel. Consequently, the PBtL process should currently be regarded as a sweet spot solution for countries like Norway, Sweden or

France. Since many countries are in the process of reducing the GWP of their power production,<sup>1</sup> the PBtL process could become more broadly applicable in the future. In the meantime, an off-grid system could be considered for production sites with high renewable power generation potential. Ireland, for instance, would serve as an excellent PBtL production site due to its high wind potential. Here, the integration of the fluctuating power supply is crucial for the process economics, as an over-dimensioned electrolyser can have a significant impact on the SAF production costs.

The availability of biomass residues has been identified as another limiting factor, besides green and inexpensive electricity. Around 25 Mt a<sup>-1</sup> of SAF can be produced in Europe, assuming that 33% of all forestry residue available for energy purposes can be used for fuel production. This would cover the 32% blending rate mandated in the ReFuel EU directive<sup>22</sup> for the year 2040. To reach the entire European aviation fuel demand of 62.8 Mt a<sup>-1</sup>, either a larger share of forest residue has to be used for fuel production or other feedstock types, such as agricultural residue or municipal solid waste. Yet, the demand for all biomass residues is bound to increase as they also serve as feedstock for low-carbon heat and power production. In situations with a high demand for biomass residues, the advantage of the PBtL process' near full carbon conversion should be considered when allocating these limited resources.

The following points should be considered in future work on this topic:

- The process configuration is fixed with the base case. The optimal plant configuration at each individual site might vary with the regional boundary conditions. For example, a slight reduction of the CO<sub>2</sub> recycling rate when producing with Finish grid electricity would lower the fuel's GWP. With this slight alteration, Finnish PBtL fuel could be produced according the RED II directive (<32.9 g<sub>CO<sub>2</sub>,eq</sub> MJ<sub>fuel</sub><sup>-1</sup>).

- The FT product fraction C<sub>5+</sub> is treated as SAF in this study. However, additional refining steps are omitted. These steps add further costs to the product and part of the product will not be converted into jet fuel. Taking this into account would improve the accuracy of the cost and fuel volume predictions made here.

- The simulated process relies on a 900 MW<sub>el</sub> AEL. However, the currently largest installed AEL system has a capacity of 10 MW.<sup>82</sup> Upscaling issues for this technology should be monitored. The development of other technologies, such as SOEC and PEMEL, should also be considered for a future choice of electrolyser.

- No carbon tax for fossil aviation fuel is considered in the calculation of the NPC and GHG abatement cost values of the FT product. The competitiveness of SAF, however, is expected to increase in the future with measures such as the fossil jet fuel tax planned in the EU with the "Fit for 55" legislative package.<sup>83</sup>

- The assumption that 33% of all forestry residue available for energy purposes can be used for the production of aviation fuel can be considered optimistic. Depending on the demand for other transport and energy applications, this percentage could be significantly lower.

- Only primary forestry residues were considered as biomass feedstock for the derivation of aviation fuel potentials in this

study. If other biomass sources were considered as well, these potentials could be significantly higher. Particularly agricultural residues have a high potential and can be similarly sustainable to forestry residues.<sup>84</sup> However, a redesign of the PBtL process, especially the gasification and gas cleaning steps, would be required for these feedstocks.

- Regarding the sustainability of the forestry residues used for fuel production, local forestry management practices need to be assessed carefully in order to ensure that the use of this type of biomass does indeed lead to a significantly lower overall climate impact. Aspects such as land-use change, carbon debt and its payback time have to be considered for each region.

## Author contributions

Conceptualisation, F. H., V. P., R.-U. D., U. B.; data curation, F. H., V. P.; formal analysis, F. H., V. P.; funding acquisition, R.-U. D., U. B.; investigation, F. H., V. P.; methodology, F. H., V. P.; project administration, F. H.; resources, R.-U. D., U. B.; software, F. H., V. P.; supervision, R.-U. D., U. B.; validation, F. H., V. P.; visualisation, F. H., V. P.; writing – original draft, F. H., V. P.; writing – review & editing, F. H., V. P., R.-U. D., U. B.

## Conflicts of interest

There are no conflicts to declare.

## Acknowledgements

The authors would like to gratefully acknowledge the constructive feedback and funding provided by Airbus SE.

## References

- 1 European Environmental Agency, *Greenhouse gas emission intensity of electricity generation by country*, [https://www.eea.europa.eu/data-and-maps/daviz/co2-emission-intensity-9/#tab-googlechartid\\_googlechartid\\_googlechartid\\_chart\\_1111](https://www.eea.europa.eu/data-and-maps/daviz/co2-emission-intensity-9/#tab-googlechartid_googlechartid_googlechartid_chart_1111), accessed 31, January, 2022.
- 2 S. Searle and C. Malins, *Availability of cellulosic residues and wastes in the EU*, International Council on Clean Transportation, Washington, DC, USA, 2013.
- 3 M. Hillestad, M. Ostadi, G. A. Serrano, E. Rytter, B. Austbø, J. Pharoah and O. S. Burheim, *Fuel*, 2018, **234**, 1431–1451.
- 4 F. Habermeyer, E. Kurkela, S. Maier and R.-U. Dietrich, *Front. Energy Res.*, 2021, **9**, 684.
- 5 I. Hannula, *Energy*, 2016, **104**, 199–212.
- 6 Agora Verkehrswende, Agora Energiewende and Frontier Economics, *The Future Cost of Electricity-Based Synthetic Fuels*, 2018.
- 7 O. Schmidt, A. Gambhir, I. Staffell, A. Hawkes, J. Nelson and S. Few, *Int. J. Hydrogen Energy*, 2017, **42**, 30470–30492.
- 8 N. Jones, K. Johnson and E. Sutti, *Future cost and performance of water electrolysis: An expert elicitation study*, Building Research Establishment Ltd, Liverpool, UK, 2015, p. 23.

- 9 F. G. Albrecht, D. H. König, N. Baucks and R.-U. Dietrich, *Fuel*, 2017, **194**, 511–526.
- 10 European Commission, *Revision of the EU ETS Directive Concerning Aviation*, [https://climate.ec.europa.eu/eu-action/transport-emissions/reducing-emissions-aviation\\_en](https://climate.ec.europa.eu/eu-action/transport-emissions/reducing-emissions-aviation_en), accessed 8, February, 2023.
- 11 E. Commission, *Renewable Energy – Recast to 2030 (RED II)*, [https://joint-research-centre.ec.europa.eu/welcome-jec-website/reference-regulatory-framework/renewable-energy-recast-2030-red-ii\\_en](https://joint-research-centre.ec.europa.eu/welcome-jec-website/reference-regulatory-framework/renewable-energy-recast-2030-red-ii_en), accessed 24, March, 2022.
- 12 S. A. Isaacs, M. D. Staples, F. Allroggen, D. S. Mallapragada, C. P. Falter and S. R. Barrett, *Environ. Sci. Technol.*, 2021, **55**, 8247–8257.
- 13 ICAO, *ICAO welcomes new net-zero 2050 air industry commitment*, <https://www.icao.int/Newsroom/Pages/ICAO-welcomes-new-netzero-2050-air-industry-commitment.aspx>, accessed 10, February, 2023.
- 14 F. G. Albrecht and R.-U. Dietrich, *Technical and Economic Optimization of Biomass-to-Liquid Processes Using Exergoeconomic Analysis*, Copenhagen, Denmark, 2018.
- 15 S. Searle and C. Malins, *GCB Bioenergy*, 2015, **7**, 328–336.
- 16 Q. Bernical, X. Joulia, I. Noirot-Le Borgne, P. Floquet, P. Baurens and G. Boissonnet, *Ind. Eng. Chem. Res.*, 2013, **52**, 7189–7195.
- 17 K. Dahal, S. Brynolf, C. Xisto, J. Hansson, M. Grahn, T. Grönstedt and M. Lehtveer, *Renew. Sustain. Energy Rev.*, 2021, **151**, 111564.
- 18 C. N. Hamelinck and A. P. Faaij, *J. Power Sources*, 2002, **111**, 1–22.
- 19 C. Panoutsou and K. Maniatis, *Sustainable Biomass Availability in the EU, to 2050*, Concawe, 2021.
- 20 R. M. Swanson, A. Platon, J. A. Satrio and R. C. Brown, *Fuel*, 2010, **89**, S11–S19.
- 21 J. O'Malley, N. Pavlenko and S. Searle, *Estimating Sustainable Aviation Fuel Feedstock Availability to Meet Growing European Union Demand*, International Council on Clean Transportation, p. 2021.
- 22 European Commission, *Proposal for a Regulation of the European Parliament and of the Council on Ensuring a Level Playing Field for Sustainable Air Transport*, [https://ec.europa.eu/info/sites/default/files/refueeu\\_aviation\\_-\\_sustainable\\_aviation\\_fuels.pdf](https://ec.europa.eu/info/sites/default/files/refueeu_aviation_-_sustainable_aviation_fuels.pdf), accessed 17, January, 2023.
- 23 M. Prussi, A. O'Connell and L. Lonza, *Biomass Bioenergy*, 2019, **130**, 105371.
- 24 F. Gerard, M. Gerner, P. Lemoine, J. Moerenhout, V. De Haas and P. Cazzola, *Assessment of the Potential of Sustainable Fuels in Transport in the Context of the Ukraine/Russia Crisis*, 2022.
- 25 E. M. Smeets, A. P. Faaij, I. M. Lewandowski and W. C. Turkenburg, *Prog. Energy Combust. Sci.*, 2007, **33**, 56–106.
- 26 M. S. Peters, K. D. Timmerhaus and R. E. West, *Plant Design and Economics for Chemical Engineers*, McGraw-Hill, New York, 2003.
- 27 Eurostat, *Preise Gas für Nichthaushaltskunde, ab 2007 – halbjährliche Daten*, [https://ec.europa.eu/eurostat/databrowser/view/nrg\\_pc\\_203/default/table?lang=de](https://ec.europa.eu/eurostat/databrowser/view/nrg_pc_203/default/table?lang=de), accessed 30, November, 2022.
- 28 H. Haberl, T. Beringer, S. C. Bhattacharya, K.-H. Erb and M. Hoogwijk, *Curr. Opin. Environ. Sustain.*, 2010, **2**, 394–403.
- 29 P. Lauri, P. Havlík, G. Kindermann, N. Forsell, H. Böttcher and M. Obersteiner, *Energy Policy*, 2014, **66**, 19–31.
- 30 L. Zhang, T. L. Butler and B. Yang, *Green Energy to Sustainability: Strategies for Global Industries*, 2020, pp. 85–110.
- 31 M. F. Shahriar and A. Khanal, *Fuel*, 2022, **325**, 124905.
- 32 E. Rytter and A. Holmen, *Catalysts*, 2015, **5**, 478–499.
- 33 Bechtel, *Aspen Process Flowsheet Simulation Model of a Battelle Biomass-Based Gasification, Fischer-Tropsch Liquefaction and Combined-Cycle Power Plant*, US Department of Energy (DOE), Pittsburgh, Pennsylvania, 1998.
- 34 A. Buttler and H. Spliethoff, *Renew. Sustain. Energy Rev.*, 2018, **82**, 2440–2454.
- 35 S. De Jong, K. Antonissen, R. Hoefnagels, L. Lonza, M. Wang, A. Faaij and M. Junginger, *Biotechnol. Biofuels*, 2017, **10**, 64.
- 36 S. E. Tanzer, J. Posada, S. Geraedts and A. Ramírez, *J. Clean. Prod.*, 2019, **239**, 117845.
- 37 C. van der Giesen, R. Kleijn and G. J. Kramer, *Environ. Sci. Technol.*, 2014, **48**, 7111–7121.
- 38 C. M. Liu, N. K. Sandhu, S. T. McCoy and J. A. Bergerson, *Sustain. Energy Fuels*, 2020, **4**, 3129–3142.
- 39 G. Haarlemmer, G. Boissonnet, E. Peduzzi and P.-A. Setier, *Energy*, 2014, **66**, 667–676.
- 40 C. Malins, S. Searle, A. Baral, D. Turley and L. Hopwood, *Wasted: Europe's Untapped Resource: An Assessment of Advanced Biofuels from Wastes and Residues*, International Council on Clean Transportation, 2014.
- 41 E. Kurkela, M. Kurkela and I. Hiltunen, *Biomass Convers. Biorefin.*, 2021, 1–22, DOI: [10.1007/s13399-021-01554-2](https://doi.org/10.1007/s13399-021-01554-2).
- 42 V. S. Sikarwar, M. Zhao, P. S. Fennell, N. Shah and E. J. Anthony, *Prog. Energy Combust. Sci.*, 2017, **61**, 189–248.
- 43 P. Basu, *Biomass Gasification, Pyrolysis and Torrefaction: Practical Design and Theory*, Academic Press, 2018.
- 44 G. Wang, J. Zhang, J. Shao, Z. Liu, H. Wang, X. Li, P. Zhang, W. Geng and G. Zhang, *Energy*, 2016, **114**, 143–154.
- 45 I. Hannula, *Biomass Bioenergy*, 2015, **74**, 26–46.
- 46 A. Padurean, C.-C. Cormos and P.-S. Agachi, *Int. J. Greenh. Gas Control*, 2012, **7**, 1–11.
- 47 S. LeViness, *Velocys Fischer-Tropsch Synthesis Technology – Comparison to Conventional FT Technologies*, San Antonio, Texas, 2013.
- 48 E. Rytter and A. Holmen, *ACS Catal.*, 2017, **7**, 5321–5328.
- 49 C. Schnuelle, T. Wassermann, D. Fuhrlaender and E. Zondervan, *Int. J. Hydrogen Energy*, 2020, **45**, 29938–29952.
- 50 C. Minke, M. Suermann, B. Bensmann and R. Hanke-Rauschenbach, *Int. J. Hydrogen Energy*, 2021, **46**, 23581–23590.
- 51 E. Kurkela, M. Kurkela, C. Frilund, I. Hiltunen, B. Rollins and A. Steele, *Johnson Matthey Technol. Rev.*, 2021, **65**, 333–345.
- 52 S. Müller, P. Groß, R. Rauch, R. Zweiler, C. Aichernig, M. Fuchs and H. Hofbauer, *Biomass Convers. Biorefin.*, 2018, **8**, 275–282.

- 53 Aspen Technology Inc., *Aspen Physical Property System – Physical Property Methods*, 2013.
- 54 B. Todic, T. Bhatelia, G. F. Froment, W. Ma, G. Jacobs, B. H. Davis and D. B. Bukur, *Ind. Eng. Chem. Res.*, 2013, **52**, 669–679.
- 55 S. Maier, S. Tuomi, J. Kihlman, E. Kurkela and R.-U. Dietrich, *Energy Convers. Manage.*, 2021, **247**, 114651.
- 56 F. Mantei, R. E. Ali, C. Baensch, S. Voelker, P. Haltenort, J. Burger, R.-U. Dietrich, N. v. d. Assen, A. Schaadt, J. Sauer and O. Salem, *Sustain. Energy Fuels*, 2022, **6**, 528–549.
- 57 M. S. A. Khan, N. Grioui, K. Halouani and R. Benelmir, *Energy Convers. Manage.: X*, 2022, **13**, 100170.
- 58 W.-C. Wang, Y.-C. Liu and R. A. A. Nugroho, *Energy*, 2022, **239**, 143–154.
- 59 International Monetary Fund and International Financial Statistics, <https://data.worldbank.org/indicator/PA.NUS.FCRF?locations=XC>, accessed 12, April, 2022.
- 60 K. Andersson, S. Brynolf, H. Landquist and E. Svensson, *Shipping and the Environment: Improving Environmental Performance in Marine Transportation*, 2016, pp. 265–293.
- 61 *Environmental management – Life cycle assessment – Requirements and guidelines (ISO 14044:2006)*, German and English version EN ISO 14044:2006, DIN Deutsches Institut für Normung e.V., 2006.
- 62 C. Mutel, *J. Open Source Softw.*, 2017, **2**, 236.
- 63 G. Wernet, C. Bauer, B. Steubing, J. Reinhard, E. Moreno-Ruiz and B. Weidema, *Int. J. Life Cycle Assess.*, 2016, **21**, 1218–1230.
- 64 DLR, *Techno Economic Assessment and LCA Report Comparing 2–3 Process Configurations*, 2021.
- 65 W. Schakel, H. Meerman, A. Talaei, A. Ramírez and A. Faaij, *Appl. Energy*, 2014, **131**, 441–467.
- 66 C. Wulf and M. Kaltschmitt, *Sustainability*, 2018, **10**, 1699.
- 67 M. Delpierre, J. Quist, J. Mertens, A. Prieur-Vernat and S. Cucurachi, *J. Clean. Prod.*, 2021, **299**, 126866.
- 68 S. Fazio, V. Castellani, S. Sala, E. Schau, M. Secchi, L. Zampori and E. Diaconu, *Supporting information to the characterisation factors of recommended EF Life Cycle Impact Assessment methods*, 2018, <https://publications.jrc.ec.europa.eu/repository/handle/JRC114822>.
- 69 P. Ruiz, A. Sgobbi, W. Nijs, C. Thiel, F. Dalla Longa, T. Kober, B. Elbersen and G. Hengeveld, *JRC Science for Policy Report*, European Commission, 2015.
- 70 P. Ruiz, W. Nijs, D. Tarvydas, A. Sgobbi, A. Zucker, R. Pilli, R. Jonsson, A. Camia, C. Thiel and C. Hoyer-Klick, *Energy Strategy Rev.*, 2019, **26**, 100379.
- 71 J. N. Van Stralen, A. Uslu, F. Dalla Longa and C. Panoutsou, *Biofuels*, *Bioprod. Biorefin.*, 2013, **7**, 147–163.
- 72 S. Teske, *Achieving the Paris Climate Agreement Goals: Global and Regional 100% Renewable Energy Scenarios with Non-energy GHG Pathways for +1.5 C and +2 C*, Springer Nature, 2019.
- 73 Eurostat, *Electricity prices for non-household consumers – bi-annual data*, <https://appsso.eurostat.ec.europa.eu/nui/submitViewTableAction.do>, accessed 31, January, 2022.
- 74 Eurostat, *Labour cost levels by NACE Rev. 2 activity*, [https://ec.europa.eu/eurostat/databrowser/product/page/LC\\_LCI\\_LEV\\$DEFAULTVIEW](https://ec.europa.eu/eurostat/databrowser/product/page/LC_LCI_LEV$DEFAULTVIEW), accessed 31, January, 2022.
- 75 J. Hengstler, M. Russ, A. Stoffregen, A. Hendrich, S. Weidner, M. Held and A. K. Briem, *Aktualisierung und Bewertung der Ökobilanzen von Windenergie- und Photovoltaikanlagen unter Berücksichtigung aktueller Technologieentwicklungen. Abschlussbericht*, 2021.
- 76 Finanzen.net, *Oil price (Brent)*, <https://www.finanzen.net/rohstoffe/oelpreis>, accessed 1, November, 2022.
- 77 European Parliament Council of the European Union, *Directive (EU) 2018/2001 of the European Parliament and of the Council of 11 December 2018 on the Promotion of the Use of Energy from Renewable Sources*, Official Journal of the European Union, 2018.
- 78 F. Habermeyer, J. Weyand, S. Maier, E. Kurkela and R.-U. Dietrich, *Biomass Convers. Biorefin.*, 2023, 1–19.
- 79 B. Vidal-Legaz, S. Sala, A. Antón, D. M. De Souza, M. Nocita, B. Putman and R. F. Teixeira, *Land-use related environmental indicators for Life Cycle Assessment*, Joint Research Centre, Luxembourg, 2016.
- 80 D. S. Lee, D. W. Fahey, P. M. Forster, P. J. Newton, R. C. N. Wit, L. L. Lim, B. Owen and R. Sausen, *Atmos. Environ.*, 2009, **43**, 3520–3537.
- 81 European Commission, *Hydrogen: Commission Supports Industry Commitment to Boost by Tenfold Electrolyser Manufacturing Capacities in the EU*, [https://ec.europa.eu/commission/presscorner/detail/en/ip\\_22\\_2829](https://ec.europa.eu/commission/presscorner/detail/en/ip_22_2829), accessed 8, December, 2022.
- 82 Asahi Kasei, <https://www.asahi-kasei.com/news/2020/ze200403.html>, accessed 10, August, 2021.
- 83 European Commission, *'Fit for 55': Delivering the EU's 2030 Climate Target on the Way to Climate Neutrality*, <https://eur-lex.europa.eu/legal-content/EN/TXT/?uri=CELEX%3A52021DC0550>, accessed 15, March, 2023.
- 84 A. Liebich, T. Fröhlich, D. Münter, H. Fehrenbach, J. Giegrich, S. Köppen, F. Dünnebeil, W. Knörr, S. Simon and S. Maier, *System comparison of storable energy carriers from renewable energies*, <https://www.umweltbundesamt.de/publikationen/system-comparison-of-storable-energy-carriers-from>.

# Chapter 4

## Results and Discussion

Some aspects of the PBtL process are discussed across multiple papers. This chapter aims to contextualize and synthesize the results from various publications to highlight overarching findings. The first subchapter marks trends in the techno-economic results across the literature on the PBtL process including the author's publications. Then, common patterns in optimal process design and the integration of fluctuating energy sources are discussed. In the final two subchapters, the findings from the second and third publication on minimizing the GHG emissions and the fuel quantity producible within Europe are summarized.

### 4.1 Techno-economic results

From the summary of techno-economic results in Table 4.1, it is apparent that the process design can strongly affect the process performance. In terms of carbon efficiency, the third publication [31] as well as the publications by Hillestad et al. [22] and Albrecht et al. [9] are above 90 % while the other studies are around 60 %. Throughout all publications, carbon efficiency refers to the fraction of biogenic carbon that can be converted to fuel. High carbon efficiency values can be reached by maximizing the hydrogen addition. The electrolyzer to gasifier capacity ratio E/G gives an indication of the amount of hydrogen added to the system in relation to the biomass input. For simulations with a carbon efficiency above 90 % these values are both above 1.7. Only the simulation by Hillestad et al. does not fit into this pattern. However, this can be explained by the technology selection for the model. Using a SOEC system reduces the electrolyzer capacity by around 33 % compared to PEM or AEL systems due to the SOEC's

**Table 4.1.** PBtL process performance for all published simulations compared to results from literature. All shown results represent the base case in each publication along with the key assumptions.

	I	II	III	Albrecht	Hillestad	Bernical
<b>Base Case Assumptions</b>	[32]	[13]	[31]	[9]	[22]	[24]
Plant size [MW <sub>th</sub> ]	200	50	400	100	435	500
Carbon intensity [kg <sub>CO<sub>2</sub>,eq</sub> /MWh <sub>el</sub> ]	-	68.6	51	-	-	55
Electricity price [€/MWh]	55.49	45.9	50.4	105	50**	70
Biomass price [€/t <sub>wet</sub> ]	84.4	84.4	84.4	97.4	-	-
E/G*** [MW <sub>el</sub> /MW <sub>th</sub> ]	0.94	0.84	2.23	1.71	0.95	-
<b>Base Case Results</b>						
Carbon efficiency [%]	61.1	59.8	92	97	91.3	62
Fuel efficiency [%]	55.2	48.9	45	51.4	0.656	39*
NPC [€/l <sub>C<sub>5+</sub></sub> ]	1	1.09	1.32	2.06	1.7**	1.5
GWP emissions [g <sub>CO<sub>2</sub>,eq</sub> /MJ]	-	19.9	28.1	-	-	11.4
Spec. FCI [M€/MW <sub>th</sub> ]	2.47	2.72	3.83	6.76	6.04	3.40

\*Including power production

\*\*Refers to price/cost in \$

\*\*\*Electrolyzer to gasifier energy input ratio

higher efficiency [22, 42]. In addition, the use of an entrained flow gasifier has the advantage over fluidized or fixed bed gasifiers of leading to a relatively high H<sub>2</sub>/CO ratio in the gasifier outlet [22]. Hence, the system has a comparatively lower hydrogen demand. The lower energy demand of the system can also be seen in the higher fuel efficiency for the simulation published by Hillestad et al. [22]. Here, fuel efficiency describes the ratio of product LHV to the process' energy inputs biomass and electrical power.

Production costs across the studies fall within a range of 1 to 2.06 €/l<sub>C<sub>5+</sub></sub> as displayed in Table 4.1. Variations in electricity and biomass prices contribute to these cost disparities, alongside notable differences in investment costs. Although paper III and the study by Hillestad et al. have a similar plant sizes and electricity prices, the NPC differ by 0.4 €/l<sub>C<sub>5+</sub></sub>. This is partly due to higher equipment costs in Hillestad et al. [22], which are in line with the more expensive technology selection of an entrained flow gasifier and a SOEC. Divergent Lang factors account

for the remaining difference.

The fuel production GWP lies in the range of 19.9 to 28.1  $g_{CO_2,eq}/kWh$  for the analyzed base cases in publication II and III. Although the carbon intensity of the electricity simulated for paper II is higher than in paper III, the former exhibits a lower fuel GWP. This can be explained by the lower  $CO_2$  recycle ratio in paper II. The  $CO_2$  recycle ratio of 44 % compared to 100 % in paper III results in a lower carbon efficiency and consequently a lower product output. At the same time, less hydrogen is needed for the lower product amount. The resulting lower electricity demand leads to the overall lower process GWP in paper II. Bernical et al. find a GWP of 11.4  $g_{CO_2,eq}/MJ$  at a similar carbon efficiency and power carbon intensity as in paper II [24]. The discrepancy in GWP can most likely also be attributed to a lower power demand for Bernical. Yet, this cannot be verified since the exact power demand of the process is not stated in this publication.

## 4.2 Process configuration

Starting from the base case results presented in Table 4.1, various alternative process configurations have been examined with the aim to find enhance process efficiencies or economics. This section summarizes the findings and categorizes these configurations based on their effects on the process.

Some variations of the process configuration lead to a trade-off between CAPEX and process efficiency. The choice of electrolyzer can be taken as an example from paper II. Here, the capital intensive SOEC technology is compared to the AEL, which features a lower electrical efficiency. The simulation in paper II shows that, the SOEC is the economically preferable electrolyzer option above an electricity price of around 50 €/MWh. At high electricity prices, the lower electricity cost due to the SOEC's higher efficiency outweighs the lower investment cost of the AEL. In the same study, the impact of increased FT off-gas recycling is explored, considering the trade-off between heightened CAPEX for all units affected by recycling and an increase in product output. Under the assumptions in paper II, it is demonstrated that higher CAPEX exerts a lower impact on production costs compared to the increased product yield. Therefore, the higher fuel efficiency results in lower NPC in this case. Furthermore, the design of the recycle can influence the process performance. Employing a short recycle, i.e., from the reactor outlet to the inlet, was found to generally increase the production cost by diminishing the

fuel output. However, the combination of a short recycle with a reformer can be economically advantageous compared to a long recycle when biomass with a high syngas cleaning effort is used as feedstock. Finally, an increase in FT temperature from 205 to 230 °C is shown to decrease NPC although the fuel efficiency is decreased. Higher FT temperatures boost FT catalyst activity, reducing the required catalyst mass to achieve the same CO conversion. The reduced cost for the catalyst and the containing FT reactor outweighs the lower product yield, given the assumption made in paper II.

Other variations of the process configuration lead to an increased product output at the expense of a higher power demand. A high CO<sub>2</sub> recycle rate is discussed in the previous section with the comparison of the base case for paper II and III but was also investigated in a dedicated simulation in paper II. In both cases the higher product output comes at the cost of a larger hydrogen demand. As shown in paper 2, the concepts with a high CO<sub>2</sub> recycle rate are especially economically favorable when electricity is available at a low price. The same principle can be applied to the comparison of the PBtL to the BtL process. The product output can be significantly increased as shown in paper I and II, at the cost of additional capital and operation costs for the electrolysis unit. Accordingly, low electricity prices make the PBtL process more economically advantageous. Lastly, a lower H<sub>2</sub>/CO ratio in the FT input can also lower the product yield of the process when assuming a constant H<sub>2</sub> conversion. At the same time, a lower hydrogen demand is shown for the lower H<sub>2</sub>/CO ratio in the PBtL case within paper I. In this example, an additional benefit is that at low H<sub>2</sub>/CO ratios the FT reactor has a higher product selectivity.

Finally, some parameter variations can be categorized as technical advancements that would generally benefit the process performance. An increased electrolyzer efficiency for instance would decrease the power consumption and thereby decrease the NPC. This is shown in a sensitivity analysis in paper II. In the same sensitivity study, an increased once-through CO conversion was shown to have a positive effect on NPC and fuel efficiency. Yet, to attain this higher CO conversion further development in the SBCR design is required [15]. The microreactor design already promises a CO conversion rate up to 80 % [43] compared to 55 % for the SBCR [44]. This is attainable for microchannel reactors due to their excellent heat management [45]. However, this reactor type is connected with higher capital investment.



### 4.3 Integration of fluctuating energy sources

Throughout this work, different options for the integration of fluctuating energy sources have been discussed. This section provides an overview of the main findings from paper I and III on this topic. In the following text, fluctuating energy source is used as an umbrella term for wind and PV power as well as power from the spot market.

In paper I, an alternating operation concept is analyzed which can adapt to the energy spot market by switching between PBtL and BtL production mode. The two modes, referred to as electrolysis assisted (EA) and biomass alone mode (BA), require different amounts of energy depending on whether the electrolyzer is operated (EA) or not (BA). For both modes a number of units are inactive and consequently passively affect the production costs of each mode. Especially, the inactive electrolyzer making up 42 % of the total FCI heavily increases the NPC in the BA mode. Consequently, operating the process in the BA mode and thereby inactivating the electrolyzer should be avoided. In general, the process should be designed such that the inactive units are as small as possible. One way to reach this design is to decrease the H<sub>2</sub>/CO ratio in the FT inlet in the EA mode. Although this lowers the product output for the EA mode, it also reduces the electrolyzer size. For the alternating concept a switch from a ratio of 2.05 to 1.6 translates into a total NPC reduction of 7 % when comparing case 1.1 and 1.3 in paper I.

Paper 3 presents PBtL NPC for European NUTS 2 regions with grid, PV and wind connected operation. For the renewable power sources two scenarios for the integration into a steady-state PBtL process are considered: In the optimistic virtual grid scenario, the fluctuating power production is turned into a steady-state power output by a grid service, which is assumed to be free of charge. In the hydrogen storage scenario, the electrolyzer unit is assumed to be over-dimensioned according to the wind or PV profile's capacity factor. The production costs for renewable energy connected PBtL operation in the hydrogen storage scenario are higher than grid operation in the majority of NUTS 2 regions. This is caused by the high cost for an oversized electrolyzer. Exceptions to this trend are wind power connected Irish NUTS 2 regions. Ireland, with a relatively high capacity factor for on-shore wind, is less affected by the over-dimensioned electrolyzer cost. When considering the virtual grid scenario, the electrolyzer does not have to be over dimensioned. Therefore, production costs in most regions are lower compared to grid operation.

## 4.4 GHG abatement cost

An emission analysis and the calculation of GHG abatement cost can be found in paper II and III. Both studies show that the electricity's carbon intensity is the most determining factor in the total PBtL fuel GWP. In fact, paper II finds electricity must have a carbon intensity lower than  $116 \text{ g}_{CO_2,eq}/\text{kWh}$  in order for the fuel to meet the RED II directive's sustainable fuel definition of  $32 \text{ g}_{CO_2,eq}/\text{MJ}$  [46]. For the plant simulated in paper III this limit is at  $63 \text{ g}_{CO_2,eq}/\text{kWh}$ . This difference can be explained by the amount of power added to the process. As seen in Table 4.1, the simulation in paper III has a higher hydrogen demand per product output than in paper II. Therefore, the process is more sensitive to the electricity's carbon intensity. Both studies find the majority of European countries to be above the RED II limit for sustainable fuel. In paper II, the EU-27 average grid mix does not qualify. For paper III, only the grid mixes of Sweden, Norway, France and Lithuania fall under the defined limit. Yet, all wind and PV connected PBtL production regions fulfil the RED II directive with the exception of Northern European PV production regions.

Promising production regions include Finland, Sweden, Norway and France. They reach abatement costs in the range of  $286 - 418 \text{ €}_{2020}/\text{t}_{CO_2,eq}$  with the national grid mixes assumed in paper II. In the same countries, the BtL abatement cost range is  $303 - 426 \text{ €}_{2020}/\text{t}_{CO_2,eq}$ . For paper III, the best production region in Norway achieves an abatement cost of  $288 \text{ €}_{2020}/\text{t}_{CO_2,eq}$  with grid electricity.

## 4.5 Production potential

The amount of fuel that can be produced within Europe is estimated in paper II and III. Both publications focus on different aspects. Paper II estimates the amount of fuel that can be produced from forest and agricultural biomass residue on a European level [47]. Under the assumption that all biomass is available for fuel production, the PBtL process yields  $63 \text{ Mt}_{C_5+}/\text{a}$ , of which  $14 \text{ Mt}_{C_5+}/\text{a}$  stem from forest residue. This fuel amount would cover the entire EU jet fuel demand [48]. Paper III, on the other hand, only considers forest residue. Contrary to paper II, an availability of 33 % is assumed, which takes into account that other sectors compete for the forest residue. Based on that, around  $25 \text{ Mt}_{C_5+}/\text{a}$  can be produced within Europe. In comparison to the results of paper II, it should be noted that the biomass conversion in paper III is higher, as shown in Table 4.1. Furthermore, paper III considers the

regional fuel production in connection with the regional GHG emissions. When regions that do not fulfil the RED II SAF limit are filtered out, only around 5 Mt<sub>C<sub>5+</sub></sub>/a can be produced with grid electricity. Only with wind or PV operation 25 Mt<sub>C<sub>5+</sub></sub>/a can be reached. Both papers also compare the PBtL results to the yield that is possible with the BtL process. Since paper II includes agricultural residues and considers no competing biomass demand, the total BtL production is estimated at 34 Mt<sub>C<sub>5+</sub></sub>/a compared to around 10 Mt<sub>C<sub>5+</sub></sub>/a in paper III.

# Chapter 5

## Conclusion

This work presents a detailed techno-economic and environmental assessment of sustainable aviation fuel production via the PBtL process in Europe. This includes a discussion of process configurations for an improved process efficiency and economics, and an assessment of integration options for fluctuating renewable energy sources. Furthermore, this work provides estimations regarding the potential sustainable aviation fuel output achievable within Europe, accounting for the constraints imposed by biomass and renewable electricity availability.

A number of methodological advances were required to conduct this analysis. Aspen flowsheet simulations were implemented for three different PBtL process models. Detailed Fischer-Tropsch kinetic reaction models were linked to the process model via a Fortran subroutine for an accurate representation of the product distribution. Moreover, an efficient analysis of various process concepts was achieved by setting up a process superstructure flowsheet and linking it to DLR's techno-economic assessment tool TEPET. Additionally, an approach for the assessment of alternating process operation with TEPET was established. Lastly, an approach for the estimation of local production cost and GHG emissions was applied to around 300 NUTS regions to attain a detailed view of region-specific PBtL production potential.

Based on the techno-economic and ecologic results including the discussion of process concepts, the following conclusions can be drawn:

- Across all the analyzed processes, the most significant cost contributors were identified as electricity, biomass, and the electrolyzer investment. The impact of each cost parameter to the resulting cost of SAF is quantified and discussed for different process configurations.

- The ideal steady-state process design is largely dependent on the economic boundary conditions of the PBtL process:
  - A solid oxide electrolyzer should be favored over an alkaline electrolyzer at high electricity costs. Under these conditions, the higher efficiency of the solid oxide system can compensate for its higher investment cost. However, the current maturity and available size makes the SOEC only a promising option future deployment.
  - With an increased CO<sub>2</sub> recycle ratio the amount of FT product can be increased. Correspondingly, the hydrogen demand of the process will increase. As a result, a production cost decrease with a higher CO<sub>2</sub> recycling rate can only be expected below a certain electricity price limit.
- The GWP of PBtL production is primarily determined by the GWP of the used electricity. Only a few countries' national grid mixes had a sufficiently low GWP to produce SAF in compliance with the RED II directive in 2020. Under the assumption of full CO<sub>2</sub> recycling to maximize the carbon efficiency, the grid mix should not be higher than 63 g<sub>CO<sub>2</sub>,eq</sub>/kWh<sub>el</sub>.

The discussion of integration options for fluctuating electricity allows for the following assertions:

- An alternating operation of the PBtL process with an intermittently operated electrolyzer is only economical on a highly volatile electricity market. Avoiding inactive process units should be prioritized when designing an alternating process.
- The process economics can be improved by minimizing the capacity of the inactive process units. This can be achieved by an under-stoichiometric H<sub>2</sub>/CO ratio in the FT feed for the electrolyzer-assisted mode decreases the electrolyzer size. The same can be accomplished by decreasing the CO<sub>2</sub> recycling rate in the electrolyzer-assisted mode.

Lastly, the examination of fuel production quantity under European biomass and renewable electricity availability constraints yields the following conclusions:

- Presently, the PBtL process is an option for sweet spots, including countries like Sweden or Norway, which offer inexpensive and low GWP grid electricity. Additionally, locations with high capacity factors for renewable energy sources can be considered good sites for off-grid production. As many European countries are in the process of decreasing their grid's GWP footprint, it could be a good option to start the production of SAF with a

BtL process first. Later, when GWP criteria can be met with the national grid mix, the process can be modified to PBtL production by adding an electrolysis unit.

- The nearly complete carbon conversion of the PBtL process is an advantage when biomass is in high demand. This could increasingly be the case for sustainably sourced biomass residue within Europe, where the fuel production would have to compete with heat and electricity production for the limited biomass. Assuming 33 % of all European forest residue is available for the production of fuel via the PBtL process in 2020, around 25 Mt<sub>C5+</sub>/a could be produced in accordance with the RED II directive.

## 5.1 Outlook

Today, the production of SAF is in its infancy. Building on the conclusions of this work, the following points should be considered or further analyzed to guarantee an effective production ramp-up.

The sustainability of different biomass sources has been subject of debate. Clear regulations towards biomass that build trust in the sustainability of forestry and harvesting practices should be introduced. This is a crucial prerequisite for the effective roll-out of any biomass-based fuel process. Secondly, a critical discussion of biomass usage should consider the full utilization of this resource. Applications like CHP plants just use the biomass' energy content for the generation of heat and electricity without making use of the biogenic carbon. These applications should be weight against fuel processes that utilize the biomass' energy and carbon content.

The production of SAF within Europe should be critically compared with an import option. Although domestic production comes with a higher supply security, production cost advantages might favor the import solution. A global sweet spot search could identify promising production sites and quantify the production cost advantages. Here, further considerations should be made regarding the optimal design of off-grid systems. For fluctuating energy sources, a detailed hydrogen production pathway including energy and hydrogen storage and an optimally sized electrolysis unit should be techno-economically analyzed. However, steady energy sources such as hydro or nuclear powerplants should be considered in regions with high biomass potential as well.

Many exemplary design studies showed that the optimal plant design is dependent on the

boundary conditions of the process. The automatic calculation of the optimal process design via an optimization tool in TEPET will increase the accuracy of cost prediction when many locations are considered. Furthermore, with this tool trade-offs between product output, production costs and GWP can be better understood. Similar tools have been presented by Peduzzi et al. with their superstructure optimizer [11] or Pandey et al. with their path optimization algorithm [49].

A detailed model of the FT refining steps would improve the cost predictions for the final SAF product. Co-processed FT product, which is certified as drop-in fuel up to a blending rate of 5 %, should be compared to the bio-refinery production with a maximum blending rate of 50 % [4]. Moreover, the FT wax fraction could be marketed as a high priced by-product due to its purity [50]. Although lowering the fuel yield, this could positively affect the process economics. A comparative techno-economic and life-cycle analysis to identify strength or weaknesses of the different SAF routes should be conducted for all SAF production routes. Other routes, such as the methanol to kerosene route, are in the process of being certified as drop-in fuel. A discussion of these routes with a focus on production volume, emissions and production costs can uncover the most promising production route under different boundary conditions.

# Bibliography

- [1] United Nations, The Paris Agreement, Web Page, **2023**, <https://unfccc.int/process-and-meetings/the-paris-agreement>, Accessed: 8. February 2023.
- [2] European Commission, 'Fit for 55': delivering the EU's 2030 Climate Target on the way to climate neutrality, Web Page, **2021**, <https://eur-lex.europa.eu/legal-content/EN/TXT/?uri=CELEX%3A52021DC0550>, Accessed: 15. March 2023.
- [3] European Commission, Proposal for a REGULATION OF THE EUROPEAN PARLIAMENT AND OF THE COUNCIL on ensuring a level playing field for sustainable air transport, Web Page, **2021**, [https://ec.europa.eu/info/sites/default/files/refueleu\\_aviation\\_-\\_sustainable\\_aviation\\_fuels.pdf](https://ec.europa.eu/info/sites/default/files/refueleu_aviation_-_sustainable_aviation_fuels.pdf), Accessed: 17. January 2023.
- [4] M. F. Shahriar, A. Khanal, *Fuel* **2022**, *325*, DOI <https://doi.org/10.1016/j.fuel.2022.124905>.
- [5] S. S. Ail, S. Dasappa, *Renewable sustainable energy reviews* **2016**, *58*, 267–286.
- [6] A. Tremel, P. Wasserscheid, M. Baldauf, T. Hammer, *International Journal of Hydrogen Energy* **2015**, *40*, 11457–11464.
- [7] S. Schemme, J. L. Breuer, M. Köller, S. Meschede, F. Walman, R. C. Samsun, R. Peters, D. Stolten, *International Journal of Hydrogen Energy* **2020**, *45*, 5395–5414.
- [8] S. Adlung, S. Maier, R.-U. Dietrich, *Sustainable Energy Technologies and Assessments* **2021**, *43*, 100897.
- [9] F. G. Albrecht, D. H. König, N. Baucks, R.-U. Dietrich, *Fuel* **2017**, *194*, 511–526.
- [10] M. Decker, F. Schorn, R. C. Samsun, R. Peters, D. Stolten, *Applied Energy* **2019**, *250*, 1099–1109.
- [11] E. Peduzzi, G. Boissonnet, G. Haarlemmer, F. Maréchal, *Sustainable Energy & Fuels* **2018**, *2*, 1069–1084.
- [12] S. Y. Searle, C. J. Malins, *Biomass and Bioenergy* **2016**, *89*, 2–10.



- [13] F. Habermeyer, J. Weyand, S. Maier, E. Kurkela, R.-U. Dietrich, *Biomass Conversion and Biorefinery* **2023**, DOI 10.1007/s13399-022-03671-y.
- [14] E. Kurkela, M. Kurkela, C. Frilund, I. Hiltunen, B. Rollins, A. Steele, *Johnson Matthey Technology Review* **2021**, *65*, 333–345.
- [15] E. Rytter, A. Holmen, *ACS Catalysis* **2017**, *7*, 5321–5328.
- [16] Thyssenkrupp AG, BioTfuel: The biofuel of the future is made from waste, Web Page, **2023**, <https://www.thyssenkrupp.com/en/stories/sustainability-and-climate-protection/biotfuel-the-biofuel-of-the-future-is-made-from-waste>, Accessed: 10. September 2023.
- [17] Fulcrum BioEnergy, A look inside the Fulcrum Process, Web Page, **2023**, <https://www.fulcrum-bioenergy.com/our-fuel-process>, Accessed: 10. September 2023.
- [18] ERNEUERBARE ENERGIEN, Choren verkauft und entlässt, Web Page, **2011**, <https://www.erneuerbareenergien.de/transformation/speicher/investor-fuer-eins-der-drei-unternehmen-gefunden-choren-verkauft-und-entlaesst>, Accessed: 10. September 2023.
- [19] I. Hannula, *Energy* **2016**, *104*, 199–212, <http://www.sciencedirect.com/science/article/pii/S0360544216303668>.
- [20] I. Hannula, *Biomass and Bioenergy* **2015**, *74*, 26–46.
- [21] H. Zhang, L. Wang, F. Maréchal, U. Desideri, *Applied Energy* **2020**, *270*, 115113.
- [22] M. Hillestad, M. Ostadi, G. A. Serrano, E. Rytter, B. Austbø, J. Pharoah, O. S. Burheim, *Fuel* **2018**, *234*, 1431–1451.
- [23] S. A. Isaacs, M. D. Staples, F. Allroggen, D. S. Mallapragada, C. P. Falter, S. R. Barrett, *Environmental Science & Technology* **2021**, *55*, 8247–8257.
- [24] Q. Bernical, X. Joulia, I. Noiroot-Le Borgne, P. Floquet, P. Baurens, G. Boissonnet, *Industrial & Engineering Chemistry Research* **2013**, *52*, 7189–7195.
- [25] M. Dossow, V. Dieterich, A. Hanel, H. Spliethoff, S. Fendt, *Renewable and Sustainable Energy Reviews* **2021**, *152*, 111670.
- [26] K. R. Putta, U. Pandey, L. Gavrilovic, K. R. Rout, E. Rytter, E. A. Blekkan, M. Hillestad, *Frontiers in Energy Research* **2022**, *9*, DOI 10.3389/fenrg.2021.758149.
- [27] S. Müller, P. Groß, R. Rauch, R. Zweiler, C. Aichernig, M. Fuchs, H. Hofbauer, *Biomass Conversion Biorefinery* **2018**, *8*, 275–282.

- [28] M. Ostadi, E. Rytter, M. Hillestad, *Biomass and Bioenergy* **2019**, *127*, 105282, <http://www.sciencedirect.com/science/article/pii/S0961953419302314>.
- [29] M. Ostadi, B. Austbø, M. Hillestad, *Chemical Engineering Transactions* **2019**, *76*, 205–210.
- [30] J. Weyand, F. Habermeyer, R.-U. Dietrich, *Fuel* **2023**, *342*, DOI 10.1016/j.fuel.2023.127763.
- [31] F. Habermeyer, V. Papantoni, Brand-Daniels, R.-U. Dietrich, *Sustainable Energy & Fuels* **2023**.
- [32] F. Habermeyer, E. Kurkela, S. Maier, R.-U. Dietrich, *Frontiers in Energy Research* **2021**, *9*, 684.
- [33] K. Koponen, I. Hannula, *Applied Energy* **2017**, *200*, 106–118.
- [34] E. Kurkela, M. Kurkela, C. Frilund, I. Hiltunen, B. Rollins, A. Steele, *Johnson Matthey Technology Review* **2021**, *65*, 333–345.
- [35] D. S. Mallapragada, E. Gençer, P. Insinger, D. W. Keith, F. M. O’Sullivan, *Cell Reports Physical Science* **2020**, *1*, 100174.
- [36] E. Kurkela, M. Kurkela, I. Hiltunen, *Biomass Conversion and Biorefinery* **2021**, 1–22.
- [37] B. Todic, T. Bhatelia, G. F. Froment, W. Ma, G. Jacobs, B. H. Davis, D. B. Bukur, *Industrial Engineering Chemistry Research* **2013**, *52*, 669–679.
- [38] B. Todic, W. Ma, G. Jacobs, N. Nikacevic, B. H. Davis, D. Bukur, *International Journal of Chemical Kinetics* **2017**, *49*, 859–874.
- [39] M. S. Peters, K. D. Timmerhaus, R. E. West, *Plant design and economics for chemical engineers*, **volume 4**, McGraw-Hill New York, **2003**.
- [40] A. De Klerk, *Fischer-tropsch refining*, John Wiley & Sons, **2012**.
- [41] F. Habermeyer, *Confidential FLEXCHX deliverable report D8.1* **2019**.
- [42] A. Buttler, H. Spliethoff, *Renewable and Sustainable Energy Reviews* **2018**, *82*, 2440–2454.
- [43] S. LeViness, S. R. Deshmukh, L. A. Richard, H. J. Robota, *Topics in Catalysis* **2014**, *57*, 518–525.
- [44] E. Rytter, A. Holmen, *Catalysts* **2015**, *5*, 478–499.
- [45] S. LeViness **in** AIChE 2013 Spring Meeting.
- [46] European Commission, Renewable Energy – Recast to 2030 (RED II), Web Page, **2018**, [https://joint-research-centre.ec.europa.eu/welcome-jec-website/reference-regulatory-framework/renewable-energy-recast-2030-red-ii\\_en](https://joint-research-centre.ec.europa.eu/welcome-jec-website/reference-regulatory-framework/renewable-energy-recast-2030-red-ii_en), Accessed: 24. March 2022.

- [47] C. Malins, S. Searle, A. Baral, D. Turley, L. Hopwood, Wasted: Europe's untapped resource: an assessment of advanced biofuels from wastes and residues, Report, International Council on Clean Transportation, **2014**, <https://theicct.org/wp-content/uploads/2021/06/WASTED-final.pdf>.
- [48] J. O'malley, N. Pavlenko, S. Searle, Estimating sustainable aviation fuel feedstock availability to meet growing European Union demand, Report, International Council on Clean Transportation, **2021**, <https://theicct.org/publication/estimating-sustainable-aviation-fuel-feedstock-availability-to-meet-growing-european-union-demand/>.
- [49] U. Pandey, K. R. Putta, K. R. Rout, E. A. Blekkan, E. Rytter, M. Hillestad, *Chemical Engineering Research and Design* **2022**, *187*, 276–289.
- [50] G. Herz, E. Reichelt, M. Jahn, *Applied Energy* **2018**, *215*, 309–320.